

N 70 20433

NASA CR 108938

# Alteration of the State of Motion of a Human Being in Free Fall

by  
M. P. Scher and T. R. Kane

Technical Report No. 198

July 1969

**CASE FILE  
COPY**



DIVISION OF APPLIED MECHANICS

STANFORD UNIVERSITY, STANFORD, CALIFORNIA

Department of Applied Mechanics

STANFORD UNIVERSITY

Technical Report No. 198

ALTERATION OF THE STATE OF MOTION  
OF A HUMAN BEING IN FREE FALL

by

M. P. Scher and T. R. Kane

July 1969

## ABSTRACT

A "weightless" astronaut can employ certain movements of his limbs to alter either the orientation or the attitude motion of his body. To study such limb maneuvers, principles of rigid body dynamics are applied to models of the human body.

Maneuvers producing pitch, yaw, and roll reorientations are described, and their effectiveness in changing the orientation of a man initially at rest as regards rotational motion is explored. The results of these analyses justify considerable optimism regarding the use of limb movements as a self-rotation technique.

When the human possesses initial rotational motion, it is theoretically possible to perform maneuvers which convert the motion to a more desirable form. The underlying rationale involves relationships between kinetic energy and the nature of the motion. Analysis shows that the maneuvers in question must be performed with such precision that it is exceedingly difficult to control tumbling motions by means of limb movements. However, the methods developed can be applied successfully to control motions of certain artificial satellites.

Portions of the material covered in this report were presented previously in Technical Report No. 190 (1968) of the Department of Applied Mechanics. They are repeated here in order to render the present report self-contained.

## ACKNOWLEDGEMENT

This work was supported financially by the National Aeronautics and Space Administration under NGR-05-020-209.

## TABLE OF CONTENTS

	page
ABSTRACT -----	ii
ACKNOWLEDGEMENT -----	iii
TABLE OF CONTENTS -----	iv
LIST OF TABLES -----	vi
LIST OF ILLUSTRATIONS -----	vii
LIST OF SYMBOLS -----	viii
1. Introduction -----	1
1.1 Background	1
1.2 Previous Investigations	4
1.3 Inertia Properties of Human Body Segments	15
CHANGES IN ORIENTATION	
2. Pitch Motion -----	27
2.1 Description	27
2.2 Analysis	29
2.3 Results	40
3. Yaw Motion -----	45
3.1 Description	45
3.2 Analysis	47
3.3 Results	59
4. Roll Motion -----	65
4.1 Description	65
4.2 Riddle's Model	66
4.3 Results	69
CHANGES IN ATTITUDE MOTION	
5. Quasi-Rigid Bodies in Free Fall -----	77
5.1 Attitude Motion and Kinetic Energy	77
5.2 Symmetric Quasi-Rigid Bodies	81

# TABLE OF CONTENTS

	page
6. Attitude Equations for Two-Body Systems -----	84
6.1 General Relative Motion	84
6.2 Kinematics of Two Hinged Bodies	90
6.3 Computer Program	98
7. Alteration of Attitude Motions of a Tumbling Man -----	115
7.1 Description	115
7.2 Model	116
7.3 Procedure	121
7.4 Results	127
8. Symmetric Two-Body Satellite -----	141
8.1 Description	141
8.2 Analytical Aspects	143
8.3 Results	146
8.4 Feasibility	150
9. Conclusion -----	156
9.1 Changes in Orientation	156
9.2 Changes in Attitude Motion	157
A. Appendix -----	159
A.1 Tables of Inertia Properties	159
A.2 Subroutines BODIES, INTRNL, TWOBOD, and DFEQS1	165
A.3 Main Program and Subroutines ALPHA and OUTPUT	176
A.4 Computer Output	181
References -----	185

# LIST OF TABLES

Table	Page
1.1 -----	22
1.2 -----	23
1.3 -----	25
1.4 -----	26
2.1 -----	39
3.1 -----	51
3.2 -----	55
3.3 -----	59
3.4 -----	63
4.1 -----	70
6.1 -----	102
6.2 -----	104
6.3 -----	106
6.4 -----	107
6.5 -----	108
6.6 -----	112

Table	Page
6.7 -----	113
6.8 -----	113
6.9 -----	114
7.1 -----	119
7.2 -----	121
7.3 -----	128
7.4 -----	133
7.5 -----	135
7.6 -----	136
8.1 -----	148
A.1 -----	159
A.2 -----	160
A.3 -----	161
A.4 -----	162
A.5 -----	163
A.6 -----	163
A.7 -----	164
A.8 -----	164

# LIST OF ILLUSTRATIONS

Figure		Page
1.1	Nine-segment model of human -----	21
1.2	Five-segment model of human -----	24
2.1	Examples of pitch maneuver -----	28
2.2	Pitch motion model -----	30
2.3	Pitch reorientation as a function of $\beta$ -----	41
2.4	Pitch reorientation as a function of $\theta$ -----	43
2.5	Pitch reorientation as a function of $\varphi$ -----	43
3.1	Yaw maneuver -----	46
3.2	Yaw motion model, phase 1 -----	48
3.3	Yaw motion model, phase 2 -----	56
3.4	Yaw reorientation as a function of $\beta_0$ -----	60
3.5	Yaw reorientation as a function of $\beta_0$ for the four- step yaw maneuver -----	64
4.1	Roll motion model -----	67
4.2	Yaw, pitch, and roll angles as functions of $\theta_0$ -----	71
4.3	Yaw, pitch, and roll angles as functions of $\beta_0$ -----	73
4.4	Roll reorientation, and appropriate values of $\alpha_0$ and $\beta_0$ , as functions of $\theta$ (legs straight) -----	74
4.5	Roll reorientation, and appropriate values of $\alpha_0$ and $\beta_0$ , as functions of $\theta_0$ (legs tucked) -----	75
4.6	Roll reorientation, and appropriate values of $\alpha_0$ and $\beta_0$ , as functions of $\theta_0$ (legs tucked and a five-pound weight in each hand) -----	75
6.1	Two bodies performing general relative motion -----	85
6.2	Two hinged bodies -----	92
7.1	Model of man moving one arm -----	117
7.2	$\gamma(\xi; \Gamma, T)$ -----	124
7.3	$\alpha$ as a function of $\tau$ -----	129
7.4	Kinetic energy as a function of $\tau$ -----	129
7.5	Angular velocity components as functions of $\tau$ -----	131
7.6	$\theta_r$ as a function of $\tau$ -----	132
7.7	Alternative solution for $\alpha$ as a function of $\tau$ -----	134
7.8	Alternative solution for $\alpha$ as a function of $\tau$ with unit lapses between cycles -----	134
7.9	$\theta_r$ as a function of $\tau$ with a 1% error in $\Gamma$ -----	137
7.10	$\alpha$ and kinetic energy as functions of $\tau$ , when convert- ing roll to yaw -----	139
8.1	Symmetric two-body satellite -----	142
8.2	Reduction of $\varphi$ from $60^\circ$ to $0^\circ$ -----	147
8.3	Reduction of $\varphi$ from $90^\circ$ to $0^\circ$ -----	149
8.4	Reduction of $\varphi$ from $60^\circ$ to $0^\circ$ when $\alpha = \Gamma \sin^3 \pi \frac{\tau}{T}$ --	151
8.5	Reduction of $\varphi$ from $60^\circ$ to $30^\circ$ -----	151



# LIST OF SYMBOLS

Numbers refer to the page on which the symbol is defined.

Symbols	page	Symbols	page
Section 1.2		P , Y	29
$\underline{h}$ , $\underline{I}$ , $\underline{\omega}$	13	$m_A$ , $I^A$	29
R , $\underline{r}_i$ , $\underline{v}_i$	13	$\underline{a}_1$ , $\underline{a}_2$ , $\underline{a}_3$	29
$m_i$ , $\underline{\omega}^R$ , $\underline{E}$	14	F	29
R	14	$\xi$	31
Section 1.3		L , $B^*$ , b	31
X , Y , Z	20	$m_B$ , $I_1^B$ , $I_2^B$	31
$B_1$ , $B_2$ , $B_2'$ , $B_3$ , $B_3'$ ,		M , $M'$ , $\underline{m}$	31
$B_4$ , $B_4'$ , $B_5$ , $B_5'$	22	$\theta$ , $\varphi$	31
$B_i^*$	22	K	31
$s_1$ , $s_2$	22	$K_{\omega}^A$ , $K_{\omega}^B$ , $K_{\omega}^{B'}$ , $K_V^A$ ,	
$L_1$ , $L_2$ , $L_3$ , $L_4$ , $L_5$	22	$K_V^B$ , $K_V^{B'}$	32
$d_1$ , $d_2$ , $d_3$ , $d_4$ , $d_5$	22	$\omega_1$ , $\omega_2$ , $\omega_3$	32
$m_i$ , $I_x^i$ , $I_y^i$ , $I_z^i$	22	$\underline{v}_B$	32
$B_1$ , $B_2$ , $B_2'$ , $B_3$ , $B_3'$	25	$S^*$	32
$L_2$ , $L_3$ , $d_2$ , $d_3$	25	$F_{\underline{\omega}}^A$	32
$m_i$ , $I_x^i$ , $I_y^i$ , $I_z^i$	25	$\underline{n}_1$ , $\underline{n}_2$ , $\underline{n}_3$ , N	33
Section 2.2		$\beta$ , $\alpha$	33
A , B , $B'$ , S	29	$\underline{A}^N$ , $\underline{N}^B$ , $\underline{F}^B$	33
0 , $0'$	29	$c_{ij}$	34
$A^*$	29	$\underline{v}^A$ , $\underline{r}^{A^*/S^*}$	34
$a_1$ , $a_2$ , $a_3$	29	$\underline{r}^{B^*/A^*}$	35

Symbols	page	Symbols	page
$\underline{v}^{B^*/0}, \underline{v}^{0/A^*}$	35	$S^*$	50
$M, J$	37	$\underline{v}_B$	50
$E_1, E_2, E_3$	37	$\underline{F}^A$	50
$F_1, F_2, F_3, F_4, F_5$	37	$\alpha, P$	51
$\Delta \xi$	38	$\underline{A}^P$	51
$\ell, \delta, \eta, E, F, G$	38	$\underline{P}^B$	52
Section 3.1		$\underline{v}_A, \underline{v}_B', \underline{v}^{B^*/0}, \underline{v}^{0/S^*}$	53
$\beta_0$	45	$P_1, P_2$	54
Section 3.2		$\Delta \xi_1$	55
$S, A, B, B'$	47	$\beta$	55
$0, 0'$	47	$\underline{A}^B$	55
$Y, M, M'$	49	$\underline{b}_1, \underline{b}_2, \underline{b}_3$	55
$A^*$	49	$q_1, q_2$	58
$m_A, I^A, a$	49	$\Delta \xi_2, \Delta \xi$	58
$\underline{a}_1, \underline{a}_2, \underline{a}_3$	49	Section 4.2	
$F$	49	(Some symbols appearing in	
$\xi$	49	Sec. 4.2 were defined in	
$B^*$	49	Sec. 2.2.)	
$L$	49	$P_1, P_2, P_3$	66
$I_1^B, I_2^B, m_B, b$	49	$\gamma$	66
$K$	50	$I_1^A, I_2^A, I_3^A$	66
$K_{\omega}^A, K_{\omega}^B, K_{\omega}^{B'}, K_v^A,$		$M_1, M_2$	68
$K_v^B, K_v^{B'}$	50	$S_1, S_2$	68
$\underline{F}^B, \omega_1^B, \omega_2^B, \omega_3^B$	50	$\alpha_1, \alpha_2, \beta_1, \beta_2$	68
$P_1, P_2, P_3$	50	$\theta_1, \theta_2, \varphi_1, \varphi_2$	68

Symbols	page	Symbols	page
Section 4.3		$A_{ij} , B_{ij}$	88
$\theta_0$	70	$F_i , T_i$	88
$\alpha_0 , \beta_0$	72	$\omega_i , \Omega_i , r_i$	88
Section 5.1		$E_{ij} , D_i$	88
$K , K_1 , K_3$	78	$C_i , \Delta$	89
$I_1 , I_2 , I_3$	80	Section 6.2	
$\underline{a}_1 , \underline{a}_2 , \underline{a}_3$	80	$L , C$	91
$\omega_1 , \omega_2 , \omega_3$	80	$\underline{a} , \underline{b}$	91
$\underline{H}$	80	$\underline{b}_1 , \underline{b}_2 , \underline{b}_3$	91
Section 5.2		$\underline{h} , \underline{n}_A , \underline{n}_B , \alpha$	91
$\varphi$	81	$I_{ij}^B$	91
$\underline{a}$	81	$[c] , c_{ij}$	91
$\varphi_0 , \varphi_f$	83	$p_{ij} , q_{ij}$	93
Section 6.1		$\underline{m}_A , \underline{m}_B$	93
$A , B , F$	84	$[p] , [q] , [r]$	94
$A^* , B^* , 0$	84	$d_{ij} , e_{ij}$	94
$\underline{I}^A , \underline{I}^B , m_A , m_B$	84	$f_{ij}$	95
$\underline{p} , \underline{r}$	84	$a_i , b_i$	95
$\underline{F} , \underline{T}$	84	$u_i , v_i , w_i$	96
$\underline{F}_A^* , \underline{F}_B^*$	84	Section 6.3	
$M$	85	$\Gamma_i , T_i$	112
$\underline{T}_A^* , \underline{T}_B^*$	86	$\xi$	114
$\underline{\omega}^A , \underline{\omega}^B , \underline{\alpha}^A , \underline{\alpha}^B$	86	Section 7.2	
$\underline{\omega}^{AB}$	87	$A , B$	116
$\underline{a}_1 , \underline{a}_2 , \underline{a}_3$	87	$C , B^*$	116

Symbols	page	Symbols	page
$b, m_B, I_1^B, I_2^B$	116	Section 7.4	
$\underline{b}_1, \underline{b}_2, \underline{b}_3$	116	$H, \theta_r$	130
$A^*$	116	Section 8.1	
$a_1, a_2, A_{ij}, m_A$	116	$\varphi$	141
$\underline{a}_1, \underline{a}_2, \underline{a}_3$	116	$A, B, P$	141
$D, B'$	116	$m, L$	141
$m_D, D_1, D_2, D_3$	116	$D, S$	141
$D^*, 0$	117	$\alpha$	141
$d_1, d_2$	117	$\underline{H}$	143
$\underline{I}^A$	119	Section 8.2	
$\underline{I}^B$	120	$\underline{I}^A, \underline{I}^B, \underline{a}, \underline{b}$	143
$\underline{a}, \underline{b}$	120	$\underline{a}_1, \underline{a}_2, \underline{a}_3$	143
$\underline{n}_A, \underline{n}_B, \underline{h}, \alpha$	120	$\underline{b}_1, \underline{b}_2$	143
$I_1, I_2, I_3$	120	$\underline{h}, \underline{n}_A, \underline{n}_B$	144
Section 7.3		$I_1, I_2, I_3$	144
$t$	121	$\omega_1, \omega_2, \omega_3$	145
$\omega_1, \omega_2, \omega_3$	121	$\Omega, \tau$	145
$\Omega_0, \tau$	121	$\varphi_0$	145
$\tau_0, \tau_n$	122	$\gamma, \xi, \Gamma, T$	146
$\Omega_n$	122	Section 8.3	
$K$	123	$\tau_0, \varphi_f$	146
$\gamma, \xi, \Gamma, T$	123	Section 8.4	
$\Gamma_i, T_i, \tau_i$	124	$K$	153
$K_1, K_3$	126	$\Delta E$	153
		$K_1, K_3$	153

## 1. Introduction

### 1.1 Background

To perform certain tasks which arise in connection with manned space flight, an astronaut must be able to control the motion of his body while in a state of free fall ("weightlessness"). This is a relatively simple matter in situations that permit the astronaut to maintain direct contact with some part of a space vehicle, for he can then exploit forces that come into play as a result of such contacts. Indeed, this method has been used extensively in space missions, and it is a practicable one whenever the vehicle is relatively small and aids, such as handgrips, can be conveniently located on the exterior of the spacecraft to facilitate extravehicular activity.

With the advent of larger space vehicles, or with more ambitious extravehicular missions, it may occur that an astronaut cannot maintain contact with his space vehicle. In this case, the only way to control translational motions of the astronaut is to supply him with a device capable of generating forces, such as a gas gun. There are, however, at least two alternatives for controlling changes in the orientation of the astronaut. One is to use a maneuvering unit which employs either gas jets or inertial devices. The other is to utilize relative motions of parts of the body of the astronaut as do trapeze performers, and divers. This option is attractive because it eliminates both the danger of mechanical failure and the weight penalties associated with carrying any device and its fuel or power supply. In any event, the ability to control orientation by means of limb maneuvers could provide a "back-up"

capability, should primary reliance be placed on the first alternative. These considerations motivated the work described in this dissertation.

Before proceeding to a brief description of the problems to be discussed, it is helpful to introduce three intersecting, mutually perpendicular lines and three planes which are fixed relative to the torso of a man. In accordance with familiar aeronautical usage, these lines are called the pitch, roll, and yaw axes. The yaw axis has the same general orientation as the spine, and the pitch axis passes from left to right. The location of the point of intersection of the axes is selected in a manner that facilitates analysis and may therefore differ from one analysis to the next. The plane determined by a pair of axes is designated by the axis normal to it; e.g., the pitch plane is the plane normal to the pitch axis.

The problems to be solved all deal with a man in free fall; that is, the system of all forces acting on the man is presumed to be equivalent to a single force acting at his mass center; and they fall into two classes: either the man is initially at rest as regards rotational motion, or he is not. In both cases, it is assumed that initially all of the man's limbs are at rest relative to the torso. The problem, then, is to discover motions of the limbs which, in the first case, lead to desired changes in orientation and, in the second case, to advantageous modifications of attitude motions. In both cases, it is required that the limbs ultimately return to their original positions relative to the torso.

For a man initially without rotational motion, it is not difficult to establish qualitative relationships between certain limb movements and associated rotations of the torso. For example, it is apparent that symmetrical rotary motions of the arms will lead to a pitch rotation of the

torso. What is more difficult is to arrive at a quantitative description of such a maneuver. This, however, is precisely what is needed in order to assess any proposed method from a practical point of view. It was decided, therefore, to undertake analytical studies of specific maneuvers which produce rotations around the pitch, yaw, and roll axes. Now, it is a fact that any change whatsoever in the orientation of a rigid body can be produced by three successive rotations about either two or three body-fixed axes. In other words, a man can achieve any desired change in orientation by performing, for example, successive pitch, yaw, and roll maneuvers or, alternatively, a yaw, a pitch, and another yaw maneuver. Accordingly, analyses of maneuvers leading to pitch, yaw, and roll reorientations are presented in Chapters 2, 3, and 4, respectively. The results of these analyses justify considerable optimism regarding the use of limb movements as a self-rotation technique.

When the man has initial rotational motion (while his limbs are at rest relative to his torso), the situation is difficult to visualize. Indeed, it seems unlikely that intuition will indicate how to convert, say, an undesired tumbling motion into a simple spinning motion. A strategy for accomplishing this task, based on energy considerations and leading to a description of suitable limb motions, is discussed in Chapter 5.

After digressing, in Chapter 6, to develop convenient equations of motion, tactics to implement the strategy set forth in Chapter 5 are devised in Chapter 7 for a man who wishes to alter his attitude motion by moving only one arm. The results of this analysis cast doubt on the feasibility of employing limb motions to control human attitude motions, but they suggest that the underlying ideas may well prove useful in the control of attitude motions of spinning spacecraft. Accordingly,

attitude control of a symmetric satellite by means of a driven pendulum is discussed in Chapter 8.

## 1.2 Previous Investigations

Even prior to the space program, the discipline of mechanics had been brought to bear on questions involving physical activity. Much of this early work was performed by coaches and others interested in understanding athletic feats. A review of such literature was presented by Smith [1], whose work will be considered shortly in more detail. Also, considerable effort has been expended on the determination of certain physical properties of the segments of the human body. Since such information is of great importance in the application of mechanics to humans, Sec. 1.3 is devoted to a thorough review of this subject.

One of the first authors to deal with the problem of changing one's orientation by means of limb maneuvers when initially at rest as regards rotational motion was Kulwicki [2], who proposed nine maneuvers, each intended to produce a rotation of the torso about either the pitch, yaw, or roll axis. Some attempt was made to invoke laws of mechanics to explain the qualitative descriptions provided by Kulwicki, but only one of the nine maneuvers was actually studied analytically. Similar work was done by Stepantsov [3] in the U.S.S.R. Smith [1] points out that, in both of these works, the analyses put forth are inadequate. However, Kulwicki and Stepantsov did demonstrate good physical intuition. Stepantsov proposed the yaw maneuver to be considered in Chapter 3 of the sequel, and both authors proposed the pitch maneuver analyzed in Chapter 2, as well as a yaw maneuver similar to the righting movements performed by a cat dropped from rest upside-down. (See the "pinwheel" maneuver in [2] and



page 10 of [3]. The maneuver which Kulwicki called the "Cat Reflex" does not appear to be used by cats. Smith [1] presents a review of research on falling cats, describes a simple analytical model, and analyzes a basic maneuver; and Kane and Scher [4] present a similar, but more complete, analysis.)

A problem of human self-rotation was attacked mathematically by Whitsett [5], who developed a relatively sophisticated mathematical model of the human body, formulated equations governing the planar motion of a system of two hinged bodies, and applied these equations to a man who rotates his arms in planes parallel to the pitch plane. Whitsett also considered a wide variety of other problems dealing with weightless man, including a planar analysis of the translation and rotation of a rigid man under the influence of a body-fixed force misaligned with his mass center, consideration of the stability of the motion of a man in a position of "attention" while spinning about his yaw axis, optimal choice for the direction of thrust of a gas gun, and estimation of the torques which a man can apply to an object by hand when the remainder of his body is unconstrained. Most of these topics were treated briefly, and those dealing with reorientation have now been pursued to greater depth. Hanavan [6,7] has provided an improved model of a human subject, Smith [1] has extended the analysis of planar motions, and Chapter 2 of the sequel treats the rotary arm maneuver in full detail.

A major step in the direction of increased analytical complexity was taken by McCrank [8], who developed equations for three-dimensional attitude motion of a nine-segment model of a human, and used these to create a computer program in which the user can prescribe the time histories of motions of the limbs relative to the torso and can specify initial values

of components of the angular velocity of the torso. A numerical integration of the equations of motion is then performed, resulting in a time history of the angular velocity components of the torso. McCrank considered several sample problems, including some in which the man is not initially at rest as regards rotational motion. His program has two drawbacks: It provides information only on angular rates, not on attitude variables; and the user must prescribe the motions of the limbs relative to the torso in terms of three-axis Euler angles, which may not be convenient in the analysis of a particular limb movement. Perhaps it is for this reason that, in considering a symmetric rotation of the arms (Motion No. 4 in [8]), McCrank prescribed a motion which violates physiological constraints at the shoulder joint. (A way to avoid this is demonstrated in Sec. 2.2 of the sequel.)

An even more ambitious task was undertaken by the Martin Marietta Corporation and reported by Tewell [9]. This was the construction of a weightlessness simulator. The essence of the simulator is as follows: The torso of a man is strapped to a gimbaled carriage capable of moving with six degrees of freedom; the man is permitted to move his limbs; the variations of certain angles which specify the orientation of the limbs relative to the torso are continuously monitored electrically, and these electrical signals are fed to a combination analog-digital computer which determines the behavior the torso would possess in free fall and causes servo-motors to drive the carriage in such a way as to give the torso the required orientation. From an analytical point of view, the system is no more sophisticated than the analysis by McCrank [8]; however, it allows the limb motion inputs, which must be prescribed mathematically for

McCrack's program, to be generated by a man; and the output is a physical reorientation of the man, rather than a time history of angular rates.

Certain difficulties arise in connection with the Martin simulator: Not all of the degrees of freedom which a human actually possesses are detected by the limb motion sensors; the mathematical modelling of the man could be improved (see Sec. 1.3 for details); and the rotations of the gimbals are limited so that some 360 degree reorientations are unattainable and some situations in which the man has rotational motion, even when moving as a single rigid body, cannot be considered. Nevertheless, the simulator is probably a convenient device on which to learn how to maneuver and to obtain a very clear idea of the results of certain limb motions.

The most elegant treatment of the problem of freely falling humans who are initially without rotational motion was presented by Smith [1]. After coining some convenient terms, he defined two problems as follows: Consider a collection of hinged rigid bodies and call one of them the main body. Let generalized coordinates which describe the attitude of the main body in inertial space be called external variables, and call generalized coordinates which describe the orientations of the other bodies relative to the main body internal variables. Then the First Problem is to prescribe time histories of the internal variables and seek the resulting time histories of the external variables, and the Second Problem is to specify the initial and final values of the internal and external variables and to seek time histories of the internal variables which lead to the desired final values. Clearly, only the First Problem was considered in [5], [8], and [9].

Using the First Problem approach, Smith considered both planar and general motions of systems of two and three bodies with zero angular momentum. In the case of three bodies in general motion, a maneuver was analyzed which can be performed either with the arms or with the legs and which produces yaw rotation accompanied by small amounts of pitch and roll. In considering the Second Problem, Smith [1,10] found that no solution may exist in certain cases and that, in others, the solution may not be unique. Using Calculus of Variations, Smith showed how to pose a well-defined problem, and then employed numerical finite-difference techniques to work out a particular example. This example was relatively simple and of little practical importance, and it appears that application of Smith's methods to more complicated problems could easily become prohibitively complex.

Employing the approach of the First Problem, Riddle [11] analyzed a general class of arm maneuvers in which one or both of the arms perform rotary motions relative to the torso. The results of this analysis are embodied in a computer program presented in the appendix of [11]. This program is very versatile and has been used by the present author to consider a wide variety of arm and leg maneuvers. Sec. 4.2 contains an explanation of Riddle's analysis, and some useful conclusions concerning roll reorientations are presented in Sec. 4.3.

Passerello [12], using a model of the human similar to those of McCrank [8] and Tewell [9], derived equations for the attitude motion of a ten-segment man. Again, a First Problem approach was used, so that this derivation is essentially a repetition of McCrank's. Passerello did not program his equations and, in order to produce numerical results,

reduced the number of degrees of freedom in his system to two and then obtained closed form solutions for the changes in orientation produced by two different arm motions. In one of these, he duplicated the planar two-body problem of Smith [1], and the other solution is similar to that for phase 2 of the yaw maneuver analyzed in Sec. 3.2 of the sequel.

Finally, the analyses and discussions of the pitch and yaw maneuvers considered in Chapters 2 and 3 of the sequel will be made more widely available in a forthcoming paper by Kane and Scher [13].

One might suppose that information regarding the effect of human limb motions could be extracted from research connected with the interaction between man and his spacecraft or maneuvering devices. However, this seems not to be the case. Poli [14], for instance, modelled the human as a point mass when considering the effect of his motions on spacecraft attitude. Tieber [15] even went to the trouble of trying to improve on Hanavan's model of the human in connection with studies of an astronaut maneuvering system. However, in the problems he considered, the entire human remained rigid. Finally, Kurzahls [16] documented an elaborate computer program for determining the effect of limb motions on spacecraft attitude, but did not present any results.

Turning to investigations concerned with a man who is initially spinning or tumbling, one finds that the analytical difficulties are considerably greater and, consequently, that relatively little work on this subject has been published. Whitsett [5] considered the stability of a man spinning about his yaw axis, regarding the man as a rigid, but energy dissipating, body. (While this seems self-contradictory, it is an idea much used in connection with satellite attitude stability studies, e.g.,

[17].) McCrank [8] considered one example in which a man moves his limbs in a manner that alters the nature of his rotational motion (e.g., see Motion No. 10 of [8]) and two examples (i.e., Motions No. 6 and No. 11 of [8]) in which the limb motions are such that the orientation in the torso of the direction about which the man is spinning remains unchanged. In this sense, these last two maneuvers resemble the well-known example of the spinning ice-skater who extends his arms to reduce his spin rate (e.g., see p. 2 of [2]). This is not a satisfactory example of the kind of attitude motion control to be discussed in the sequel, for, when the arms are retracted, the skater recovers his initial spin rate.

There exists a small body of literature which deals directly with the problem of altering the attitude motions of multi-body systems by means of prescribed relative motions of the parts. As early as 1896, Fouché [18] recognized that such alterations could be achieved employing cyclical relative motions of the parts, that is, relative motions which ultimately restore the system to its initial relative configuration. Fouché also realized that changes in the kinetic energy of such systems are possible. More recently, Fang [19] made the same observations and suggested that satellite attitude control schemes could be based on these considerations. However, both of these investigations stopped short of actually describing suitable relative motions. Determination of these motions is a central feature of Chapters 7 and 8 and of a forthcoming paper by Kane and Scher [20].

A closely related problem was considered by Letvin-Sedoy [21], namely, the possibility of prescribing the inertial angular rates of the main body of a system and seeking the angular velocities which the other

bodies must possess relative to the main body in order to produce the prescribed motion. When the system angular momentum is zero, this becomes a relatively simple algebraic problem, provided that there are only three possible degrees of freedom in the relative motion. Smith [1] considered a very similar problem, that of finding time histories of the internal variables, rather than the internal rates, which lead to prescribed angular rates of the main body. This latter problem is more formidable than the former because, once the algebraic manipulations are completed, a forward integration is required. However, Smith rightly pointed out that difficulties may occur in the algebraic part of the problem in that, when attempting to solve the scalar equations of motion to obtain expressions for the time derivatives of the internal variables in terms of the prescribed angular rates of the main body, it may occur that the matrix of coefficients of the derivatives of the internal variables becomes singular, in which case the existence of a solution is in doubt. In any event, these two problems differ from those to be considered in the sequel in that, in the latter, a non-zero angular momentum is assumed and the internal variables are required to return to their initial values.

There exists a large body of literature concerned with the attitude control and stability of multi-body artificial satellites, and with specific control devices, such as reaction wheels, gravity gradient booms, and nutation dampers. A few of these investigations bear a close conceptual, visual, or analytical resemblance to the work at hand, and will thus be discussed briefly.

Studies of the behavior of satellites with moving parts can be divided into three categories: First, the parts of a system may perform

prescribed relative motions which are independent of the attitude motion of the main body of the system. For instance, Kane [22] considers a satellite comprised of a symmetric rigid body on whose symmetry axis two particles oscillate in a prescribed fashion. At first glance, this seems to be a good example of a case in which prescribed relative motions serve to control a system, but, since the choice of oscillation parameters has no relation to the satellite motion, this is actually a stability problem.

Next, appendages of a satellite may be continuously driven in a manner dependent on the instantaneous attitude motion of the main body. All feedback control systems, such as those employing reaction wheels or control moment gyroscopes, belong to this category. Some of these control systems employ mechanisms consisting of rods or booms which, at least visually, resemble the open-loop satellite control system discussed in Chapter 8. Gutman [23], for instance, proposed a system consisting of a pendulum which is attached to a rigid vehicle and which is driven with an amplitude proportional to the magnitude of the undesired attitude oscillations of the satellite and with a period governed by the period of the satellite oscillations. Gatlin [24] and Lelikov [25] suggest construction of satellites attached by gimbals to long booms. Control is to be effected by exploiting reaction torques applied between the satellite and its booms. It is assumed that gravitational torques will serve to keep the booms in or near some nominal attitude, despite the presence of the occasional torques exerted by the satellite. Since all of these systems are intended to exploit gravitational torques in some fashion, the assumption of free fall has been rejected.

Finally, the parts of a space vehicle may be free to move under the



action of inertia forces as the main vehicle performs various attitude motions. Analyses of situations of this kind have been performed in connection with the role of energy dissipation in passive attitude control, and a report by Likins [26] contains an extensive bibliography on this subject. Although there are pronounced differences between the passive damping of attitude motions and the active control scheme considered in Chapter 8, some passive systems employ pendulous dampers which, at least superficially, resemble the system described in Sec. 8.1. The reader who would like to examine passive pendulous damping systems in more detail is referred to the works of Alper [27] and Haseltine [28].

The problem of developing appropriate attitude equations for multi-body systems has received a great deal of attention and can be confusing, especially when one strives to preserve the appearance of classical equations for the rotational motion of a single rigid body. Witness, for instance, the recent attempt of Hrushow [29], who differentiated the equation  $\underline{h} = \underline{I} \cdot \underline{\omega}$  with respect to time in an inertial reference frame to obtain  $\dot{\underline{h}} = \dot{\underline{I}} \cdot \underline{\omega} + \underline{I} \cdot \dot{\underline{\omega}}$  where  $\underline{h}$  is the angular momentum of a non-rigid system of particles about the system mass center,  $\underline{I}$  is the centroidal inertia dyadic, and  $\underline{\omega}$  is the angular velocity of "something." Exactly what that "something" is, is difficult to say since no rigid reference frame has been defined. Moreover, even if one introduces some reference frame  $R$  in which the particles of the system move in some specified way, the original expression for  $\underline{h}$  is incomplete since the angular momentum for a system of  $n$  particles about their mass center is given by  $\underline{h} = \sum_{i=1}^n m_i \underline{r}_i \times \underline{v}_i$  where  $\underline{r}_i$  and  $\underline{v}_i$  are the position and

velocity vectors, respectively, of the  $i^{\text{th}}$  particle of mass  $m_i$  relative to the system mass center. Expressing  $\underline{v}_i$  as  $\frac{R_d}{dt} \underline{r}_i + \underline{\omega}^R \times \underline{r}_i$  where  $\frac{R_d}{dt}$  denotes time differentiation in  $R$  and  $\underline{\omega}^R$  is the inertial angular

velocity of  $R$ , one obtains  $\underline{h} = \underline{I} \cdot \underline{\omega}^R + \sum_{i=1}^n m_i \underline{r}_i \times \frac{R_d}{dt} \underline{r}_i$  where

$$\underline{I} = \sum_{i=1}^n m_i (\underline{r}_i^2 \underline{E} - \underline{r}_i \underline{r}_i) \text{ and where } \underline{E} \text{ is a unit dyadic. The last}$$

term in this expression for  $\underline{h}$  is omitted by Hrushow.

A different point of confusion was encountered by Chobotov [30] in taking the time derivative of  $\underline{I} \cdot \underline{\omega}^R$  in an inertial reference frame where  $\underline{I}$  now represents the inertia dyadic of a rigid body  $R$  whose angular velocity is  $\underline{\omega}^R$ . This differentiation led to terms analogous to  $\frac{R_d}{dt} \underline{I}$  (e.g., see  $[\dot{\underline{I}}]$  and  $[\dot{\underline{I}}^j]$  in Fig. 4 of [30]) which clearly must

vanish if  $R$  is rigid as hypothesized. Indeed, Chobotov's equations become correct when these terms are omitted.

Satisfactory equations for the attitude motions of multi-body systems have been derived by a number of authors. These equations fall into two classes, depending on the nature of the physical system. The first class, which will be of interest in the sequel, deals with situations in which it is assumed that the parts of a system perform prescribed motions relative to a main body and, therefore, three components of angular velocity of the main body are the only unknowns. McCrank [8] and Tewell [9] present equations of this nature for the motion of a nine-segment model of a man; Grubin [31] derives them for a multi-body system under the

action of an arbitrary force system; and Smith [1] derives them for two and three body systems with no angular momentum. Equations belonging to the second class are applicable when it is assumed that the appendages of the system are free to move under the influence of inertia forces and, perhaps, elastic and viscous forces exerted on them by the main body of the system. In this case, there are more than three unknown quantities, and a corresponding number of scalar equations must be derived. Equations of this nature for multi-body systems under the influence of a general force system have been derived by Hooker [32]; and for a system of two bodies under the influence of gravitational torques, the appropriate attitude equations have been presented by Fletcher [33]. Despite this abundance of attitude equations, none is well suited for present purposes, and it is thus preferable to derive equations cast in a form that permits the exploitation of particular features of the problem under consideration. This course is followed in Sec. 6.1 for a system of two bodies which perform prescribed relative motions and are acted upon by a general force system. If the two bodies are connected by a simple hinge, certain simplifications arise, as discussed in Sec. 6.2.

### 1.3 Inertia Properties of Human Body Segments

Analyses in which the human is modelled as a system of hinged rigid segments generally involve certain segment properties such as mass, mass center locations, centroidal inertia dyadic, and hinge point locations. Numerous attempts to obtain meaningful values for these properties have been made [34-42]. A brief review of these investigations will indicate deficiencies in currently available values and will reveal the origins of values employed in the sequel.

Experimenters seeking values for segment properties have studied cadavers as well as living humans. During the first half of this century, the most noted investigations were those of Braune and Fischer [34,35], who dismembered four cadavers and performed numerous measurements. More recently, Dempster [36] dismembered eight cadavers and published similar data.

By estimating segment volumes, either photographically or by direct measurements, and by assuming the body to be of uniform density, Weinbach [37] demonstrated how to calculate segment properties of living subjects. However he did not publish such data. Most recently, Drillis [38] estimated segment properties by employing a wide variety of experimental techniques such as immersion and plaster casting and by making occasional assumptions regarding mass distribution. This latter work is significant because it presents a thorough review of previous experimental work and employs a population of living subjects whose weight and height distribution roughly resembles that of today's Air Force personnel.

In addition to frequent large discrepancies in segment parameter values (e.g., see Tables IX or XIII in [38]), the aforementioned investigations share one major deficiency: they do not involve enough measurements to enable one to determine the centroidal inertia dyadic of any body segment. Consequently, they fail to provide sufficient information for certain three-dimensional analyses involving the dynamics of body segments.

Some investigators have sought inertia properties of the human as a whole when the limbs are held fixed relative to the torso. With the aid

of a compound pendulum, Santschi [39] measured mass center locations and moments of inertia about three mutually perpendicular, but not necessarily principal, centroidal axes on sixty-six subjects, each in eight different limb configurations. The height and weight distribution of the subjects was chosen to roughly approximate that of the 1950 U.S. Air Force flying population as recorded by Hertzberg [40], who also recorded the distribution among USAF personnel of a wide variety of other anthropometric measurements. Ref. [39] also includes a tabulation of anthropometric measurements performed on each of the sixty-six subjects in accordance with procedures outlined by Hertzberg.

An alternative procedure for estimating the inertia properties of the human as a whole, but yielding values of segment properties as a by-product, was employed by Hanavan [6,7]. He modelled the human as a system of fifteen hinged rigid segments, each possessing a uniform mass distribution and a relatively simple geometrical shape, e.g., the arm, leg, and foot segments were modelled as frustra of right circular cones. The dimensions of the geometrical figures and the locations of hinge points were to be obtained by performing twenty-four anthropometric measurements on the particular subject being modelled. Thus a "personalized" model could be obtained for a given individual. Based on relations derived by Barter [41], the total mass of the subject was to be distributed among the fifteen segments. Once the mass and dimensions of each segment were determined, the mass center locations and centroidal principal moments of inertia could be computed. After prescribing angles relating the orientation of the segments to one another, the combined mass center and centroidal moments and products of inertia of the entire human could be calculated.

The particular anthropometric measurements required by the Hanavan model were chosen to coincide with those recorded in Refs. [39] and [40]. Thus Hanavan computed the mass center location, centroidal principal moments of inertia, and orientation of the corresponding principal axes for the 5<sup>th</sup>, 25<sup>th</sup>, 50<sup>th</sup>, 75<sup>th</sup>, and 95<sup>th</sup> percentile USAF man in each of thirty-one different limb configurations. Unfortunately, Hanavan failed to publish the individual segment parameters. To determine the accuracy of his computations, Hanavan modelled each of the sixty-six subjects measured by Santschi and compared his computed mass center and moment of inertia calculations with those determined experimentally, finding discrepancies of less than ten percent in most cases .

Perhaps the most suspect part of the Hanavan procedure is the use of Barter's relations, which are linear regression equations expressing segment weights as a function of total body weight and were obtained by a least-squares fit to the segment mass data presented in [34], [35], and [36]. Thus a part of the experimental work on cadavers is incorporated in the Hanavan model. The nature of the regression equations is such that the sum of the segment weights does not necessarily equal the total body weight. Hanavan surmounted this difficulty by distributing the difference proportionally among the segments. A far more serious question concerns the applicability of the regression equations to the USAF flying population since the height and weight distribution of the cadavers from which the equations were derived is far removed from that of USAF personnel.

The results of Hanavan and Santschi were employed by Woolley [42], who wished to obtain values for the segment properties which are

dependent on the build of the particular man being modelled, yet wanted to avoid arduous anthropometric measurements. Woolley inserted the measurements made on each of Santschi's subjects into the Hanavan model and computed the segment properties for each. By using a least-squares technique, he obtained linear regression equations providing segment properties as functions of total body weight. Thus a short stout man and a tall lean man with equal total weights would be assigned the same values for segment properties. In this sense, Woolley "impersonalized" the "personalized" Hanavan model. The user of Woolley's results should be cautioned that the foot and lower leg segments were combined incorrectly so that the regression equations for moments of inertia of the lower leg and foot about the "X" and "Y" axes (e.g., see Eqs. (31) and Fig. 22 in [42]) should be interchanged.

Some refinements in the Hanavan model were introduced by Tieber [15] in an attempt to bring the calculated moments of inertia of the entire body closer to those measured in [39]. To this end, three additional anthropometric measurements were introduced and Barter's equations were replaced with new regression equations obtained from as yet unpublished work at the USAF Aerospace Medical Research Laboratories. Tieber, like Hanavan, neglected to publish any values for the segment properties. The resulting improvements in the values of moments of inertia of the entire man are small (e.g., compare Fig. 6 of [15] to Fig. 16 of [6]) and, due to the inadequacy of the experimental work on segment properties, there is no way to tell whether or not these modifications of the Hanavan model lead to improvements in values of segment properties.

Analysts in need of values for segment properties have obtained them

in various ways. Pre-Hanavan investigators, such as Kulwicksi [2] and Whitsett [5], developed their own models using the measurements reported in [36] and [40]. Kulwicksi's model is relatively crude while Whitsett's appears to be a precursor of Hanavan's. McCrank [8] attempted to substitute the anthropometric measurements of the sixty-third subject measured by Santschi into the Hanavan model, but gave no reason for the choice of the particular subject and performed the substitutions incorrectly (e.g., compare Table I of [8] with case 63 in Appendix II of [42]). Tewell [9] employed Woolley's regression equations and conveniently tabulated values of segment properties appropriate for men weighing between 140 and 220 pounds. Unfortunately, Tewell failed to notice the error in Woolley's equations (e.g., the user of Tewell's tables should reverse IXX and IYY of segments 8 and 9 in Appendix A of [9]).

Values of segment properties employed in the sequel, as well as in the work of Smith [1], Riddle [11], and Passerello [12],\* were obtained by inserting the anthropometric measurements for the USAF 50<sup>th</sup> percentile man into the fifteen segment Hanavan model and by combining segments when practical. As a convenience to the reader, the properties of some of the combinations of segments in the Hanavan model are now presented. Fig. 1.1 depicts a nine-segment model of a man in a position of "attention." In this position, the X, Y, Z axes (shown in Fig. 1.1) are parallel to principal axes of each of the nine segments; and all linear dimensions indicated in Fig. 1.1 are measured parallel to either the Y or Z directions. Table 1.1 contains a list of the symbols appearing

---

\* Values cited in [1], [11], and [12] were calculated by slide rule and therefore differ from those in the sequel, which were obtained by computer.



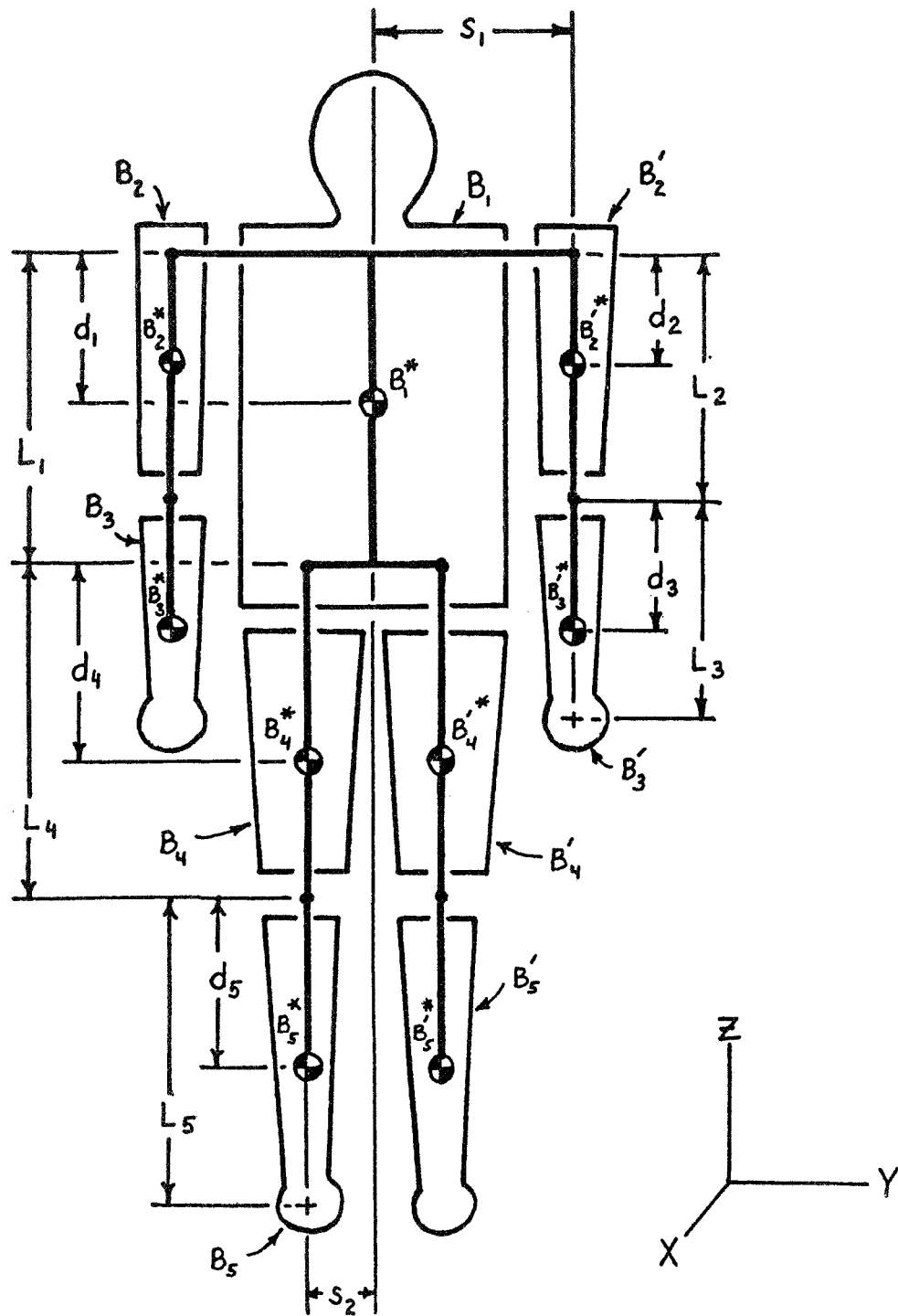


Fig. 1.1

Nine-segment model of human

Table 1.1

(Refer to Fig. 1.1 and Table 1.2.)

Symbol	Definition
$B_1$	Rigid body representing torso, neck, and head.
$B_2, B_2'$	Rigid bodies representing right and left upper arms.
$B_3, B_3'$	Rigid bodies representing right and left forearms and hands.
$B_4, B_4'$	Rigid bodies representing right and left thighs.
$B_5, B_5'$	Rigid bodies representing right and left lower legs and feet.
$B_i^*$	Mass center of body $B_i$ .
$s_1$	Distance from torso centerline to shoulder joint.
$s_2$	Distance from torso centerline to hip joint.
$L_1$	Distance from line joining shoulders to line joining hips.
$d_1$	Distance from line joining shoulders to $B_1^*$ .
$L_2$	Distance from shoulder joint to elbow.
$d_2$	Distance from shoulder joint to $B_2^*$ or $B_2'^*$ .
$L_3$	Distance from elbow to center of fist.
$d_3$	Distance from elbow to $B_3^*$ or $B_3'^*$ .
$L_4$	Distance from hip joint to knee.
$d_4$	Distance from hip joint to $B_4^*$ or $B_4'^*$ .
$L_5$	Distance from knee to center of foot.
$d_5$	Distance from knee to $B_5^*$ or $B_5'^*$ .
$m_i$	Mass of body $B_i$ .
$I_x^i$	Moment of inertia of body $B_i$ about a line parallel to X and passing through $B_i^*$ .
$I_y^i$	Moment of inertia of body $B_i$ about a line parallel to Y and passing through $B_i^*$ .
$I_z^i$	Moment of inertia of body $B_i$ about a line parallel to Z and passing through $B_i^*$ .

in Fig. 1.1 and definitions of these symbols. Some additional symbols representing inertia properties are defined in Table 1.1; and values for both inertia and geometrical properties of a nine-segment, 50th percentile man are presented in Table 1.2. Similar material for a five-segment model of the USAF 50th percentile man is presented in Fig. 1.2 and Tables 1.3 and 1.4. Appendix A.1 contains tables analogous to Table 1.2 and Table 1.4 for the 5th, 25th, 75th, and 95th percentile USAF man.

Table 1.2  
Inertia Properties for a Nine-Segment Model  
of the USAF 50th Percentile Man  
(Refer to Fig. 1.1 and Table 1.1.)

Segment	$m_i$	$I_x^i$	$I_y^i$	$I_z^i$	$L_i$	$d_i$
$B_1$	2.78	1.743	1.644	0.257	1.544	0.632
$B_2, B_2'$	0.1585	0.01760	0.01760	0.00191	0.961	0.374
$B_3, B_3'$	0.1308	0.01889	0.01889	0.00105	1.062	0.575
$B_4, B_4'$	0.510	0.0721	0.0721	0.01632	1.508	0.788
$B_5, B_5'$	0.326	0.0745	0.0788	0.00797	1.379	0.727

$$s_1 = 0.664$$

$$s_2 = 0.253$$

$$\text{Total mass} = 5.03$$

(All lengths in feet, masses in slugs, and moments of inertia in slug-feet<sup>2</sup>.)

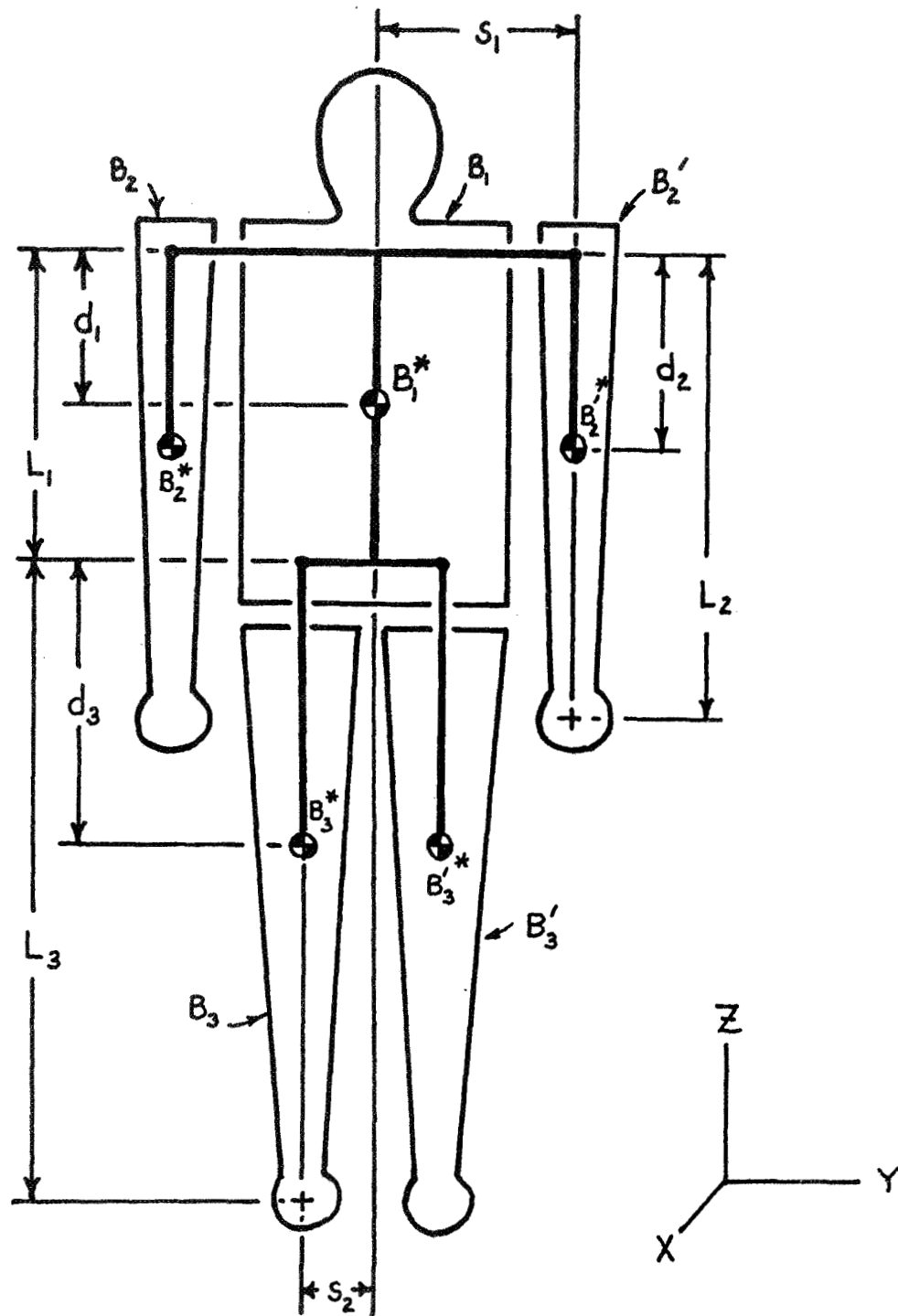


Fig. 1.2

Five-segment model of human

Table 1.3

(Refer to Fig. 1.2 and Table 1.4)

Symbol	Definition
$B_1$	Rigid body representing torso, neck, and head.
$B_2, B_2'$	Rigid bodies representing right and left arms and hands.
$B_3, B_3'$	Rigid bodies representing right and left legs and feet.
$B_i^*$	Mass center of body $B_i$ .
$s_1$	Distance from torso centerline to shoulder joint.
$s_2$	Distance from torso centerline to hip joint.
$L_1$	Distance from line joining shoulders to line joining hips.
$d_1$	Distance from line joining shoulders to $B_1^*$ .
$L_2$	Distance from shoulder joint to center of fist.
$d_2$	Distance from shoulder joint to $B_2^*$ or $B_2'^*$ .
$L_3$	Distance from hip joint to center of foot.
$d_3$	Distance from hip joint to $B_3^*$ or $B_3'^*$ .
$m_i$	Mass of body $B_i$ .
$I_x^i$	Moment of inertia of body $B_i$ about a line parallel to X and passing through $B_i^*$ .
$I_y^i$	Moment of inertia of body $B_i$ about a line parallel to Y and passing through $B_i^*$ .
$I_z^i$	Moment of inertia of body $B_i$ about a line parallel to Z and passing through $B_i^*$ .

Table 1.4  
Inertia Properties for a Five-Segment Model  
of the USAF 50<sup>th</sup> Percentile Man  
(Refer to Fig. 1.2 and Table 1.3.)

Segment	$m_i$	$I_x^i$	$I_y^i$	$I_z^i$	$L_i$	$d_i$
$B_1$	2.78	1.743	1.644	0.257	1.544	0.632
$B_2, B_2'$	0.289	0.1331	0.1331	0.00296	2.02	0.899
$B_3, B_3'$	0.836	0.563	0.567	0.0243	2.89	1.352
$s_1 = 0.664$		$s_2 = 0.253$				

Total mass = 5.03

(All lengths in feet, masses in slugs, and moments of inertia in slug-feet<sup>2</sup>.)

## CHANGES IN ORIENTATION

### 2. Pitch Motion

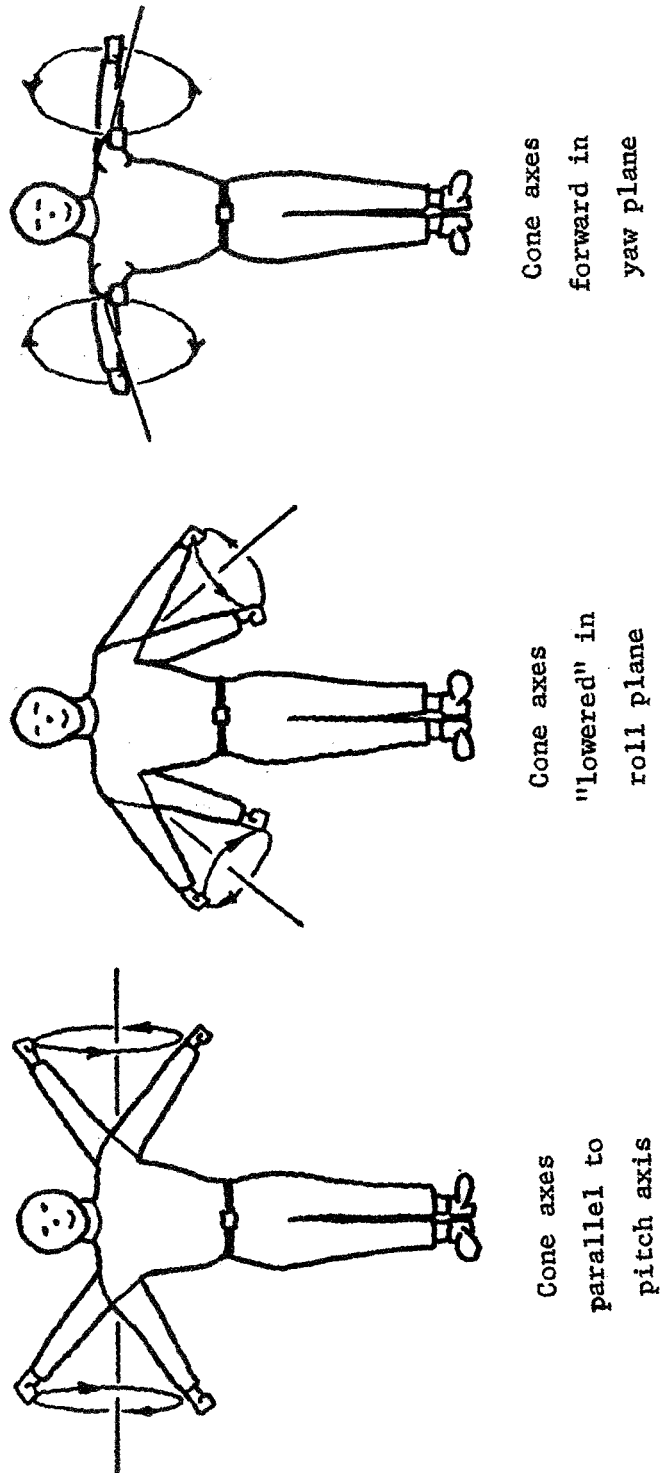
#### 2.1 Description

The pitch maneuver under consideration was suggested by Kulwicki [2] and Stepantsov [3] and was analyzed by McCrank [8] who, however, failed to investigate its effectiveness and postulated an arm motion which cannot be performed for physiological reasons.

During the maneuver, the arms are held straight at the elbows and perform a rotary motion with respect to the torso, remaining symmetrically disposed with respect to the pitch plane at all times. The longitudinal axis of each arm travels on the surface of an imaginary, torso-fixed cone whose vertex is at the shoulder. The arm motion can be described in terms of the cone semi-vertex angle and the orientation of the cone axis relative to the torso, any physically attainable orientation being permissible, as illustrated by the examples in Fig. 2.1. (Symmetry considerations show that these cone parameters need to be specified for only one of the arms.) The legs must be kept fixed relative to the torso and symmetrically located with respect to the pitch plane.

Consider the motion of the torso (and legs) during one cycle of the maneuver. The sense of pitching of the torso is opposite to that in which the arms travel on the surfaces of the cones. A reversal in the sense of motion of the arms produces a reversal in the sense of pitching.

Prior to starting the maneuver, the subject may have his limbs disposed in any way satisfying the requirements of symmetry with respect to the pitch plane, and the arms may then be brought to the starting position



Examples of pitch maneuver

Fig. 2.1



in any manner compatible with this requirement. After an integral number of cycles of the maneuver have been performed, the arms can be returned to their initial positions by retracing the paths followed in bringing them to the starting positions. Any pitching of the torso obtained while starting will be nullified during the return.

## 2.2 Analysis

For purposes of analysis, the human is modelled as a system  $S$  of three rigid bodies. One of these, designated  $A$ , represents the torso, head, and legs. The remaining two,  $B$  and  $B'$ , each represent an arm.  $B$  and  $B'$  are connected to  $A$  at points  $O$  and  $O'$  (see Fig. 2.2), which represent shoulder joints.

Body  $A$  is presumed to be symmetric with respect to the pitch plane, so that its mass center  $A^*$  lies in this plane. Points  $O$  and  $O'$  are symmetrically located at a distance  $a_2$  to either side of the pitch plane, and the line  $P$  passing through them is designated the pitch axis. The yaw axis  $Y$  is oriented in  $A$  so as to pass through the mass center of a body comprised of only the torso and head. Consequently,  $A^*$  lies on  $Y$  only when the legs are held in certain positions; and, in general,  $A^*$  is located at a distance  $a_1$  from  $Y$  and at a distance  $a_3$  from the yaw plane. The mass of  $A$  is  $m_A$ , and the moment of inertia of  $A$  about a line through  $A^*$  parallel to  $P$  is  $I^A$ . Unit vectors  $\underline{a}_1$ ,  $\underline{a}_2$ ,  $\underline{a}_3$  are fixed in  $A$  parallel to the roll, pitch, and yaw axes, respectively. In view of symmetry considerations, only pitch motions of  $A$  need to be considered so that the orientation of  $A$  in an inertial reference frame  $F$  can be described by means of a single



angle, such as an angle  $\xi$  between  $Y$  and a line fixed in  $F$  and normal to  $P$ .

Body  $B$  possesses an axis of symmetry, designated  $L$ . The mass center  $B^*$  of  $B$  is located on  $L$  at a distance  $b$  from point  $O$ . The mass of  $B$  is  $m_B$ , the moment of inertia of  $B$  about  $L$  is  $I_2^B$ , and the moment of inertia of  $B$  about any line passing through  $B^*$  and normal to  $L$  is  $I_1^B$ . The geometrical and inertia properties of  $B'$  are identical to those of  $B$ .

The kinematical analysis in the sequel involves the cone axes,  $M$  and  $M'$ , which are fixed with respect to  $A$  and are located symmetrically with respect to the pitch plane. Line  $M$  passes through  $O$  and its orientation is determined by angles  $\theta$  and  $\varphi$  as shown in Fig. 2.2. (The lines forming  $\theta$  lie in the yaw plane, and those forming  $\varphi$  lie in a plane normal to the yaw plane.) Symmetry considerations permit one to locate  $M'$ . Unit vector  $\underline{m}$  is parallel to  $M$ .

The equation of motion for this system will be obtained by employing a Lagrangian approach. When  $S$  is in free fall, the attitude variable  $\xi$  does not enter the expressions for the kinetic and potential energies and, consequently, a first integral of Lagrange's equation may be obtained. The assumption that  $S$  is initially rotationally at rest leads to a choice of zero for the constant of integration, and Lagrange's equation thus becomes

$$\frac{\partial K}{\partial \dot{\xi}} = 0 \quad (2.1)$$

where  $\dot{\xi}$  is the time derivative of the angle  $\xi$ , and  $K$ , the kinetic energy associated with motions of  $S$  relative to the system mass center,

can be expressed as

$$K = K_{\omega}^A + K_{\omega}^B + K_{\omega}^{B'} + K_v^A + K_v^B + K_v^{B'} \quad (2.2)$$

The first three terms on the right-hand side of this equation represent the rotational kinetic energies of A, B, and B'. For example, if  $I_1^B, I_2^B, I_3^B$  are principal moments of inertia of B for  $B^*$ , and  $\omega_1^B, \omega_2^B, \omega_3^B$  are components of the angular velocity of B in F when this angular velocity is referred to principal axes of B for  $B^*$ , then

$$K_{\omega}^B = \frac{1}{2} [I_1^B (\omega_1^B)^2 + I_2^B (\omega_2^B)^2 + I_3^B (\omega_3^B)^2] \quad (2.3)$$

The last three terms in Eq. (2.2) reflect the motions of the mass centers of A, B, and B'. For instance, if  $\underline{v}_B$  is the velocity of  $B^*$  relative to the system mass center  $S^*$ , then

$$K_v^B = \frac{1}{2} m_B \underline{v}_B^2 \quad (2.4)$$

In the following kinematical analysis, only pitch motions of A are considered. Consequently, the angular velocity of A in F can be expressed as

$$\underline{\omega}^A = \dot{\xi} \underline{a}_2 \quad (2.5)$$

Symmetry considerations demand that  $\underline{a}_2$  be parallel to a principal axis of A for  $A^*$ . Hence  $I^A$  is a principal moment of inertia and<sup>†</sup>

$$K_{\omega}^A = \frac{1}{2} I^A \dot{\xi}^2 \quad (2.6)$$

(2.3, 2.5)

---

<sup>†</sup> Numbers beneath equal signs are intended to direct attention to corresponding equations.

The motions of B and B' are described in terms of the "coning" motion outlined in Sec. 2.1. Line L intersects cone axis M at O, thereby defining a plane N, and the angle  $\beta$  between L and M remains constant throughout the maneuver. Mutually perpendicular unit vectors  $\underline{n}_1$ ,  $\underline{n}_2$ ,  $\underline{n}_3$  are fixed in N, with  $\underline{n}_2$  parallel to L and  $\underline{n}_1$  normal to N.

If the angle between N and a plane passing through M and normal to the yaw plane is designated  $\alpha$ , then the angular velocity of N in A is given by

$$\underline{\omega}^A_N = \dot{\alpha} \underline{m} \quad (2.7)$$

When  $\alpha$  increases from 0 to  $2\pi$ , L travels once around the surface of a cone of semi-vertex angle  $\beta$ . During this motion, B must rotate in N in such a manner that no twisting of the arm relative to the torso occurs at the shoulder. This can be accomplished by specifying the angular velocity of B in N as follows:

$$\underline{\omega}^N_B = -\dot{\alpha} \underline{n}_2 \quad (2.8)$$

The angular velocity of B in F can be expressed as

$$\underline{\omega}^F_B = \underline{\omega}^N_B + \underline{\omega}^A_N + \underline{\omega}^F_A \quad (2.9)$$

In order to resolve this vector into components parallel to  $\underline{n}_1$ ,  $\underline{n}_2$ ,  $\underline{n}_3$ , we note that

$$\underline{n}_i = \sum_{j=1}^3 c_{ij} \underline{a}_j \quad i=1, 2, 3 \quad (2.10)$$

where the  $c_{ij}$  of interest are

$$\left. \begin{aligned}
 c_{12} &= -\sin \theta \cos \alpha - \cos \theta \sin \varphi \sin \alpha \\
 c_{21} &= \cos \theta \sin \beta \sin \alpha + \sin \theta \cos \varphi \cos \beta + \sin \theta \sin \varphi \sin \beta \cos \alpha \\
 c_{22} &= -\sin \theta \sin \beta \sin \alpha + \cos \theta \cos \varphi \cos \beta + \cos \theta \sin \varphi \sin \beta \cos \alpha \\
 c_{23} &= -\sin \varphi \cos \beta + \cos \varphi \sin \beta \cos \alpha \\
 c_{32} &= -\sin \theta \cos \beta \sin \alpha - \cos \theta \cos \varphi \sin \beta + \cos \theta \sin \varphi \cos \beta \cos \alpha
 \end{aligned} \right\} \quad (2.11)$$

Furthermore,

$$\underline{m} = \cos \beta \underline{n}_2 - \sin \beta \underline{n}_3 \quad (2.12)$$

It now follows that (see Eqs. (2.9), (2.5), (2.10), (2.7), (2.12), (2.8))

$$\underline{F}_w^B = [\dot{\xi} c_{12}] \underline{n}_1 + [\dot{\xi} c_{22} + \dot{\alpha}(\cos \beta - 1)] \underline{n}_2 + [\dot{\xi} c_{32} - \dot{\alpha} \sin \beta] \underline{n}_3 \quad (2.13)$$

and, since  $\underline{n}_1, \underline{n}_2, \underline{n}_3$  are parallel to principal axes of B for  $B^*$ ,

$$\begin{aligned}
 K_w^B &= \frac{1}{2} \left\{ \dot{\xi}^2 [I_1^B (c_{12}^2 + c_{32}^2) + I_2^B c_{22}^2] \right. \\
 &\quad + 2 \dot{\xi} \dot{\alpha} [I_2^B c_{22} (\cos \beta - 1) - I_1^B c_{32} \sin \beta] \\
 &\quad \left. + \dot{\alpha}^2 [I_1^B \sin^2 \beta + I_2^B (\cos \beta - 1)^2] \right\} \quad (2.14)
 \end{aligned}$$

In a similar fashion, an identical expression is obtained for  $K_w^{B'}$ .

The velocity  $\underline{v}_A$  of  $A^*$  relative to  $S^*$  is the time derivative in F of  $\underline{r}^{A^*/S^*}$ , the position vector of  $A^*$  relative to  $S^*$ ; i.e.,

$$\underline{v}_A = \frac{F_d}{dt} \underline{r}^{A^*/S^*} \quad (2.15)$$

Symmetry requires that  $S^*$  lie in the pitch plane. This fact makes it possible to express  $\underline{r}^{A^*/S^*}$  as

$$\underline{r}^{A^*/S^*} = - \frac{2m_B}{m_A + 2m_B} \left[ \left( \underline{r}^{B^*/A^*} \cdot \underline{a}_1 \right) \underline{a}_1 + \left( \underline{r}^{B^*/A^*} \cdot \underline{a}_3 \right) \underline{a}_3 \right] \quad (2.16)$$

where  $\underline{r}^{B^*/A^*}$  is the position vector of  $B^*$  relative to  $A^*$ , which, by reference to Fig. 2.2, is seen to be given by

$$\underline{r}^{B^*/A^*} = - a_1 \underline{a}_1 + a_2 \underline{a}_2 + a_3 \underline{a}_3 + b \underline{n}_2 \quad (2.17)$$

Consequently, (see Eqs. (2.15), (2.16), (2.17), (2.10), (2.11), (2.5))

$$\underline{v}_A = \frac{2m_B}{m_A + 2m_B} \left\{ - \left[ b \frac{dc_{21}}{d\alpha} \dot{\alpha} + \dot{\xi} (bc_{23} + a_3) \right] \underline{a}_1 + \left[ \dot{\xi} (bc_{21} - a_1) - b \frac{dc_{23}}{d\alpha} \dot{\alpha} \right] \underline{a}_3 \right\} \quad (2.18)$$

and it follows that

$$\begin{aligned} K_v^A &= \frac{1}{2} m_A \left( \frac{2m_B}{m_A + 2m_B} \right)^2 \left\{ \dot{\xi}^2 \left[ b^2 (c_{23}^2 + c_{21}^2) + 2b(a_3 c_{23} - a_1 c_{21}) + a_1^2 + a_3^2 \right] \right. \\ &\quad + 2 \dot{\xi} \dot{\alpha} \left[ b^2 \left( c_{23} \frac{dc_{21}}{d\alpha} - c_{21} \frac{dc_{23}}{d\alpha} \right) + b \left( \frac{dc_{21}}{d\alpha} a_3 + \frac{dc_{23}}{d\alpha} a_1 \right) \right] \\ &\quad \left. + \dot{\alpha}^2 b^2 \left[ \left( \frac{dc_{21}}{d\alpha} \right)^2 + \left( \frac{dc_{23}}{d\alpha} \right)^2 \right] \right\} \quad (2.19) \end{aligned}$$

Next,  $\underline{v}_B$  is given by

$$\underline{v}_B = \underline{v}^{B^*/O} + \underline{v}^{O/A^*} + \underline{v}_A \quad (2.20)$$

where

$$\underline{v}^{B^*/O} = \underline{\omega}^B \times b \underline{n}_2 \quad (2.21)$$

and

$$\underline{v}^{O/A^*} = \underline{\omega}^A \times (-a_1 \underline{a}_1 + a_2 \underline{a}_2 + a_3 \underline{a}_3) \quad (2.22)$$

Thus (see Eqs. (2.20), (2.18), (2.21), (2.13), (2.10), (2.22), (2.5))

$$\begin{aligned} \underline{v}_B = & \left\{ \frac{m_A}{m_A + 2m_B} \left[ \dot{\xi} (bc_{23} + a_3) + \dot{\alpha} b \frac{dc_{21}}{d\alpha} \right] \right\} \underline{a}_1 + \left\{ \dot{\alpha} b \sin \beta c_{12} \right\} \underline{a}_2 \\ & + \left\{ \frac{m_A}{m_A + 2m_B} \left[ \dot{\xi} (a_1 - bc_{21}) + \dot{\alpha} b \frac{dc_{23}}{d\alpha} \right] \right\} \underline{a}_3 \end{aligned} \quad (2.23)$$

$K_V^B$  is, therefore, given by

$$\begin{aligned} K_V^B = & \frac{1}{2} m_B \left\{ \dot{\xi}^2 \left( \frac{m_A}{m_A + 2m_B} \right)^2 \left[ b^2 (c_{21}^2 + c_{23}^2) + 2b(c_{23}a_3 - c_{21}a_1) + (a_1^2 + a_3^2) \right] \right. \\ & + 2\dot{\xi}\dot{\alpha} \left( \frac{m_A}{m_A + 2m_B} \right)^2 \left[ b^2 \left( c_{23} \frac{dc_{21}}{d\alpha} - c_{21} \frac{dc_{23}}{d\alpha} \right) + b \left( a_3 \frac{dc_{21}}{d\alpha} + a_1 \frac{dc_{23}}{d\alpha} \right) \right] \\ & \left. + \dot{\alpha}^2 b^2 \left[ \sin^2 \beta c_{12}^2 + \left( \frac{m_A}{m_A + 2m_B} \right)^2 \left( \left( \frac{dc_{21}}{d\alpha} \right)^2 + \left( \frac{dc_{23}}{d\alpha} \right)^2 \right) \right] \right\} \end{aligned} \quad (2.24)$$

and the expression for  $K_V^{B'}$  is identical. The kinetic energy associated with motions of S relative to  $S^*$  can now be expressed as (see Eqs. (2.2), (2.6), (2.14), (2.19), (2.24))

$$\begin{aligned} K = & \dot{\xi}^2 \left\{ \frac{1}{2} I_1^B (c_{12}^2 + c_{32}^2) + I_2^B c_{22}^2 \right. \\ & + \frac{m_A m_B}{m_A + 2m_B} \left[ b^2 (c_{21}^2 + c_{23}^2) + 2b(a_3 c_{23} - a_1 c_{21}) + (a_1^2 + a_3^2) \right] \left. \right\} \\ & + 2 \dot{\xi} \dot{\alpha} \left\{ I_2^B c_{22} (\cos \beta - 1) - I_1^B c_{32} \sin \beta \right. \\ & + \frac{m_A m_B}{m_A + 2m_B} \left[ b^2 \left( c_{23} \frac{dc_{21}}{d\alpha} - c_{21} \frac{dc_{23}}{d\alpha} \right) + b \left( \frac{dc_{21}}{d\alpha} a_3 + \frac{dc_{23}}{d\alpha} a_1 \right) \right] \left. \right\} \\ & + \dot{\alpha}^2 \left\{ 2I_2^B (1 - \cos \beta) + (I_1^B - I_2^B + m_B b^2) \sin^2 \beta \right. \\ & \left. + \frac{m_A m_B}{m_A + 2m_B} b^2 \left[ \left( \frac{dc_{21}}{d\alpha} \right)^2 + \left( \frac{dc_{23}}{d\alpha} \right)^2 \right] \right\} \end{aligned} \quad (2.25)$$



The equation of motion can thus be formulated as

$$\begin{aligned}
 \ddot{\alpha} & \left\{ \frac{I^A}{2} + I_1^B (c_{12}^2 + c_{32}^2) + I_2^B c_{22}^2 \right. \\
 & + \frac{m_A m_B}{m_A + 2m_B} \left[ b^2 (c_{21}^2 + c_{23}^2) + 2b(a_3 c_{23} - a_1 c_{21}) + (a_1^2 + a_3^2) \right] \left. \right\} \\
 & + \dot{\alpha} \left\{ I_2^B c_{22} (\cos \beta - 1) - I_1^B c_{32} \sin \beta \right. \\
 & + \frac{m_A m_B}{m_A + 2m_B} \left[ b^2 \left( c_{23} \frac{dc_{21}}{d\alpha} - c_{21} \frac{dc_{23}}{d\alpha} \right) + b \left( a_3 \frac{dc_{21}}{d\alpha} + a_1 \frac{dc_{23}}{d\alpha} \right) \right] \left. \right\} \\
 & = 0
 \end{aligned} \tag{2.26}$$

(2.1, 2.25)

and, eliminating time and making the substitutions

$$\begin{aligned}
 M &= \frac{m_A m_B}{m_A + 2m_B} \\
 J &= I_1^B - I_2^B + Mb^2 \\
 E_1 &= \cos \theta \cos \varphi [J \sin^2 \beta - I_2^B (\cos \beta - 1)] \\
 E_2 &= \sin \beta [\sin \theta (J \cos \beta + I_2^B - Mba_3 \sin \varphi) - \cos \varphi Mba_1] \\
 E_3 &= \cos \theta \sin \beta [Mba_3 - \sin \varphi (J \cos \beta + I_2^B)] \\
 F_1 &= \frac{I^A}{2} + M(a_1^2 + a_3^2) + I_2^B + J[\cos^2 \beta (\sin^2 \theta - \cos^2 \varphi \cos^2 \theta) + \cos^2 \theta] \\
 &\quad - 2Mb \cos \beta (\sin \varphi a_3 + \cos \varphi \sin \theta a_1) \\
 F_2 &= J \sin^2 \beta (\sin^2 \theta - \sin^2 \varphi \cos^2 \theta) \\
 F_3 &= 2J \sin \theta \cos \theta \sin \varphi \sin^2 \beta \\
 F_4 &= 2 \sin \beta \cos \theta (J \cos \beta \sin \theta \cos \varphi - Mba_1) \\
 F_5 &= 2 \sin \beta [Mb(a_3 \cos \varphi - a_1 \sin \theta \sin \varphi) - J \cos^2 \theta \sin \varphi \cos \varphi \cos \beta]
 \end{aligned} \tag{2.27}$$

one finds that

$$\frac{d\xi}{d\alpha} = - \frac{E_1 + E_2 \sin \alpha + E_3 \cos \alpha}{F_1 + F_2 \cos^2 \alpha + F_3 \sin \alpha \cos \alpha + F_4 \sin \alpha + F_5 \cos \alpha} \quad (2.28)$$

Integration of this equation for  $0 \leq \alpha \leq 2\pi$  yields  $\Delta\xi$ , the pitch reorientation per cycle of the maneuver. An analytical solution is not readily available except in the special case when the cone axes coincide with the pitch axis. In this case,  $\theta = \varphi = 0$  and, after making the definitions

$$\left. \begin{aligned} \ell &= \sqrt{a_1^2 + a_3^2} \\ \delta &= \arccos \frac{a_1}{\ell} = \arcsin \frac{a_3}{\ell} \\ \eta &= \alpha - \delta \\ E &= J \sin^2 \beta + I_2^B (1 - \cos \beta) \\ F &= I^A/2 + M\ell^2 + I_2^B + J \sin^2 \beta \\ G &= Mb \ell \sin \beta \end{aligned} \right\} \quad (2.29)$$

one can bring Eq. (2.28) into the form

$$\frac{d\xi}{d\eta} = - \frac{E - G \sin \eta}{F - 2G \sin \eta} \quad (2.30)$$

and integration for  $\eta$  between the limits zero and  $2\pi$  now leads directly to  $\Delta\xi$  (in radians), i.e.,

$$\Delta\xi = \pi \left[ 1 + \frac{2E - F}{\sqrt{F^2 - 4G^2}} \right] \quad (2.31)$$

Eqs. (2.28) and (2.31) cannot be used until suitable values have been selected for the inertia properties. Moreover,  $I^A$ ,  $a_1$ , and  $a_3$

depend on the position in which the legs are held, as well as on the inertia properties of the limbs. Table 2.1 presents appropriate values for two arm configurations as well as values suitable for two leg positions. These values are based on the Hanavan model discussed in Sec. 1.3.

Table 2.1

Symbol	Arm	Arm with 5 lb. weight in hand	Units
$m_B$	0.289	0.445	slugs
$b$	0.899	1.291	feet
$I_1^B$	0.1331	0.261	slug-ft. <sup>2</sup>
$I_2^B$	0.0030	0.0030	slug-ft. <sup>2</sup>

Symbol	Legs Straight	Legs Tucked*	Units
$m_A$	4.45	4.45	slugs
$a_1$	0	0.309	feet
$a_3$	1.483	1.028	feet
$I^A$	8.13	3.87	slug-ft. <sup>2</sup>

\* In the "legs tucked" position, the longitudinal axes of the thighs are normal to the roll plane and the knees are bent through 150°.

### 2.3 Results

It is of interest to observe how the pitch obtained per cycle,  $\Delta\bar{\xi}$ , varies as a function of the cone semi-vertex angle,  $\beta$ . In Fig. 2.3,  $\Delta\bar{\xi}$  is plotted as a function of  $\beta$  for three cases:

- (1) the maneuver performed with the legs straight as in the position of "attention,"
- (2) the maneuver performed with the legs tucked close to the body,\* and
- (3) the maneuver performed with the legs tucked and a five-pound weight (0.156 slugs) held in each hand.

In all three cases, the cone axes are parallel to the pitch axis, Eq. (2.31) is used, and the requisite inertia properties are taken from Table 2.1.

It can be seen that pitch increases monotonically with  $\beta$ . Since the construction of the shoulder joints places an upper limit on  $\beta$  once a particular cone axis has been chosen, the maximum possible  $\beta$  being about 45 degrees when the cone axes are parallel to the pitch axis, a man with his legs straight can expect only about 12 degrees of pitch when performing a cycle of the maneuver in this fashion. Tucking the legs in markedly improves the effectiveness of the maneuver. For instance, with  $\beta$  equal to 45 degrees, the value of  $\Delta\bar{\xi}$  is doubled to 24 degrees by tucking.

The addition of five-pound weights to the hands more than doubles  $\Delta\bar{\xi}$ ; e.g., if the weights are used while the legs are tucked and  $\beta$

---

\*A detailed explanation of this "tucked" position is presented in the footnote accompanying Table 2.1.

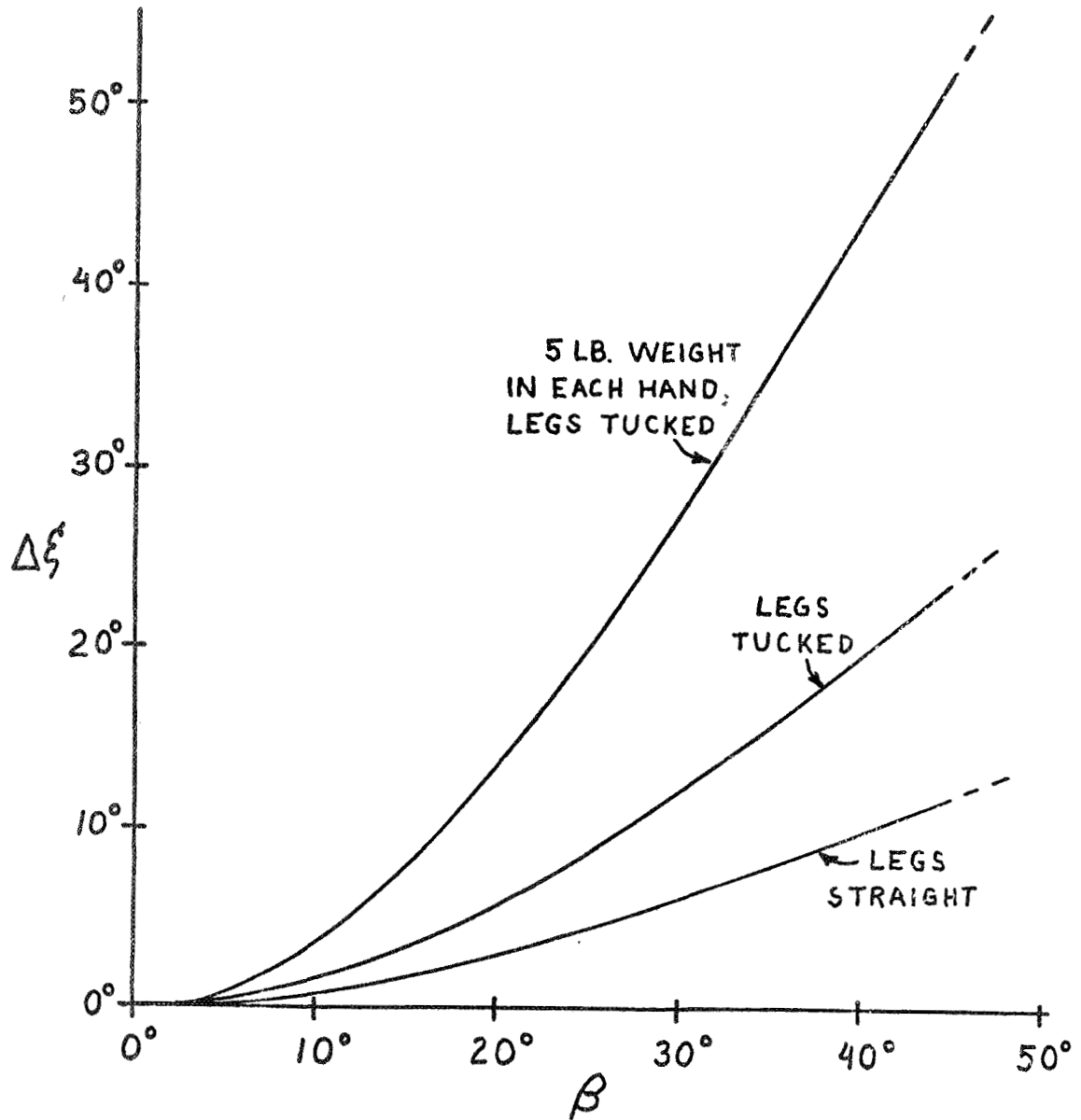


Fig. 2.3 Pitch reorientation as a function of  $\beta$  ( $\theta = \varphi = 0$ )

equals 45 degrees, 52 degrees of pitch per cycle can be obtained.

The location of the cone axes relative to the torso has a significant effect on the amount of pitch obtained per cycle. For instance, the pitch per cycle  $\Delta\bar{\xi}$  may be plotted as a function of  $\theta$  while  $\varphi$  and  $\beta$  are held constant (see Fig. 2.2 for  $\theta$ ,  $\varphi$ , and  $\beta$ ). In this case, the values of  $\theta$  to be considered are bounded from above by that value of  $\theta$  for which the hands collide in the pitch plane, this value being dependent on the constant  $\beta$  and on the arm length and shoulder width of the man. Such a graph of  $\Delta\bar{\xi}$  as a function of  $\theta$  is shown in Fig. 2.4 for the case where  $\varphi = 0$ , the legs are tucked, and for two values of  $\beta$ , i.e., 20 and 45 degrees.  $\Delta\bar{\xi}$  is seen to decrease with increasing  $\theta$  until, when  $\theta$  becomes equal to 90 degrees (i.e., when the cone axes become parallel to the roll axis), no pitch is obtained. This suggests that it is advantageous to maintain the cone axes nearly parallel to the roll plane.

When the cone axes are "lowered" in the roll plane,  $\Delta\bar{\xi}$  may increase or decrease. This can be seen in Fig. 2.5, which shows pitch per cycle as a function of  $\varphi$ , with  $\theta = 0$ , the legs tucked, and  $\beta$  again equal to 20 and 45 degrees. An upper bound on values of  $\varphi$  is provided by  $(90^\circ - \beta)$  since, for greater values of  $\varphi$ , the arms collide with the torso during the maneuver. The curves for both values of  $\beta$  possess a maximum when  $\varphi$  is about 15 degrees. The relative flatness of the curves between 0 and 30 degrees is important since physiological constraints at the shoulder joint are such that the semi-vertex angles  $\beta$  that can be used become larger if  $\varphi$  is increased from zero. For instance, while the upper bound on  $\beta$  is about 45 degrees with  $\varphi$  equal to zero, it is closer to 60 degrees when  $\varphi$  is 30 degrees. Consequently,

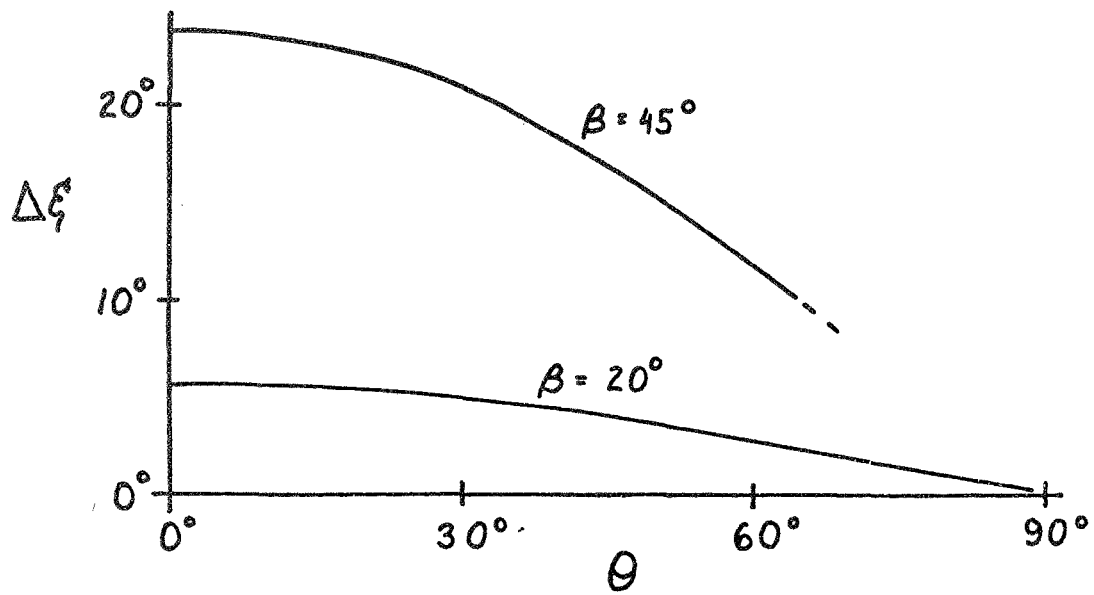


Fig. 2.4 Pitch reorientation as a function of  $\theta$  ( $\varphi = 0$ , legs tucked)

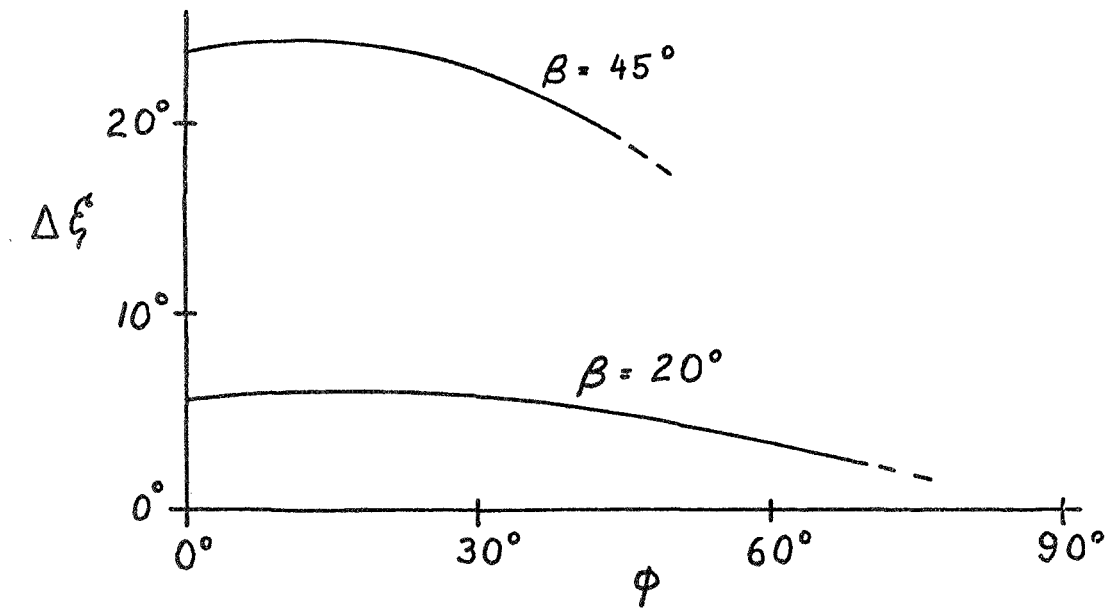


Fig. 2.5 Pitch reorientation as a function of  $\varphi$  ( $\theta = 0$ , legs tucked)

the greatest amount of pitch per cycle obtained without weights in the tucked position is about 33 degrees, and this is achieved by taking  $\beta$  equal to 60 degrees,  $\varphi$  equal to 30 degrees, and  $\theta$  nearly equal to zero.

The limb motions just described are reasonable ones for an unencumbered man in a "shirt sleeve" environment. For an astronaut in a pressure suit, the range of mobility may be sharply reduced, and the added mass of the suit may have a substantial effect on performance. In particular,  $\Delta \xi$  seems to be most sensitive to changes in the distance  $b$  from the shoulder to the mass center of the arm and in the distance  $a_3$  from the yaw plane to the mass center of the torso, head, and legs.

Finally, we consider the possibility that a small asymmetry in the performance of the maneuver could lead to "instability" in the motion, that is, to large amounts of undesired yaw and roll. It is indeed true that errors in performance may lead to unwanted yaw and roll motions but, since the equations of motion are continuous, the stability question becomes one of precision. Whenever a finite number of cycles of the maneuver are to be performed, the unwanted motions can be kept arbitrarily small by performing the maneuver with sufficient care.



### 3. Yaw Motion

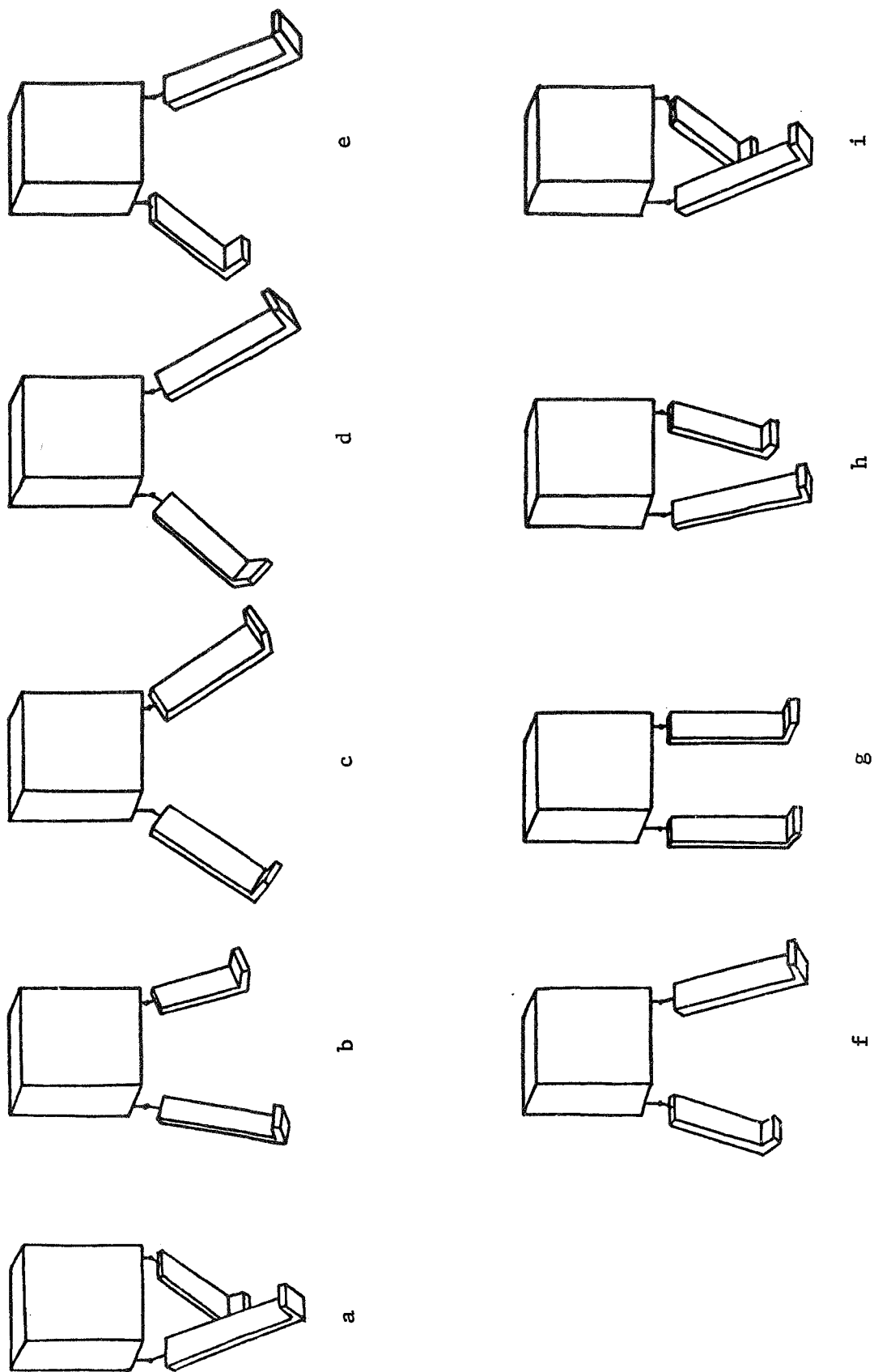
#### 3.1 Description

The limb movements to be discussed were suggested independently by James Jones of the NASA Ames Research Center and by Stepantsov [3]. The description and illustrations that follow, deal with a maneuver performed with the legs. However, the description applies also to a maneuver performed with the arms (but not with the arms and legs together).

In all cases, the limbs remain straight at the knees and elbows, and the pair of limbs that is not used must remain fixed relative to the torso in such a way that the yaw axis is a principal axis of inertia; e.g., if the legs are used, the arms may be kept at the sides, as in a position of "attention."

The maneuver is performed in two phases. For definiteness, suppose that a rotation of the torso to the left is desired. Then phase 1 begins with the right leg extended forward from the torso, and the left leg extended rearward, through equal angles  $\beta_0$  (see Fig. 3.1a): The right leg is swept to the right and then to the rear (relative to the torso) while the left leg is swept leftward and forward (see Figs. 3.1b to 3.1e); that is, the longitudinal axis of each leg moves on the surface of an imaginary, torso-fixed cone whose vertex is at the hip and whose axis is parallel to the yaw axis. In the course of this "coning" motion, no twisting of the leg occurs. Thus, the toes always point nearly forward. At the conclusion of phase 1, the right leg is extended rearward and the left leg forward relative to the torso (see Fig. 3.1e).

In phase 2, the legs travel simultaneously in planes parallel to the



Yaw maneuver

Fig. 3.1

pitch plane until each leg has returned to the position it occupied (with respect to the torso) at the beginning of phase 1 (see Figs. 3.1f through 3.1i). The entire cycle may then be repeated. During both phases, the two legs move at the same rate relative to the torso, so that their longitudinal axes maintain digonal symmetry about the yaw axis.

Consider the behavior of the torso during this maneuver. As phase 1 progresses, the torso rotates in an inertial reference frame to its left about the yaw axis, as desired, while the orientation of the yaw axis remains fixed. During phase 2, the torso turns back to the right, but this regression is not sufficient to nullify the rotation obtained in phase 1. A net rotation to the left is thus obtained from each complete cycle of the maneuver. The direction of rotation can be reversed by starting phase 1 with the left leg forward, rather than the right one.

An astronaut may be in a position of "attention" prior to starting the maneuver. The starting position for phase 1 may then be attained by moving the legs in planes parallel to the pitch plane. This will cause a regressive rotation of the torso about the yaw axis. After an integral number of cycles of the maneuver have been completed (a cycle consists of one performance of phase 1 and phase 2), the legs may be returned to a position of "attention," and the resulting yaw motion then nullifies the regressive rotation obtained while starting.

### 3.2 Analysis

For purposes of analysis, the human is modelled as a system  $S$  of three rigid bodies. One of these, designated  $A$ , represents the torso, head, and arms. The remaining two,  $B$  and  $B'$ , each represent a leg.  $B$  and  $B'$  are connected to  $A$  at points  $O$  and  $O'$ , which represent the hips (see Fig. 3.2).

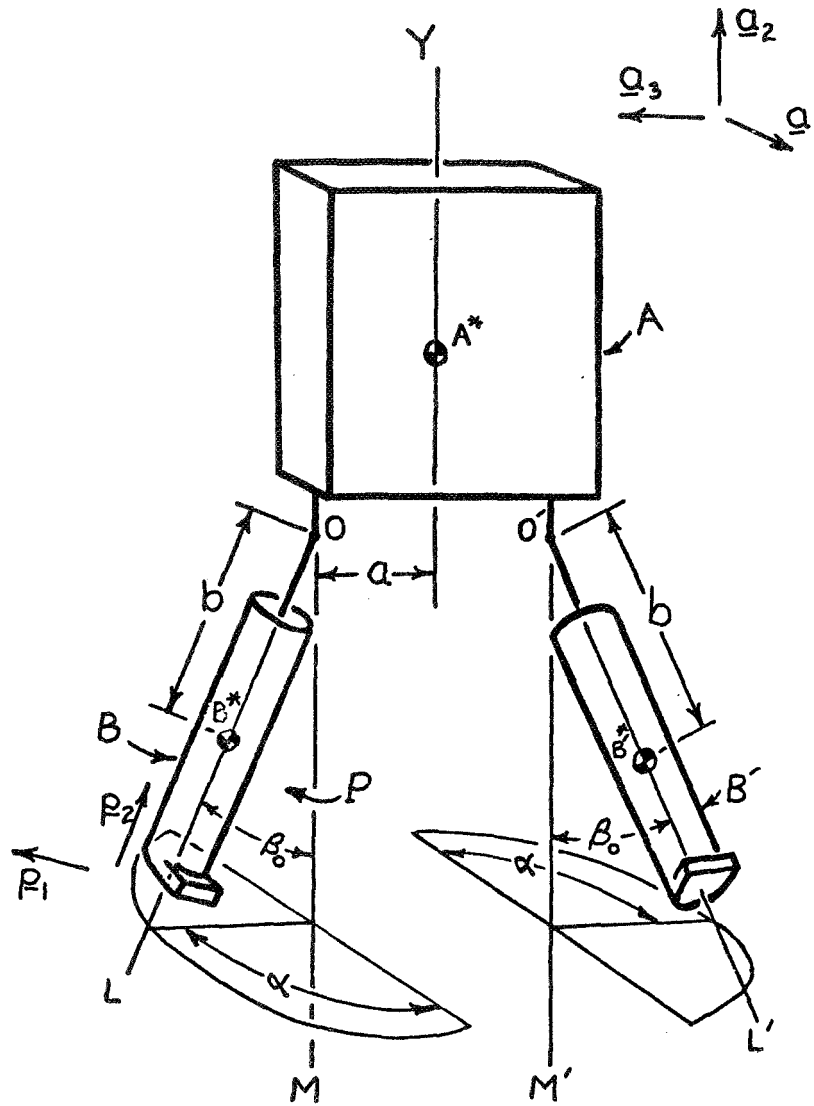


Fig. 3.2

Yaw motion model, phase 1

The yaw axis  $Y$  is presumed to coincide with a principal axis of  $A$  for its mass center  $A^*$ . The pitch axis is chosen so that points  $O$  and  $O'$  lie thereon, each at a distance  $a$  from  $Y$ . The analysis in the sequel involves two additional lines fixed in  $A$ , namely  $M$  and  $M'$ , which are parallel to  $Y$  and pass through  $O$  and  $O'$ , respectively. Body  $A$  has a mass  $m_A$  and a moment of inertia  $I^A$  about  $Y$ . Mutually perpendicular unit vectors  $\underline{a}_1, \underline{a}_2, \underline{a}_3$  are fixed in  $A$  parallel to the roll, yaw, and pitch axes, respectively. Since only yaw motions of  $A$  are to be considered, the attitude of  $A$  in an inertial reference frame  $F$  can be described by a single angle  $\xi$  between the pitch axis and a line fixed in  $F$  and normal to  $Y$ .

It is assumed that bodies  $B$  and  $B'$  each possess an axis of symmetry.<sup>†</sup> The axis of minimum moment of inertia of  $B$  for its mass center  $B^*$  is designated  $L$ , and the associated principal moment of inertia has the value  $I_2^B$ . The moment of inertia of  $B$  about any line perpendicular to  $L$  and passing through  $B^*$  is  $I_1^B$ , and the mass of  $B$  is  $m_B$ . Line  $L$  passes through  $O$ , and the distance from  $B^*$  to  $O$  is  $b$ . The inertia properties of leg  $B'$  are identical to those of  $B$ .

As different variables are used for the mathematical description of the two phases of the maneuver, two analyses are required. In both cases, confining our attention solely to yaw motions of  $A$ , we exploit a consequence of Lagrange's equations of motion, namely the fact that

---

<sup>†</sup>The maximum and intermediate principal moments of inertia of a leg for its mass center differ from each other by less than 1% in the Hanavan model (see Table 1.4).

$$\frac{\partial K}{\partial \dot{\xi}} = 0 \quad (3.1)$$

where  $\dot{\xi}$  is the time derivative of the angle  $\xi$ , and  $K$  is the kinetic energy associated with motion of  $S$  relative to the system mass center, which can be expressed as

$$K = K_{\omega}^A + K_{\omega}^B + K_{\omega}^{B'} + K_v^A + K_v^B + K_v^{B'} \quad (3.2)$$

The first three terms on the right-hand side of this equation represent the rotational kinetic energies of bodies  $A$ ,  $B$ , and  $B'$ , respectively, whereas the last three reflect the motions of the mass centers of  $A$ ,  $B$ , and  $B'$ . For example, if  $\omega_{F B}$ , the angular velocity of  $B$  in  $F$ , is expressed as

$$\omega_{F B} = \omega_1^B p_1 + \omega_2^B p_2 + \omega_3^B p_3 \quad (3.3)$$

where  $p_1$ ,  $p_2$ ,  $p_3$  are unit vectors, each parallel to a principal axis of  $B$  for  $B^*$ , and  $I_1^B$ ,  $I_2^B$ ,  $I_3^B$  are the corresponding principal moments of inertia, then

$$K_{\omega}^B = \frac{1}{2} [I_1^B (\omega_1^B)^2 + I_2^B (\omega_2^B)^2 + I_3^B (\omega_3^B)^2] \quad (3.4)$$

and, if  $v_B$  denotes the velocity of  $B^*$  relative to the mass center  $S^*$  of  $S$ , then

$$K_v^B = \frac{1}{2} m_B v_B^2 \quad (3.5)$$

Turning to the kinematical analysis for phase 1, we hypothesize that  $A$  has a simple angular velocity in  $F$ , i.e.,

$$\omega_{F A} = \dot{\xi} a_2 \quad (3.6)$$

Since  $\underline{Y}$  is a principal axis of  $A$ , and  $\underline{F}_W^A$  is parallel to  $\underline{Y}$ ,

$$K_W^A = \frac{1}{2} I^A \dot{\xi}^2 \quad (3.7)$$

(3.4,3.6)

The motions of  $B$  and  $B'$  are described in terms of the "coning" motion outlined in Sec. 3.1. We regard line  $M$  as the axis of a cone on whose surface  $L$  moves. The angle  $\beta_0$  between  $L$  and  $M$  remains fixed, and if  $P$  is the plane determined by  $L$  and  $M$ , and mutually perpendicular unit vectors  $\underline{p}_1, \underline{p}_2, \underline{p}_3$  are fixed in  $P$ , with  $\underline{p}_2$  parallel to  $L$  and  $\underline{p}_3$  normal to  $P$ , then  $\underline{p}_1, \underline{p}_2, \underline{p}_3$  are related to  $\underline{a}_1, \underline{a}_2, \underline{a}_3$  as indicated in Table 3.1, where  $\alpha$  is the angle between  $P$  and the pitch plane. The angular velocity of  $P$  in  $A$  is given by

$$\underline{\omega}^{AP} = -\dot{\alpha} \underline{a}_2 \quad (3.8)$$

Table 3.1

	$\underline{a}_1$	$\underline{a}_2$	$\underline{a}_3$
$\underline{p}_1$	$\cos \beta_0 \cos \alpha$	$\sin \beta_0$	$\cos \beta_0 \sin \alpha$
$\underline{p}_2$	$-\sin \beta_0 \cos \alpha$	$\cos \beta_0$	$-\sin \beta_0 \sin \alpha$
$\underline{p}_3$	$-\sin \alpha$	0	$\cos \alpha$

Leg B must rotate in P about L in order to avoid twisting in a physically impossible manner, as mentioned in Sec. 3.1. A suitable rotation of B in P results if the angular velocity of B in P is taken to be

$$\underline{\omega}^{P B} = \dot{\alpha} p_2 \quad (3.9)$$

The angular velocity of B in F is then given by

$$\underline{\omega}^{F B} = \underline{\omega}^{P B} + \underline{\omega}^{A P} + \underline{\omega}^{F A} = \dot{\alpha} p_2 - \dot{\alpha} a_2 + \dot{\xi} a_2 \quad (3.10)$$

(3.9, 3.8, 3.6)

or, in view of Table 3.1, by

$$\underline{\omega}^{F B} = \omega_1^B p_1 + \omega_2^B p_2 \quad (3.11)$$

(3.10)

where

$$\omega_1^B = (\dot{\xi} - \dot{\alpha}) \sin \beta_o \quad (3.12)$$

and

$$\omega_2^B = \dot{\alpha} + (\dot{\xi} - \dot{\alpha}) \cos \beta_o \quad (3.13)$$

Consequently ,

$$\begin{aligned} K_{\omega}^B &= \frac{1}{2} [I_1^B (\omega_1^B)^2 + I_2^B (\omega_2^B)^2] \\ &\quad (3.4) \\ &= \frac{1}{2} \left\{ \dot{\xi}^2 [I_1^B \sin^2 \beta_o + I_2^B \cos^2 \beta_o] \right. \\ &\quad (3.12, 3.13) \\ &\quad - 2\dot{\xi}\dot{\alpha} [I_1^B \sin^2 \beta_o + I_2^B \cos^2 \beta_o - I_2^B \cos \beta_o] \\ &\quad \left. + \dot{\alpha}^2 [I_1^B \sin^2 \beta_o + I_2^B \cos^2 \beta_o + I_2^B (1 - 2 \cos \beta_o)] \right\} \quad (3.14) \end{aligned}$$



In the same manner, an identical expression is obtained for  $K_{(u)}^{B'}$ .

Evaluation of  $K_V^A$ ,  $K_V^B$ , and  $K_V^{B'}$  necessitates determination of  $\underline{v}_A$ ,  $\underline{v}_B$ , and  $\underline{v}_{B'}$ , the velocities relative to  $S^*$  of the mass centers of A, B, and B'. In phase 1, the position of  $S^*$  remains fixed in A, so that  $\underline{v}_A$  vanishes.  $\underline{v}_B$  can be expressed as

$$\underline{v}_B = \underline{v}^{B^*/0} + \underline{v}^{0/S^*} \quad (3.15)$$

where

$$\underline{v}^{B^*/0} = \underline{F}_u^B \times (-b \underline{p}_2) \quad (3.16)$$

and, since  $S^*$  is fixed in body A and lies on line Y,

$$\underline{v}^{0/S^*} = \underline{F}_u^A \times (a \underline{a}_3) \quad (3.17)$$

Referring to Table 3.1, one can thus obtain (see Eqs. (3.15), (3.16), (3.10), (3.17), (3.6))

$$\begin{aligned} \underline{v}_B = & [\dot{\xi}a + (\dot{\xi} - \dot{\alpha})b \sin \beta_0 \sin \alpha] \underline{a}_1 \\ & - [(\dot{\xi} - \dot{\alpha})b \sin \beta_0 \cos \alpha] \underline{a}_3 \end{aligned} \quad (3.18)$$

and it follows that

$$\begin{aligned} K_V^B = & \frac{1}{2} m_B \left\{ \dot{\xi}^2 [a^2 + b^2 \sin^2 \beta_0 + 2ab \sin \beta_0 \sin \alpha] \right. \\ & \left. - 2 \dot{\xi} \dot{\alpha} [b^2 \sin^2 \beta_0 + ab \sin \beta_0 \sin \alpha] + \dot{\alpha}^2 [b^2 \sin^2 \beta_0] \right\} \end{aligned} \quad (3.19)$$

The expression for  $K_V^{B'}$  is identical to that for  $K_V^B$ . Hence

$$\begin{aligned}
 K &= \ddot{\xi}^2 \left[ \frac{I^A}{2} + I_2^B + m_B a^2 + (I_1^B - I_2^B + m_B b^2) \sin^2 \beta_o \right. \\
 &\quad \left. + 2m_B ab \sin \beta_o \sin \alpha \right] - 2 \ddot{\xi} \dot{\alpha} \left[ I_2^B (1 - \cos \beta_o) \right. \\
 &\quad \left. + (I_1^B - I_2^B + m_B b^2) \sin^2 \beta_o + m_B ab \sin \beta_o \sin \alpha \right] \\
 &\quad + \dot{\alpha}^2 \left[ 2I_2^B (1 - \cos \beta_o) + (I_1^B - I_2^B + m_B b^2) \sin^2 \beta_o \right] \quad (3.20)
 \end{aligned}$$

and the dynamical equation of motion for phase 1 is

$$\begin{aligned}
 &\ddot{\xi} \left[ \frac{I^A}{2} + I_2^B + m_B a^2 + (I_1^B - I_2^B + m_B b^2) \sin^2 \beta_o + 2m_B ab \sin \beta_o \sin \alpha \right] \\
 &\quad - \dot{\alpha} \left[ I_2^B (1 - \cos \beta_o) + (I_1^B - I_2^B + m_B b^2) \sin^2 \beta_o + m_B ab \sin \beta_o \sin \alpha \right] \\
 &= 0 \quad (3.21)
 \end{aligned}$$

(3.1, 3.20)

Dependence on time can be eliminated and, making the substitutions

$$\left. \begin{aligned}
 p_1 &= \frac{\left( \frac{I^A}{2} + I_2^B + m_B a^2 \right) + (I_1^B - I_2^B + m_B b^2) \sin^2 \beta_o}{2m_B ab \sin \beta_o} \\
 p_2 &= \frac{I_2^B (1 - \cos \beta_o) + (I_1^B - I_2^B + m_B b^2) \sin^2 \beta_o}{2m_B ab \sin \beta_o}
 \end{aligned} \right\} \quad (3.22)$$

one can relate the yaw angle  $\xi$  to the cone "sweep" angle  $\alpha$  by means of the differential equation

$$\frac{d\xi}{d\alpha} = \frac{p_2 + \frac{1}{2} \sin \alpha}{p_1 + \sin \alpha} \quad (3.23)$$

(3.21, 3.22)

This equation can be integrated in closed form for  $0 \leq \alpha \leq \pi$  to yield an expression for  $\Delta \xi_1$ , the change in yaw during phase 1 (in radians), as a function of the inertia properties and the semi-angle of limb spread:

$$\Delta \xi_1 = \frac{\pi}{2} + \frac{2p_2 - p_1}{\sqrt{p_1^2 - 1}} \left\{ \frac{\pi}{2} - \tan^{-1} \left( \frac{1}{\sqrt{p_1^2 - 1}} \right) \right\} \quad (3.24)$$

(3.23)

In phase 2, the legs move parallel to the pitch plane. A convenient variable is  $\beta$  (see Fig. 3.3), the angle between L and M (or L' and M').  $\beta$  ranges from  $-\beta_0$  to  $\beta_0$ .

In the kinematical analysis of phase 2,  $K_{\omega}^A$  is again furnished by Eq. (3.7). The angular velocity of B in F may be written as

$$\underline{\omega}^B = \underline{\omega}^A + \underline{\omega}^F \quad (3.25)$$

where  $\underline{\omega}^A$  is given by Eq. (3.6) while

$$\underline{\omega}^B = \dot{\beta} \underline{a}_3 \quad (3.26)$$

If unit vectors  $\underline{b}_1, \underline{b}_2, \underline{b}_3$  are fixed in body B, with  $\underline{b}_2$  parallel to L and  $\underline{b}_3$  parallel to the pitch axis, so that they are related to  $\underline{a}_1, \underline{a}_2, \underline{a}_3$  as shown in Table 3.2, then

Table 3.2

	$\underline{a}_1$	$\underline{a}_2$	$\underline{a}_3$
$\underline{b}_1$	$\cos \beta$	$\sin \beta$	0
$\underline{b}_2$	$-\sin \beta$	$\cos \beta$	0
$\underline{b}_3$	0	0	1

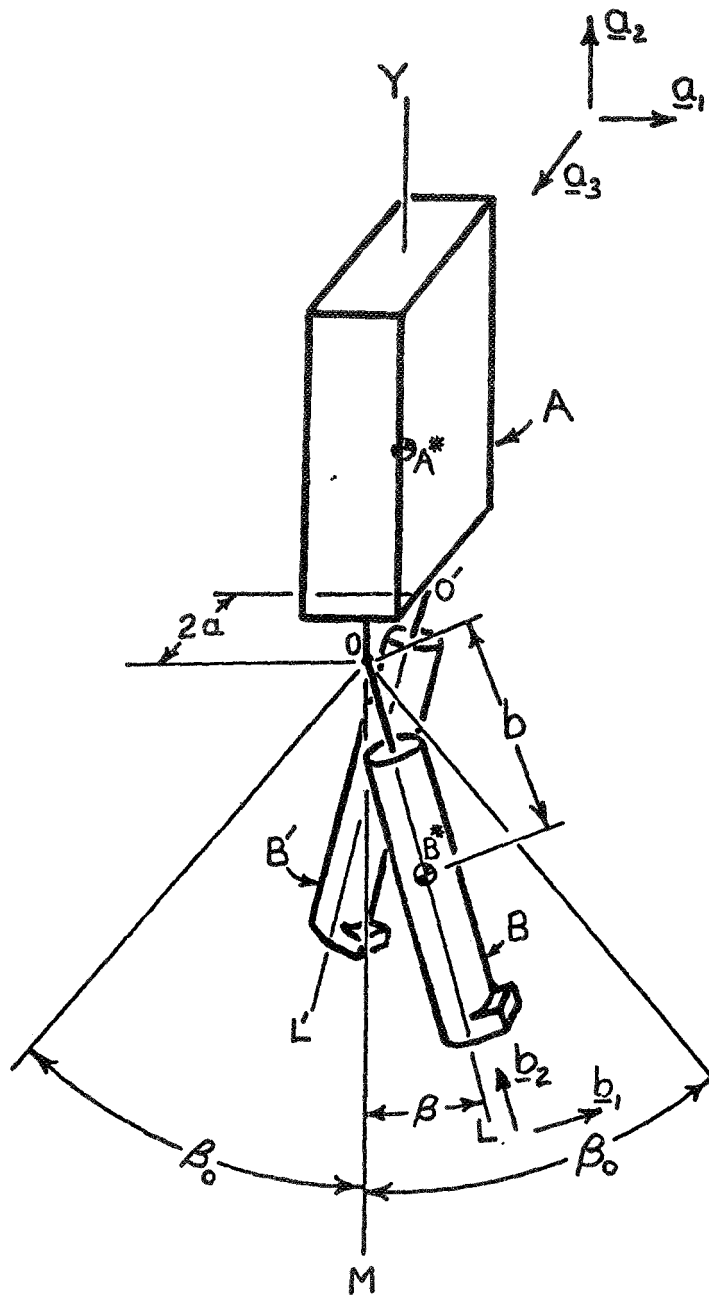


Fig. 3.3

Yaw motion model, phase 2

$$\begin{aligned} \underline{\dot{F}}^B_B &= \dot{\xi} \sin \beta \underline{b}_1 + \dot{\xi} \cos \beta \underline{b}_2 + \dot{\beta} \underline{b}_3 \\ (3.25, 3.6, 3.26) \end{aligned} \quad (3.27)$$

and, since  $\underline{b}_1, \underline{b}_2, \underline{b}_3$  are parallel to principal axes of  $B$  for  $B^*$ ,

$$\begin{aligned} K^B_w &= \frac{1}{2} \left[ \dot{\xi}^2 (I_1^B \sin^2 \beta + I_2^B \cos^2 \beta) + I_1^B \dot{\beta}^2 \right] \\ (3.4, 3.27) \end{aligned} \quad (3.28)$$

An identical expression is obtained for  $K^{B'}_w$ .

In this phase,  $K^A_v$  does not vanish. It is, however, independent of  $\dot{\xi}$  and therefore does not contribute to the equation of motion.  $\underline{v}_B$  is again given by Eq. (3.15) and  $\underline{v}^{B^*}/0$  by Eq. (3.16), but Eq. (3.17) must be replaced with a relationship that reflects the motion of  $S^*$  in  $A$ . Thus

$$\underline{v}_B = (\dot{\xi}a + b\dot{\beta} \cos \beta) \underline{a}_1 + \frac{m_A}{m_A + 2m_B} b \sin \beta \dot{\beta} \underline{a}_2 - \dot{\xi} b \sin \beta \underline{a}_3 \quad (3.29)$$

Consequently,

$$\begin{aligned} K^B_v &= \frac{1}{2} m_B \left\{ \dot{\xi}^2 [a^2 + b^2 \sin^2 \beta] + 2\dot{\xi}\dot{\beta} [ab \cos \beta] \right. \\ (3.5, 3.29) \quad &\left. + \dot{\beta}^2 \left[ b^2 \cos^2 \beta + \left( \frac{m_A}{m_A + 2m_B} \right)^2 b^2 \sin^2 \beta \right] \right\} \end{aligned} \quad (3.30)$$

and the expression for  $K^{B'}_v$  is again identical. Hence

$$\begin{aligned} K &= \left\{ \dot{\xi}^2 \left[ \frac{I^A}{2} + m_B a^2 + I_2^B + (I_1^B - I_2^B + m_B b^2) \sin^2 \beta \right] \right. \\ (3.2, 3.7, 3.28, 3.30) \quad &\left. + 2\dot{\xi}\dot{\beta} [m_B ab \cos \beta] \right. \\ &\left. + \dot{\beta}^2 \left[ I_1^B + m_B b^2 \cos^2 \beta + \left( \frac{m_A m_B}{m_A + 2m_B} \right) b^2 \sin^2 \beta \right] \right\} \end{aligned} \quad (3.31)$$

The appropriate dynamical equation is again Eq. (3.1), and, when time is eliminated and two non-dimensional constants  $q_1$  and  $q_2$  are defined as

$$\left. \begin{aligned} q_1 &= \frac{m_B ab}{I_1^B - I_2^B + m_B b^2} \\ q_2 &= \frac{\frac{I^A}{2} + I_2^B + m_B a^2}{I_1^B - I_2^B + m_B b^2} \end{aligned} \right\} \quad (3.32)$$

the relation between yaw and limb position is provided by the differential equation

$$\frac{d\xi}{d\beta} = - q_1 \frac{\cos \beta}{q_2 + \sin^2 \beta} \quad (3.33)$$

(3.1, 3.31, 3.32)

The change in yaw during phase 2,  $\Delta\xi_2$ , is obtained by integrating Eq. (3.33) for  $-\beta_0 \leq \beta \leq \beta_0$ :

$$\Delta\xi_2 = \frac{-2q_1}{\sqrt{q_2}} \tan^{-1} \left( \frac{\sin \beta_0}{\sqrt{q_2}} \right) \quad (3.34)$$

(3.33)

The total yaw rotation per cycle of the maneuver,  $\Delta\xi$ , is the sum of  $\Delta\xi_1$  and  $\Delta\xi_2$ . With  $p_1$ ,  $p_2$ ,  $q_1$ ,  $q_2$  as defined in Eqs. (3.22) and (3.32), the yaw per cycle (in radians) is thus given by

$$\Delta\xi = \frac{\pi}{2} + \frac{2p_2 - p_1}{\sqrt{p_1^2 - 1}} \left[ \frac{\pi}{2} - \tan^{-1} \left( \frac{1}{\sqrt{p_1^2 - 1}} \right) \right] - \frac{2q_1}{\sqrt{q_2}} \tan^{-1} \left( \frac{\sin \beta_0}{\sqrt{q_2}} \right) \quad (3.35)$$

(3.24, 3.34)

In Sec. 3.1, it was mentioned that the maneuver could be performed either with the arms or with the legs. Different values for the inertia properties must be used, depending upon which limbs are employed. Table 3.3

Table 3.3

Symbol	Leg Maneuver (Arms at sides)	Arm Maneuver (Legs parallel to yaw axis)	Units
$I^A$	0.519	0.413	slug-ft. <sup>2</sup>
a	0.253	0.664	feet
$m_B$	0.836	0.289	slugs
b	1.352	0.899	feet
$I_1^B$	0.565	0.1331	slug-ft. <sup>2</sup>
$I_2^B$	0.0243	0.0030	slug-ft. <sup>2</sup>

shows representative values for the two cases. These values are based on the Hanavan model for the U.S. Air Force 50th percentile man (see Sec. 1.3).

### 3.3 Results

It is of interest to know how the yaw obtained per cycle,  $\Delta\bar{\xi}$ , varies as a function of the semi-angle of leg spread,  $\beta_0$ . In Fig. 3.4,  $\Delta\bar{\xi}$  is plotted as a function of  $\beta_0$  for three cases:

- (1) the maneuver performed with the legs while the arms are held at the sides,
- (2) the maneuver performed with the arms while the legs are parallel to the yaw axis, and
- (3) the maneuver performed with the arms when a five-pound weight (0.156 slg.) is held in each hand.

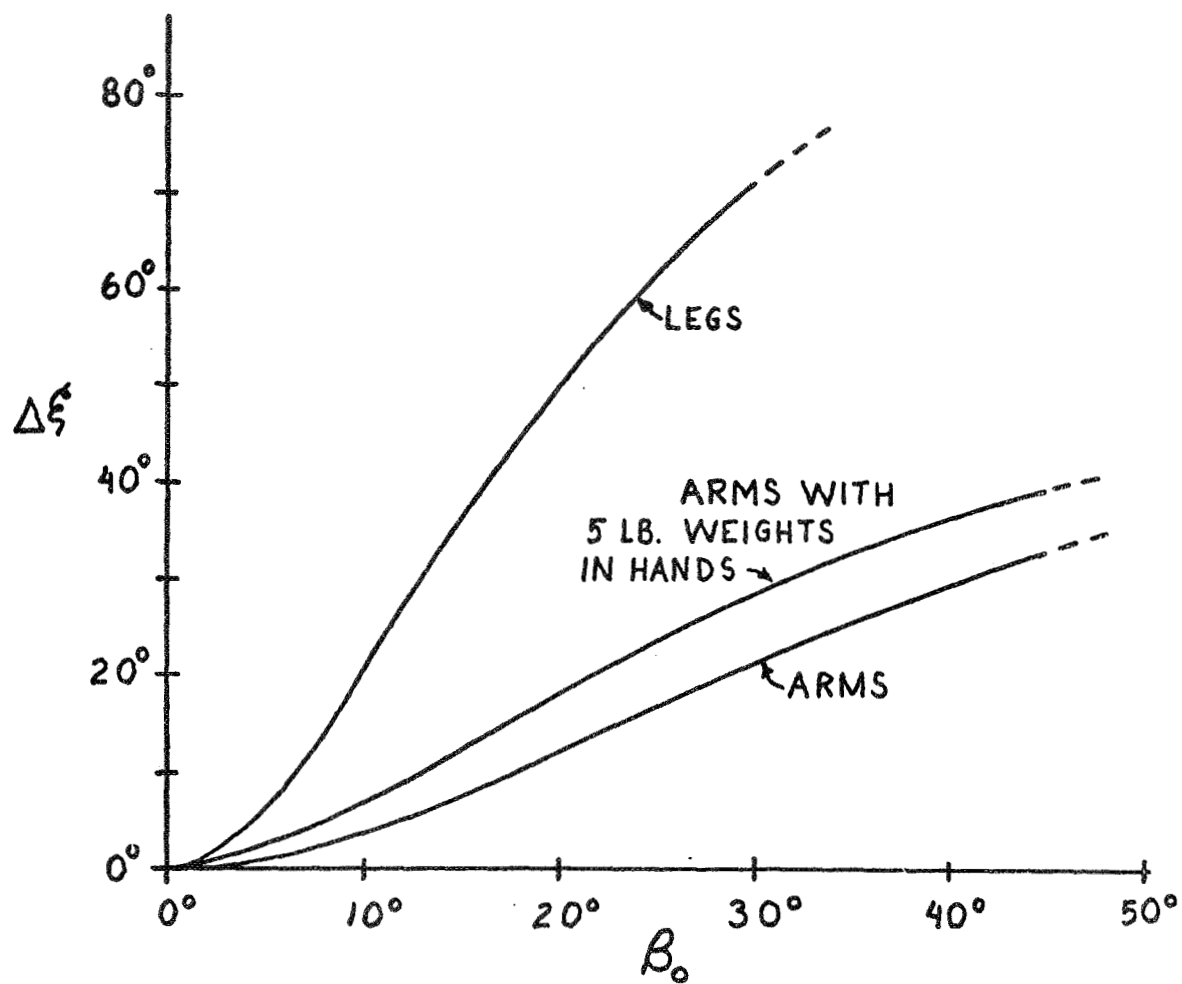


Fig. 3.4

Yaw reorientation as a function of  $\beta_0$



It can be seen that yaw increases monotonically with  $\beta_0$ . Of course, the construction of the human hip and shoulder joints places an upper bound on  $\beta_0$ . For the legs, a maximum of 30 degrees is reasonable, whereas for the arms  $\beta_0$  may be as large as 45 degrees. Consequently, realistic values for the maximum yaw obtainable per cycle are 71 degrees with the legs and 33 degrees with the arms. Holding a five-pound weight in each hand improves the performance, but not spectacularly, a reasonable upper limit for the yaw per cycle obtainable with five-pound weights being 40 degrees.

Use of the legs can be seen to be more effective than that of the arms. However, occasions may arise in which the arms are the more convenient limbs. For example, constraints imposed by an astronaut's pressure suit might be such as to render the arms more mobile than the legs.

It may occur to the reader that it is possible to perform a maneuver in which the arms and the legs are used simultaneously. However, this case is not covered by the analysis of Sec. 3.2, and the reader should be aware that the results plotted in Fig. 3.4 are not additive. In fact, rough calculations indicate that such a maneuver would be less effective than the one involving the legs alone.

Finally, the astronaut who wishes to use both his arms and legs can, in fact, enhance the effectiveness of the present two-phase yaw maneuver. Assuming that the maneuver is to be performed with the legs and that the arms are initially at the sides, a four-step sequence can be performed as follows:

- (1) Perform phase 1 with the legs, as described in Sec. 3.1.
- (2) Raise the arms in the roll plane while maintaining their

symmetry about the pitch plane until the arms lie parallel to the pitch axis.

- (3) Perform phase 2 with the legs, as described in Sec. 3.1.
- (4) Lower the arms to the sides while keeping them in the roll plane and maintaining symmetry about the pitch plane. At the conclusion of this step, all limbs have returned to their initial positions relative to the torso so that the sequence may be repeated.

Steps (2) and (4) produce no change in the orientation of the torso. They do, however, alter  $I^A$ , the moment of inertia of the torso, head, and arms about the yaw axis. Thus,  $I^A$  has a greater value during the performance of phase 2 (step (3)) than during the performance of phase 1 (step (1)). Consequently,  $|\Delta \xi_2|$ , the amount of regression during phase 2, is reduced. This four-step sequence can also be employed when the arms, rather than the legs, are used in steps (1) and (3). In this case, the legs are spread in step (2) and retracted in step (4), the spread angle of each leg being limited to about 30 degrees by constraints at the hip.

To analyze this four-step sequence,  $\Delta \xi$ , as given by Eq. (3.35), must be computed using a different value for  $I^A$  in the determination of  $q_2$  (see (3.32)) than is used in the determination of  $p_1$  (see (3.22)). Table 3.4 indicates the appropriate values of  $I^A$  for  $p_1$  and  $q_2$  when the maneuver is performed with the legs or with the arms.

The effectiveness of this four-step sequence is illustrated by Fig. 3.5, in which  $\Delta \xi$ , the yaw obtained per cycle, is plotted as a function of the semi-angle of limb spread  $\beta_0$  for the case where steps (1) and

Table 3.4

	Value of $I^A$ in $p_1$	Value of $I^A$ in $q_2$	Units
Maneuver performed with legs in steps (1) and (3)	0.519 (arms at sides)	1.938 (arms spread 90°)	slug-ft. <sup>2</sup>
Maneuver performed with arms in steps (1) and (3)	0.413 (legs straight)	2.02 (legs spread 30°)	slug-ft. <sup>2</sup>

(3) are performed with the legs and for the case where steps (1) and (3) are performed with the arms. Again, yaw increases monotonically with  $\beta_0$ , but now the effectiveness of the maneuver is found to be significantly enhanced. For example, the four-step sequence using the legs produces up to 93 degrees of yaw per cycle (i.e., when  $\beta_0 = 30^\circ$ ) as compared to 71 degrees for the two-phase maneuver performed with the legs (see Fig. 3.4). Likewise, when the arms are used in steps (1) and (3), the four-step sequence produces up to 58 degrees of yaw (i.e., when  $\beta_0 = 45^\circ$ ), an increase of 25 degrees over that obtained from the two-phase arm maneuver. Thus, at first glance, the four-step sequence appears more attractive. However, the sequence probably takes twice as long to perform and does not double the effectiveness of the two-phase maneuver. Consequently, it may be more desirable to employ the two-phase maneuver with the understanding that more cycles must be performed to obtain a desired yaw reorientation.

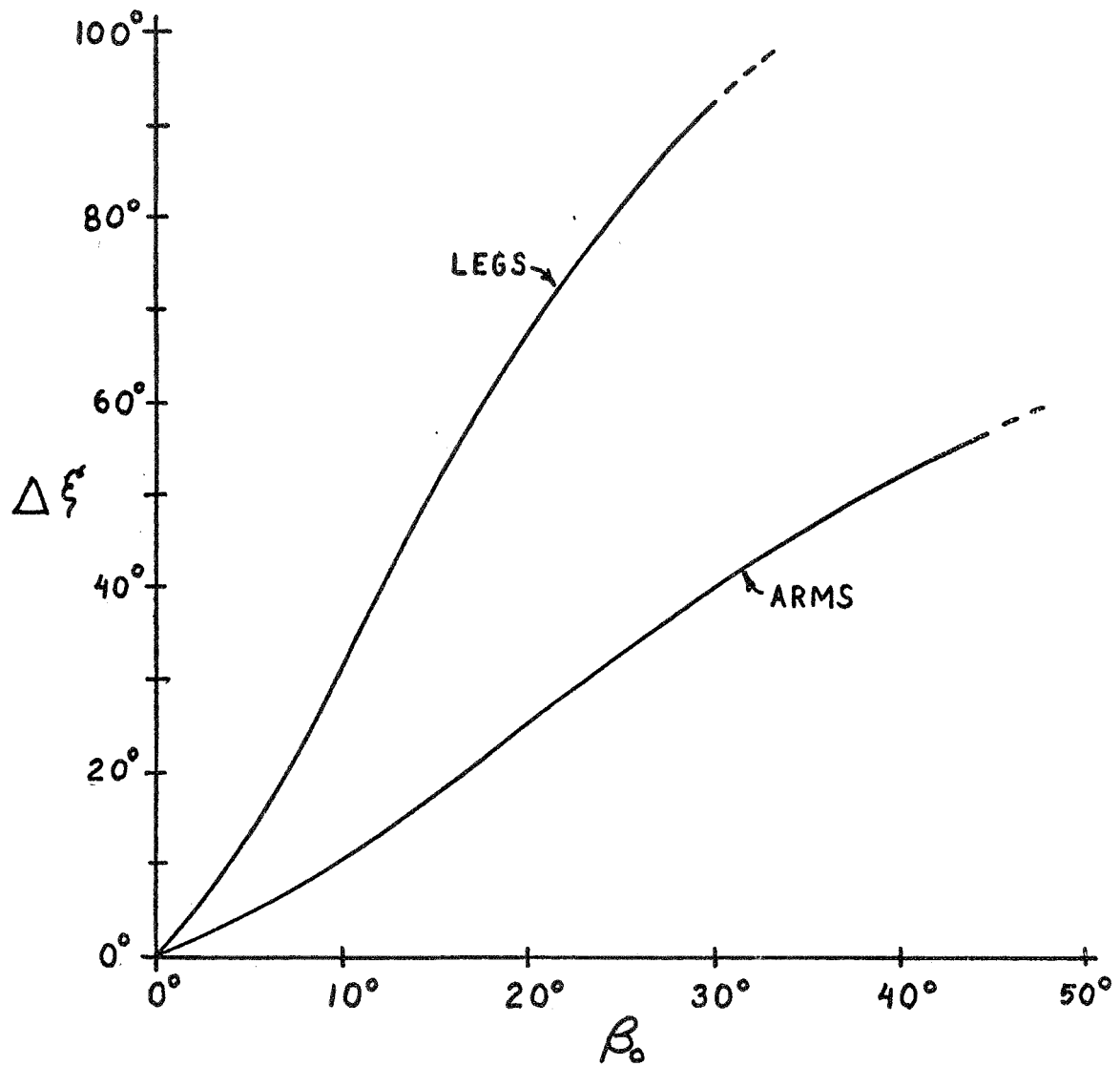


Fig. 3.5 Yaw reorientation as a function of  $\beta_0$  for the four-step yaw maneuver

#### 4. Roll Motion

##### 4.1 Description

An analysis and computer program suitable for the study of several arm maneuvers producing roll reorientation have been presented by Riddle [11] and are described in Sec. 4.2. The program is employed to examine a particular maneuver possessing many similarities to the pitch motion of Sec. 2.1.

The roll maneuver under consideration consists of rotary motions of the straightened arms on the surfaces of imaginary torso-fixed cones with equal semi-vertex angles, both arms describing their cones at the same rate. The legs are held fixed relative to the torso and are symmetrically located with respect to the pitch plane. The cone axes, however, are not located symmetrically and must, in fact, possess orientations which are dependent both on the cone semi-vertex angles employed and on the inertia properties of the subject. Furthermore, both arms must move around their cones in the same sense; i.e., both hands appear to the subject to be moving, say, clockwise. A reversal in the sense of motion of the arms produces a reversal in the direction of the roll reorientation.

In general, the motion of the torso and legs during this maneuver is not simple; that is, pitching, yawing, and rolling motions occur simultaneously. However, when the cone axes are located with care, the torso's orientation at the end of a cycle may be equivalent to one obtained by a simple rotation about the roll axis. We refer to such an attitude change as a roll reorientation.

If the subject is in a position of "attention" prior to performing the maneuver, he may find it difficult to move his arms to the starting position for the maneuver without introducing undesired amounts of pitch, roll, and yaw. For this reason the roll maneuver may be less desirable than those in Secs. 2.1 and 3.1. (Of course, any desired change in attitude, including a roll reorientation, can be obtained by performing a sequence of pitch and yaw maneuvers.)

#### 4.2 Riddle's Model

The analysis and computer program in [11] were derived to compute the reorientation of the torso obtained from one cycle of the "coning" maneuver of the arms when the axis and semi-vertex angle of each of the cones is chosen arbitrarily. To this end, the human is modelled as a system of three rigid bodies identical to those used for the pitch motion and, unless noted otherwise, symbols appearing in this section have the same definitions as in Sec. 2.2.

Three major differences distinguish the Riddle model from that of Sec. 2.2. First, the inertia properties of the main body must be given more generality. Since the main body  $A$ , representing the head, torso, and legs, is assumed to be symmetric about the pitch plane, a line  $p_2$  passing through the mass center  $A^*$  parallel to the pitch axis is a principal axis of  $A$ . The remaining two centroidal principal axes,  $p_1$  and  $p_3$ , lie in the pitch plane with orientations such that a right-hand rotation in  $A$  of  $p_1$  about  $p_2$  through an angle  $\gamma$  would cause  $p_1$  to lie parallel to the roll axis (see Fig. 4.1). The centroidal principal moments of inertia of  $A$  about  $p_1$ ,  $p_2$ , and  $p_3$  are  $I_1^A$ ,  $I_2^A$  (equivalent to  $I^A$  of Sec. 2.2), and  $I_3^A$ , respectively.



Second, the representation of the attitude of A in inertial space must be suitable for three-dimensional attitude motions. Changes in orientation will be described by three Euler angles measuring rotations performed successively about the yaw, pitch, and roll axes. These angles will be called the yaw angle, pitch angle, and roll angle and will be regarded as positive when they correspond to positive rotations about the  $\underline{a}_3$ ,  $\underline{a}_2$ , and  $\underline{a}_1$  directions, respectively. The outputs from the computer program in [11] are the values of these Euler angles at the completion of one cycle of the maneuver, assuming them to be zero initially.

Third, the location of the cone axes and the motion of the arms about them will be described employing, in part, the notation in [11]. The left and right cone axes,  $M_1$  and  $M_2$ , intersect planes  $S_1$  and  $S_2$  passing through the shoulders parallel to the pitch plane with angles  $\beta_1$  and  $\beta_2$ , respectively, the angles being positive when the cone axes are to the left (see Fig. 4.1). The projections of the left and right cone axes on  $S_1$  and  $S_2$  intersect the yaw plane with angles  $\alpha_1$  and  $\alpha_2$ , respectively. These angles are regarded as positive when the cone axes are "below" the yaw plane. Thus the cone axes are parallel to the roll axis when  $\alpha_1$ ,  $\alpha_2$ ,  $\beta_1$ , and  $\beta_2$  are zero. The cone "sweep" angles,  $\phi_1$  and  $\phi_2$ , remain equal, increasing from 0 to  $2\pi$  during one cycle of the maneuver; and they are chosen so that, at the beginning and end of a cycle, the symmetry axes of the arms lie in planes normal to  $S_1$  and  $S_2$  and containing the respective cone axes. The cone semi-vertex angles,  $\theta_1$  and  $\theta_2$ , are defined as positive when, at the beginning and end of a cycle, the symmetry axes of the arms lie to the left of their respective cone axes.



The program user can specify  $\alpha_1$  ,  $\alpha_2$  ,  $\beta_1$  ,  $\beta_2$  ,  $\theta_1$  , and  $\theta_2$  arbitrarily and can thus consider a vast variety of arm motions producing general reorientations of the torso in inertial space. For instance, the single example cited in [11] (see pp. 47 and 61) produces primarily yaw reorientation, with lesser amounts of pitch and roll. Pure yawing motions can be obtained by requiring that the cone axes lie in the roll plane and the arms move while maintaining digonal symmetry about the yaw axis (e.g.,  $\alpha_1 = \alpha_2 = 90^\circ$  ,  $\beta_1 = -\beta_2 = \theta_1 = -\theta_2 = \text{constant}$ ) . This case is very similar to the yaw motion described in Sec. 3.1 and produces reorientations of the same order of magnitude. Pitch motions identical to those discussed in Sec. 2.1 can be obtained by requiring the cone axes to be located symmetrically about the pitch plane and by modifying the program , so that the arms sweep out their cones in opposite senses (e.g.,  $\alpha_1 = \alpha_2 = \text{constant}$  ,  $\beta_1 = -\beta_2 = \text{constant}$  ,  $\theta_1 = -\theta_2 = \text{constant}$ ,  $\phi_1 = -\phi_2$  , and  $\dot{\phi}_1 = -\dot{\phi}_2$  ) . Motions involving only one arm can be analyzed by setting the cone semi-vertex angle of the other arm equal to zero.

In addition to specifying the angles which describe the arm motion, the user of Riddle's program must also provide values for the inertia properties of the arms and main body. The first half of Table 2.1 contains values for the requisite properties of the arms, and the second half contains some of the values for the properties of body A . A complete list of values of the inertia properties of A for two leg positions is contained in Table 4.1.

#### 4.3 Results

One might expect efficient roll reorientations to occur when the "coning" motions are performed with the cone axes parallel to the

Table 4.1

Symbol	Legs Straight	Legs * Tucked	Units
$m_A$	4.45	4.45	slugs
$a_1$	0	0.309	feet
$a_2$	0.664	0.664	feet
$a_3$	1.483	1.028	feet
$\gamma$	0	0.380	radians
$I_1^A$	8.32	3.49	slug-ft. <sup>2</sup>
$I_2^A$	8.13	3.87	slug-ft. <sup>2</sup>
$I_3^A$	0.413	1.000	slug-ft. <sup>2</sup>

\*The "legs tucked" position is defined in the footnote accompanying Table 2.1.

roll axis and the cone semi-vertex angles equal to a constant, say,  $\theta_0$  (i.e.,  $\alpha_1 = \alpha_2 = \beta_1 = \beta_2 = 0$ ,  $\theta_1 = \theta_2 = \theta_0$ ). In Fig. 4.2, the yaw, pitch, and roll angles obtained by performing one cycle of this maneuver are plotted as functions of  $\theta_0$  for the case where the legs are held straight. The roll angle increases monotonically with the cone semi-vertex angles, a conclusion which might have been anticipated on the basis of the results of pitch and yaw motion analyses. Here, however, the yaw and pitch angles become as much as 33 percent of the roll angle (e.g., when  $\theta_0 = 60^\circ$ ), so that the resulting attitude changes are not necessarily close to roll reorientations.

As indicated previously, judicious choice of the cone axes locations can eliminate undesired pitch and yaw angles. To narrow the field

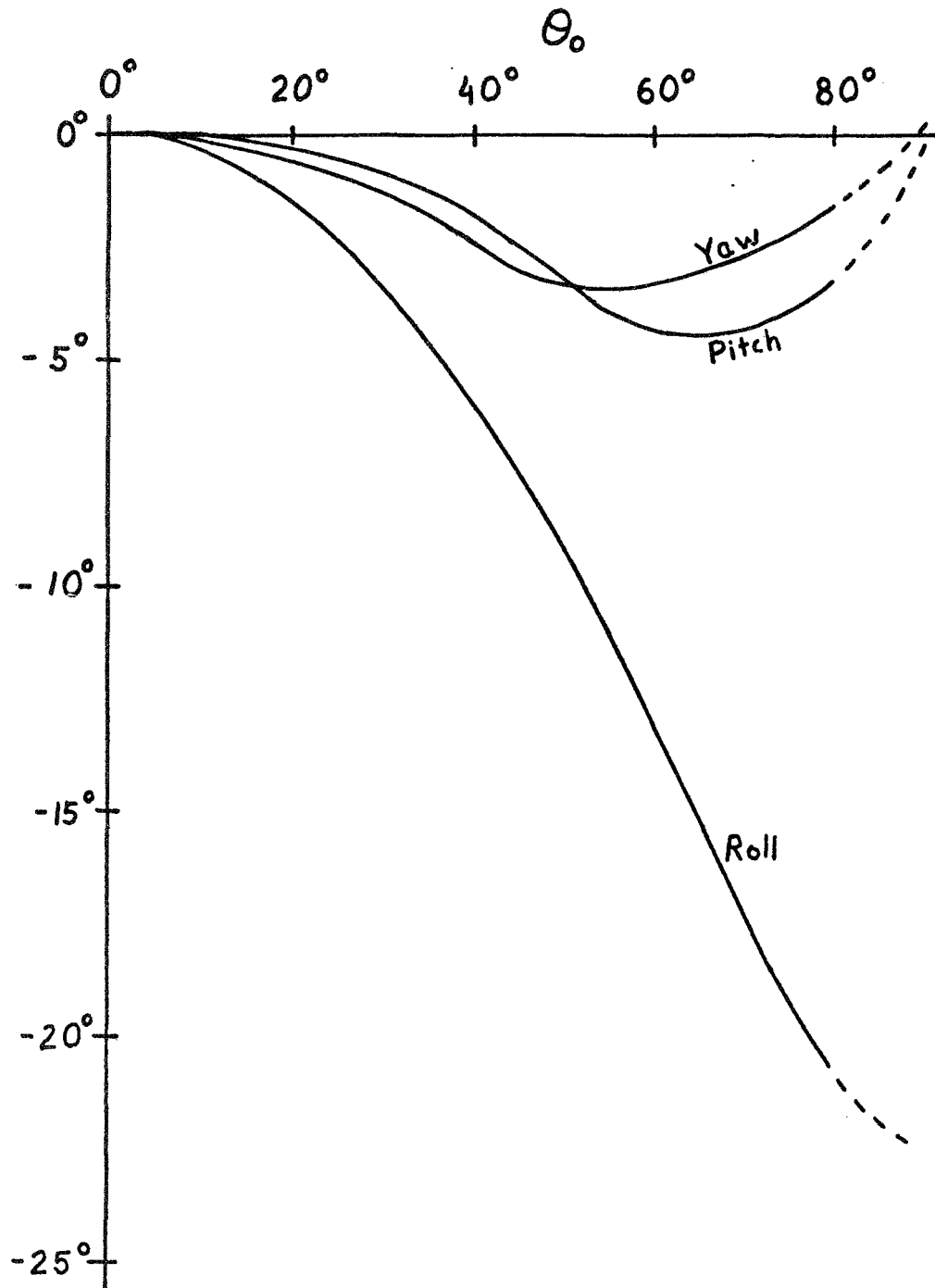


Fig. 4.2 Yaw, pitch, and roll angles as functions of  $\theta_0$   
 $(\alpha_1 = \alpha_2 = \beta_1 = \beta_2 = 0$  , legs straight)

of possible axes locations, let us consider only those in which  $\alpha_1 = \alpha_2 = \alpha_0$  and  $\beta_1 = \beta_2 = \beta_0$ . (Note that the axes are not symmetrically located about the pitch plane since  $\beta_1$  and  $\beta_2$  are positive to the left.) We will also restrict cone semi-vertex angles to values such that  $\theta_1 = \theta_2 = \theta_0$ . Thus, for a given  $\theta_0$ , there is a two-dimensional parameter space  $(\alpha_0, \beta_0)$  of possible cone axes locations. For given values of  $\beta_0$  and  $\theta_0$ , the dominant effect of increasing  $\alpha_0$  is an increase in the yaw angle. Similarly, for given values of  $\theta_0$  and  $\alpha_0$ , increases in  $\beta_0$  produce decreases in the pitch angle while the yaw and roll angles remain roughly constant. The latter phenomenon is illustrated by the graph in Fig. 4.3, in which the yaw, pitch, and roll angles produced by one cycle of the maneuver are plotted as functions of  $\beta_0$  for the case where  $\alpha_0$  is zero,  $\theta_0$  is 60 degrees, and the legs are held straight. Note that when  $\beta_0$  is -18 degrees, the pitch angle becomes zero.

Armed with this knowledge, one could attempt to vary  $\alpha_0$  and  $\beta_0$  so that, for a fixed value of  $\theta_0$ , the resulting yaw and pitch angles are both zero at the completion of a cycle of the maneuver. In this way, one could obtain a reorientation equivalent to that which would be produced by a simple rotation about the roll axis. Such an attempt, employing a trial-and-error procedure for the choice of  $\alpha_0$  and  $\beta_0$ , has been performed and the results are shown in Fig. 4.4, where the appropriate values of  $\alpha_0$  and  $\beta_0$  and the resulting roll angle are plotted as functions of the cone semi-vertex angles  $\theta_0$  for the case where the legs are straight. For example, a man wishing to roll 7.5 degrees to his left should choose cone semi-vertex angles of 45 degrees and locate

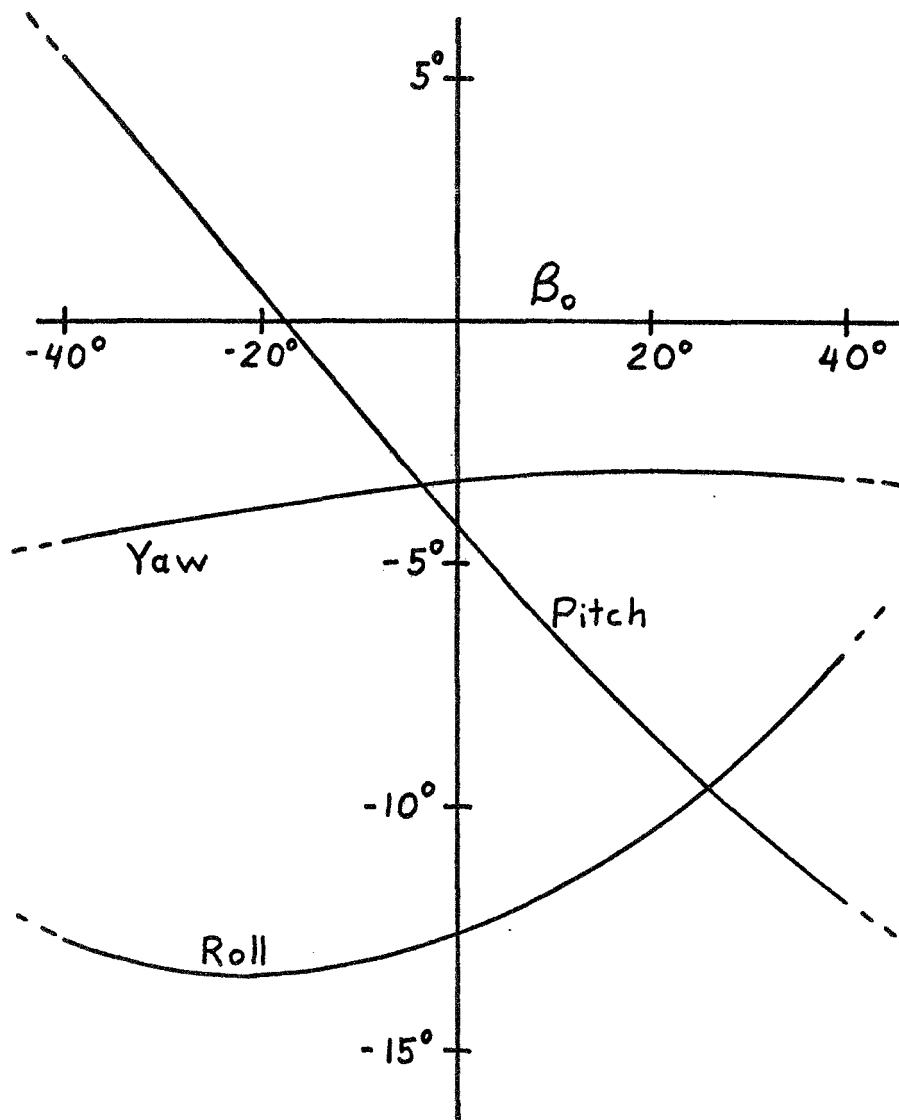


Fig. 4.3 Yaw, pitch, and roll angles as functions of  $\beta_0$   
( $\alpha_0 = 0$  ,  $\theta_0 = 60^\circ$  , legs straight)

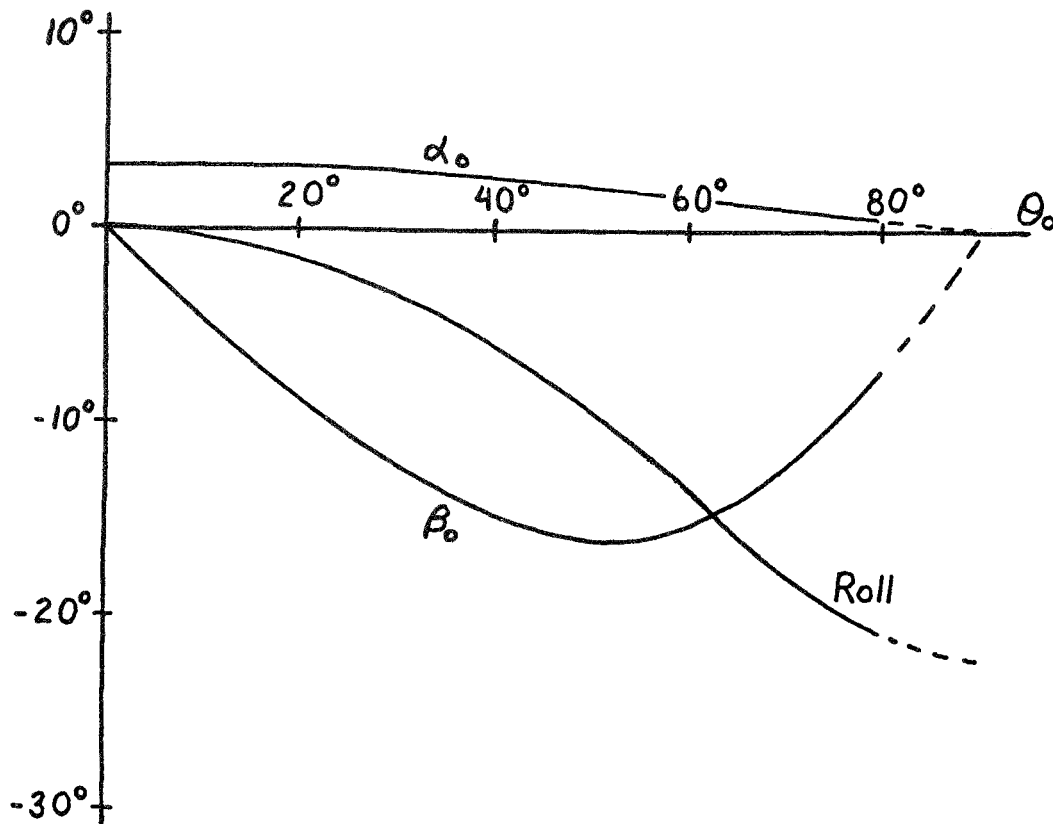


Fig. 4.4 Roll reorientation, and appropriate values of  $\alpha_0$  and  $\beta_0$ , as functions of  $\theta_0$  (legs straight)

the cone axes at  $\alpha_1 = \alpha_2 = 2.4$  degrees and  $\beta_1 = \beta_2 = -15.7$  degrees. Note that the order of magnitude of the roll reorientations is considerably less than that of pitch. For instance, when the cone axes are parallel to the pitch axis, cone semi-vertex angles of 45 degrees produce about 12 degrees of pitch when the legs are straight (see Fig. 2.3).

Tucking the legs (see footnote accompanying Table 2.1 for details) more than doubles the amount of roll obtained per cycle as can be seen by comparing Figs. 4.4 and 4.5. In the latter, the appropriate  $\alpha_0$  and  $\beta_0$  and the resulting roll angle are plotted as functions of  $\theta_0$  for

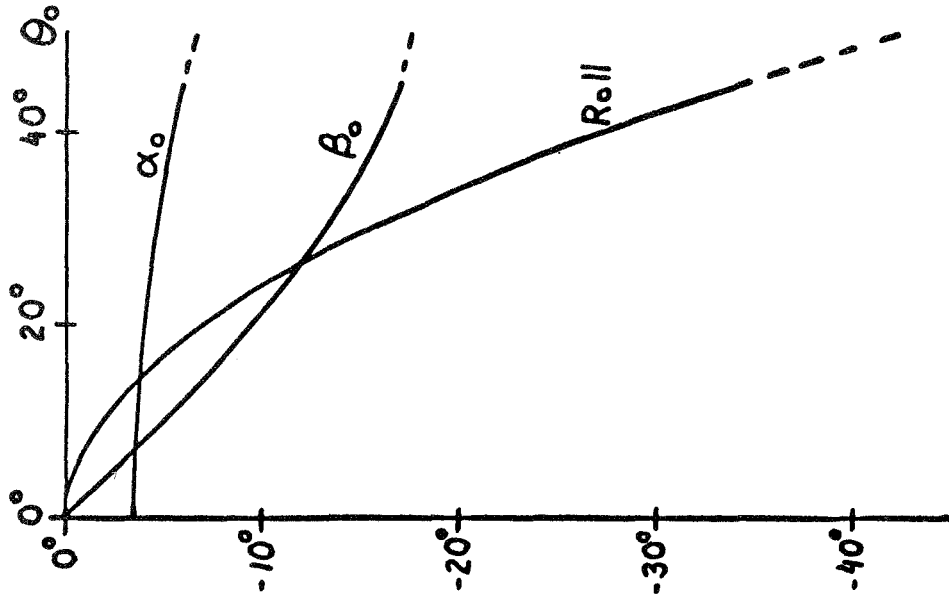


Fig. 4.6 Roll reorientation, and appropriate values of  $\alpha_0$  and  $\beta_0$ , as functions of  $\theta_0$  (legs tucked and a five-pound weight in each hand)

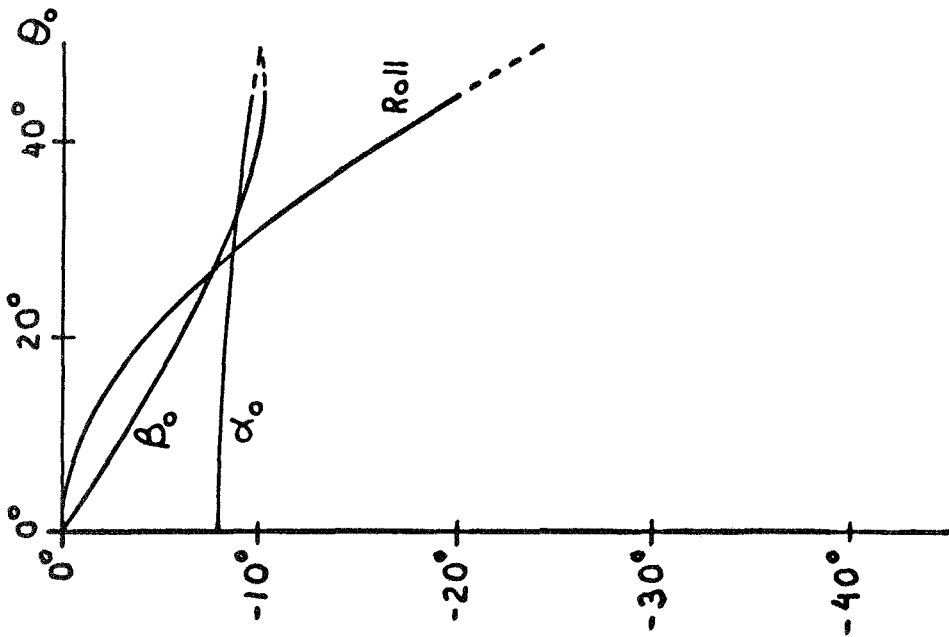


Fig. 4.5 Roll reorientation, and appropriate values of  $\alpha_0$  and  $\beta_0$ , as functions of  $\theta_0$  (legs tucked)

the case where the legs are tucked. Note that the appropriate values of  $\alpha_0$  and  $\beta_0$  are markedly different from those employed with the straightened legs. For example, when the legs are tucked, cone semi-vertex angles of 45 degrees produce 20 degrees of leftward roll reorientation. However the cone axes must be located at  $\alpha_1 = \alpha_2 = -9.9$  degrees and  $\beta_1 = \beta_2 = -10.1$  degrees. In Fig. 4.5,  $\theta_0$  is restricted to less than 45 degrees, larger semi-vertex angles being physically prohibited due to interference from the upper legs when tucked.

Finally, holding five-pound (.156 slugs) weights in the hands, while keeping the legs tucked, also doubles the attainable roll angle as illustrated by the graph in Fig. 4.6 which is analogous to those in Figs. 4.4 and 4.5. In this case, semi-vertex angles of 45 degrees produce 35 degrees of leftward roll and the appropriate cone axes are obtained by setting  $\alpha_1 = \alpha_2 = -6$  degrees and  $\beta_1 = \beta_2 = -16.8$  degrees .



## CHANGES IN ATTITUDE MOTION

### 5. Quasi-Rigid Bodies in Free Fall

#### 5.1 Attitude Motion and Kinetic Energy

In the preceding sections, specific maneuvers producing changes in the orientation of the human body are discussed. A principal feature of these problems is that, when the segments of the body come to rest relative to one another, the rotational motion of the entire system ceases. In other words, the angular momentum of the system of rigid bodies about its combined mass center is at all times equal to zero. This fact is used explicitly in Riddle's analysis, described in Sec. 4.2, and it manifests itself more subtly in the pitch and yaw motion analyses, in each of which an arbitrary constant in a first integral of Lagrange's equation (see Eqs. (2.1) and (3.1)) is set equal to zero.

We now turn to problems in which the angular momentum of a system of particles and rigid bodies is not equal to zero. The stipulation that the system be in free fall guarantees that the angular momentum will remain constant, both in magnitude and direction. When all parts of such a system are at rest relative to one another, the system as a whole must be in a state of rotational motion. The remainder of this section, and those immediately following, deal with such systems in general terms. Discussion of the human in free fall is resumed in Sec. 7.1.

The systems under consideration are comprised of particles and rigid bodies which can perform prescribed motions relative to one another. In particular, the systems can move as quasi-rigid bodies; that is, all the parts can remain at rest relative to one another. We shall limit

consideration to relative motions which begin and terminate with the parts in a given configuration, and this configuration will be called the system's quasi-rigid state.

It is helpful at this point to briefly discuss the nature of the attitude motions of a rigid body in free fall since such a discussion is directly applicable to any quasi-rigid body. If a body possesses a general inertia ellipsoid (i.e., if the three centroidal principal moments of inertia are unequal), then the most general motions of the body are difficult to visualize because the angular velocity of the body has neither a constant magnitude nor a fixed direction. Such motions are, perhaps, best characterized as "tumbling." In principle, however, it is possible for a body to simply "spin," that is, for the orientation of a centroidal principal axis of the body to remain fixed in inertial space, in which case the direction of the angular velocity vector must remain fixed both in the body and in space.

In some cases of practical significance (e.g., see Secs. 7.1 and 8.1) it may be desirable to convert a given attitude motion (e.g., undesired tumbling) of a quasi-rigid body into a simple spin. Such a feat can frequently be accomplished by moving the parts of the system relative to each other in such a manner as to ultimately restore the system to its quasi-rigid state. One strategy for determining appropriate relative movements of the parts involves the rotational kinetic energy of the quasi-rigid body about its mass center (hereafter referred to simply as the "kinetic energy") and is based on the following four statements:

(1) Whenever a system in free fall moves in a quasi-rigid state,

its kinetic energy  $K$  lies between two bounds,  $K_1$  and  $K_3$  :

$$K_1 \geq K \geq K_3 \quad (5.1)$$

- (2) If the system remains in its quasi-rigid state during some finite time interval, then the kinetic energy remains constant during this interval.
- (3) Whenever the kinetic energy of the quasi-rigid body equals  $K_1$  or  $K_3$ , then the angular velocity is parallel to a principal axis for the mass center.
- (4) If the system ceases to be rigid and the parts are made to move relative to one another, but are ultimately restored to their initial relative positions, then the value of the kinetic energy of the quasi-rigid body subsequent to relative motion may differ from that possessed prior to the motion; and the final value may be greater than, equal to, or less than the initial value (provided that (1) is not violated).

It is a consequence of (4) that particular relative motions of the parts may cause the value of the kinetic energy to become either  $K_1$  or  $K_3$  at the instant when the system is restored to its quasi-rigid state. By virtue of (2), the value of the kinetic energy must then remain fixed as long as no further relative motions occur, and from (3) it follows that the angular velocity remains parallel to a principal axis, so that the motion is one of simple spin. Thus a possible strategy for converting tumbling to simple spin is to seek relative motions which cause the kinetic energy to assume the value  $K_1$  or  $K_3$  at the instant when relative motion is terminated.

Statements (1) through (4) in the previous paragraph require some

justification. Suppose that the centroidal principal moments of inertia of the quasi-rigid body,  $I_1$ ,  $I_2$ , and  $I_3$ , are ordered so that

$$I_1 < I_2 < I_3 \quad (5.2)$$

If  $\underline{a}_1$ ,  $\underline{a}_2$ ,  $\underline{a}_3$  are unit vectors parallel to body-fixed principal axes for the mass center, and  $\omega_1$ ,  $\omega_2$ ,  $\omega_3$  are measure numbers of the inertial angular velocity of the quasi-rigid system referred to these unit vectors, then the angular momentum vector  $\underline{H}$  of the quasi-rigid system about its mass center can be expressed as

$$\underline{H} = I_1 \omega_1 \underline{a}_1 + I_2 \omega_2 \underline{a}_2 + I_3 \omega_3 \underline{a}_3 \quad (5.3)$$

and the kinetic energy of rotation,  $K$ , of the quasi-rigid body is given by

$$K = \frac{1}{2}(I_1 \omega_1^2 + I_2 \omega_2^2 + I_3 \omega_3^2) \quad (5.4)$$

Elimination of  $\omega_1$  between Eqs. (5.3) and (5.4) leads to

$$K = \frac{H^2}{2I_1} \left\{ 1 - \left[ \frac{I_2(I_2 - I_1) \omega_2^2 + I_3(I_3 - I_1) \omega_3^2}{H^2} \right] \right\} \quad (5.5)$$

while elimination of  $\omega_3$  yields

$$K = \frac{H^2}{2I_3} \left\{ 1 + \left[ \frac{I_1(I_3 - I_1) \omega_1^2 + I_2(I_3 - I_2) \omega_2^2}{H^2} \right] \right\} \quad (5.6)$$

The terms in the square brackets in (5.5) and (5.6) are positive by virtue of (5.2). Hence

$$K \leq \frac{H^2}{2I_1} \quad (5.7)$$

$$K \geq \frac{H^2}{2I_3} \quad (5.8)$$

(5.6)

and statement (1) follows from the definitions

$$K_1 = \frac{H^2}{2I_1} \quad (5.9)$$

$$K_3 = \frac{H^2}{2I_3} \quad (5.10)$$

Statement (2) is a consequence of the well-known (e.g., see [43]) energy integral of Euler's equations of motion for a rigid body in free fall; and statement (3) may be verified by examining Eqs. (5.7) and (5.8), the equality in (5.7) holding only when  $\omega_2$  and  $\omega_3$  are zero, in which case the angular velocity is parallel to  $\underline{a}_1$ , while the equality in (5.8) holds only when the angular velocity is parallel to  $\underline{a}_3$ . Finally, the validity of statement (4) can be established by citing a single example, and several such examples appear in Secs. 7.4 and 8.3.

## 5.2 Symmetric Quasi-Rigid Bodies

A special case of practical importance occurs when a system in a quasi-rigid state possesses an axially symmetric mass distribution, i.e., when  $I_2$  equals either  $I_1$  or  $I_3$ .

The most general motion of a symmetric rigid body consists of spin about the axis of symmetry, combined with precession of the symmetry axis. If a unit vector  $\underline{a}$  is parallel to the symmetry axis, then the angle  $\varphi$  between  $\underline{a}$  and  $\underline{H}$  is given by

$$\cos \varphi = \frac{\underline{a} \cdot \underline{H}}{|\underline{H}|} \quad (5.11)$$

Notice that  $\varphi$  can be calculated without knowledge of the attitude of the quasi-rigid system as long as  $\omega_1$ ,  $\omega_2$ ,  $\omega_3$  are known. Suppose that the inertia ellipsoid of the body is a prolate spheroid, so that the "1" axis is the symmetry axis. Then

$$\underline{a} = \underline{a}_1 \quad (5.12)$$

$$I_2 = I_3 \quad (5.13)$$

and

$$\varphi = \text{arc cos} \frac{I_1 \omega_1}{\sqrt{I_1^2 \omega_1^2 + I_3^2 (\omega_2^2 + \omega_3^2)}} \quad (5.14)$$

(5.11,5.3,5.12,5.13)

On the other hand, if the inertia ellipsoid of the quasi-rigid body is an oblate spheroid, then

$$\underline{a} = \underline{a}_3 \quad (5.15)$$

$$I_2 = I_1 \quad (5.16)$$

and

$$\varphi = \text{arc cos} \frac{I_3 \omega_3}{\sqrt{I_1^2 (\omega_1^2 + \omega_2^2) + I_3^2 \omega_3^2}} \quad (5.17)$$

(5.11,5.3,5.15,5.16)

Four claims, analogous to statements (1) through (4) of Sec. 5.1, are applicable to symmetric quasi-rigid bodies, but involve  $\varphi$  rather than  $K$  :

- (1) When the system assumes its quasi-rigid state in free fall,  
then

$$0 \leq \varphi \leq \pi \quad (5.18)$$

- (2) The angle  $\varphi$  remains constant as long as the system remains in its quasi-rigid state.
- (3) If  $\varphi$  equals 0 or  $\pi$ , then the quasi-rigid body is performing simple spin about its symmetry axis; moreover, if  $\varphi$  equals  $\frac{\pi}{2}$ , the system is spinning about an axis normal to the symmetry axis, in which case the component of angular velocity parallel to the symmetry axis is zero and the other two components remain constant.
- (4) Relative motions of the parts of the system which ultimately restore the system to its initial quasi-rigid state may alter the value of  $\varphi$  within the limits imposed by Eq. (5.18).

Consequently, a strategy for converting a motion in which  $\varphi$  has an initial value  $\varphi_0$  to one such that  $\varphi$  has a final value  $\varphi_f$  is to seek relative motions of the parts which restore the system to its quasi-rigid state at an instant when  $\varphi$  is equal to  $\varphi_f$ .

## 6. Attitude Equations for Two-Body Systems

### 6.1 General Relative Motion

Two rigid bodies (or a particle and a rigid body) which can move relative to one another comprise the simplest system which can exhibit quasi-rigid body motion. In this section, equations governing attitude motions of such systems are derived.

The two rigid bodies, A and B, have mass centers  $A^*$  and  $B^*$ , masses  $m_A$  and  $m_B$ , and centroidal inertia dyadics  $\underline{I}^A$  and  $\underline{I}^B$ , respectively. The position vector of  $A^*$  relative to a point O that is fixed in an inertial reference frame F is denoted by  $\underline{p}$ , and the position vector of  $B^*$  relative to  $A^*$  by  $\underline{r}$  (see Fig. 6.1).

Although only "free fall" problems are to be studied, it is desirable at this point to assume the presence of a general force system, thus broadening the applicability of the equations to be developed. To this end, the system of all forces acting on A and B is replaced with an equivalent system comprised of a force  $\underline{F}$  applied at  $A^*$  and a couple of torque  $\underline{T}$ . ( $\underline{F}$  is equal to the resultant of the actual forces, and  $\underline{T}$  is equal to the sum of the moments of these forces about  $A^*$ .)

In accordance with D'Alembert's principle,

$$\underline{F} + \underline{F}_A^* + \underline{F}_B^* = 0 \quad (6.1)$$

where  $\underline{F}_A^*$  and  $\underline{F}_B^*$ , the inertia forces for A and B, are given by

$$\underline{F}_A^* = - m_A \ddot{\underline{p}} \quad (6.2)$$

and



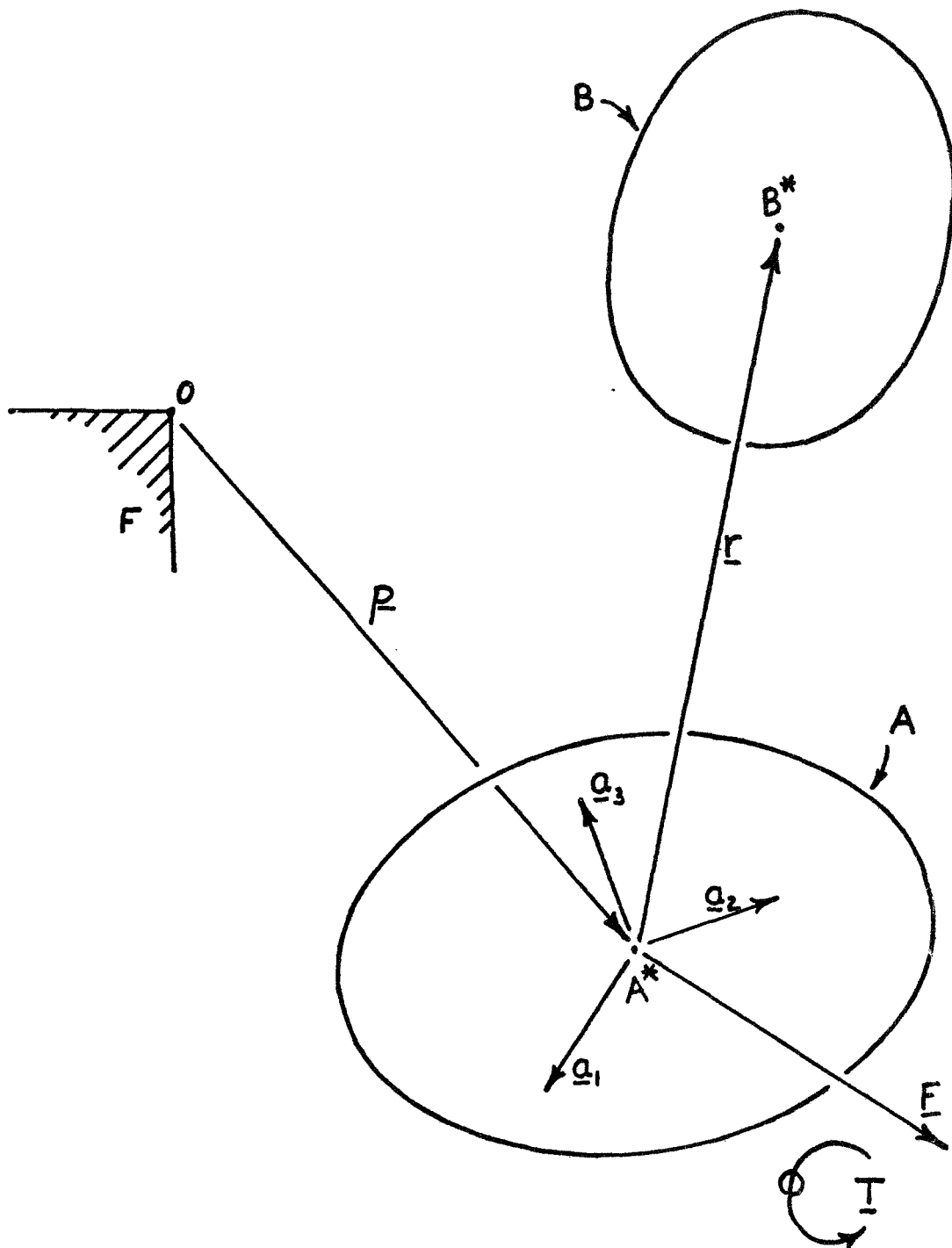


Fig. 6.1 Two bodies performing general relative motion

$$\underline{F}_B^* = - m_B (\ddot{\underline{p}} + \ddot{\underline{r}}) \quad (6.3)$$

(Dots over vectors denote time differentiation in F .) After defining M as

$$M = m_A + m_B \quad (6.4)$$

substitution from Eqs. (6.2) and (6.3) into (6.1) gives

$$\underline{F} = M \ddot{\underline{p}} + m_B \ddot{\underline{r}} \quad (6.5)$$

A second dynamical equation may be obtained from a summation of moments about A\* :

$$\underline{T} + \underline{T}_A^* + \underline{T}_B^* + \underline{r} \times \underline{F}_B^* = 0 \quad (6.6)$$

where  $\underline{T}_A^*$  and  $\underline{T}_B^*$  , the inertia torques for A and B , are given by

$$\underline{T}_A^* = \underline{I}^A \cdot \underline{\omega}^A \times \underline{\omega}^A - \underline{I}^A \cdot \underline{\alpha}^A \quad (6.7)$$

$$\underline{T}_B^* = \underline{I}^B \cdot \underline{\omega}^B \times \underline{\omega}^B - \underline{I}^B \cdot \underline{\alpha}^B \quad (6.8)$$

and  $\underline{\omega}^A$  and  $\underline{\omega}^B$  are the inertial angular velocities, and  $\underline{\alpha}^A$  and  $\underline{\alpha}^B$  the inertial angular accelerations of bodies A and B , respectively.

Substitution of (6.3) into (6.6) then leads to

$$\underline{T} + \underline{T}_A^* + \underline{T}_B^* - m_B \underline{r} \times (\ddot{\underline{p}} + \ddot{\underline{r}}) = 0 \quad (6.9)$$

and elimination of  $\ddot{\underline{p}}$  between (6.9) and (6.5) yields

$$\underline{T} + \underline{T}_A^* + \underline{T}_B^* - \frac{m_B}{M} \underline{r} \times \underline{F} - \frac{m_A m_B}{M} \underline{r} \times \ddot{\underline{r}} = 0 \quad (6.10)$$

Note that this equation does not involve the positions of A and B in F .

If the angular velocity of  $B$  relative to  $A$  is denoted by  $\underline{\omega}^{A/B}$ , then

$$\underline{\omega}^B = \underline{\omega}^A + \underline{\omega}^{A/B} \quad (6.11)$$

and, differentiating with respect to time, one obtains

$$\underline{\alpha}^B = \underline{\alpha}^A + \frac{A_d}{dt} \underline{\omega}^{A/B} + \underline{\omega}^A \times \underline{\omega}^{A/B} \quad (6.12)$$

where  $\frac{A_d}{dt}$  denotes time-differentiation in a reference frame fixed in body  $A$ ; and  $\ddot{\underline{r}}$  may be expressed as

$$\ddot{\underline{r}} = \frac{A_d^2}{dt^2} \underline{r} + 2\underline{\omega}^A \times \frac{A_d}{dt} \underline{r} + \underline{\alpha}^A \times \underline{r} + \underline{\omega}^A \times (\underline{\omega}^A \times \underline{r}) \quad (6.13)$$

Consequently (see Eqs. (6.10), (6.7), (6.8), (6.11), (6.12), (6.13)), the inertial angular acceleration  $\underline{\alpha}^A$  of body  $A$  is related to the forces acting on the system, to the angular velocity  $\underline{\omega}^A$  of  $A$ , and to the vectors  $\underline{\omega}^{A/B}$  and  $\underline{r}$ , which govern the motion of  $B$  relative to  $A$ , as follows:

$$\begin{aligned} (\underline{I}^A + \underline{I}^B) \cdot \underline{\alpha}^A + \frac{m_A m_B}{M} \underline{r} \times (\underline{\alpha}^A \times \underline{r}) = \\ \underline{T} + [(\underline{I}^A + \underline{I}^B) \cdot \underline{\omega}^A] \times \underline{\omega}^A - \underline{I}^B \cdot \left( \frac{A_d}{dt} \underline{\omega}^{A/B} + \underline{\omega}^A \times \underline{\omega}^{A/B} \right) + (\underline{I}^B \cdot \underline{\omega}^A) \times \underline{\omega}^{A/B} \\ + (\underline{I}^B \cdot \underline{\omega}^{A/B}) \times (\underline{\omega}^A + \underline{\omega}^{A/B}) - \frac{m_B}{M} \underline{r} \times \underline{F} \\ - \frac{m_A m_B}{M} \underline{r} \times \left[ \frac{A_d^2}{dt^2} \underline{r} + 2\underline{\omega}^A \times \frac{A_d}{dt} \underline{r} + \underline{\omega}^A \times (\underline{\omega}^A \times \underline{r}) \right] \end{aligned} \quad (6.14)$$

Three scalar equations equivalent to Eq. (6.14) are obtained by introducing three mutually perpendicular unit vectors  $\underline{a}_1, \underline{a}_2, \underline{a}_3$  fixed in body  $A$  and by defining the following quantities:

$$\omega_i = \underline{\omega}^A \cdot \underline{a}_i \quad i = 1, 2, 3 \quad (6.15)$$

$$A_{ij} = \underline{a}_i \cdot \underline{I}^A \cdot \underline{a}_j \quad i, j = 1, 2, 3 \quad (6.16)$$

$$\underline{F}_i = \underline{F} \cdot \underline{a}_i \quad i = 1, 2, 3 \quad (6.17)$$

$$\underline{T}_i = \underline{T} \cdot \underline{a}_i \quad i = 1, 2, 3 \quad (6.18)$$

$$B_{ij} = \underline{a}_i \cdot \underline{I}^B \cdot \underline{a}_j \quad i, j = 1, 2, 3 \quad (6.19)$$

$$\underline{r}_i = \underline{r} \cdot \underline{a}_i \quad i = 1, 2, 3 \quad (6.20)$$

$$\Omega_i = \underline{\omega}^{AB} \cdot \underline{a}_i \quad i = 1, 2, 3 \quad (6.21)$$

Eq. (6.14) is then equivalent to the three scalar equations

$$\sum_{j=1}^3 E_{ij} \dot{\omega}_j = D_i \quad i = 1, 2, 3 \quad (6.22)$$

where

$$E_{11} = A_{11} + B_{11} + \frac{m_A m_B}{M} (r_2^2 + r_3^2) \quad (6.23)$$

$$E_{12} = E_{21} = A_{12} + B_{12} - \frac{m_A m_B}{M} r_1 r_2 \quad (6.24)$$

$$\begin{aligned} D_1 = & \underline{T}_1 + \omega_3 \sum_{i=1}^3 (A_{2i} + B_{2i}) \omega_i - \omega_2 \sum_{i=1}^3 (A_{3i} + B_{3i}) \omega_i \\ & - \sum_{i=1}^3 B_{1i} \dot{\Omega}_i - B_{11} (\omega_2 \Omega_3 - \omega_3 \Omega_2) - B_{12} (\omega_3 \Omega_1 - \omega_1 \Omega_3) \\ & - B_{13} (\omega_1 \Omega_2 - \omega_2 \Omega_1) + \Omega_3 \sum_{i=1}^3 B_{2i} \omega_i - \Omega_2 \sum_{i=1}^3 B_{3i} \omega_i \end{aligned}$$

$$\begin{aligned}
 & +(\omega_3 + \Omega_3) \sum_{i=1}^3 B_{2i} \Omega_i - (\omega_2 + \Omega_2) \sum_{i=1}^3 B_{3i} \Omega_i - \frac{m_B}{M} (r_2 F_3 - r_3 F_2) \\
 & - \frac{m_A m_B}{M} \left\{ r_2 \ddot{r}_3 - r_3 \ddot{r}_2 + 2[r_2(\omega_1 \dot{r}_2 - \omega_2 \dot{r}_1) - r_3(\omega_3 \dot{r}_1 - \omega_1 \dot{r}_3)] \right. \\
 & \left. + (r_2 \omega_3 - r_3 \omega_2) \sum_{i=1}^3 \omega_i r_i \right\} \quad (6.25)
 \end{aligned}$$

and all remaining E's and D's may be obtained by cyclic permutations of the subscripts in Eqs. (6.23)-(6.25).

Eqs. (6.22) may be solved to obtain explicit expression for  $\dot{\omega}_1$ ,  $\dot{\omega}_2$ ,  $\dot{\omega}_3$ . If one first defines

$$C_1 = E_{22} E_{33} - E_{23}^2 \quad (6.26)$$

$$C_2 = E_{13} E_{23} - E_{12} E_{33} \quad (6.27)$$

$$C_3 = E_{12} E_{23} - E_{22} E_{13} \quad (6.28)$$

$$C_4 = E_{11} E_{33} - E_{13}^2 \quad (6.29)$$

$$C_5 = E_{13} E_{12} - E_{11} E_{23} \quad (6.30)$$

$$C_6 = E_{11} E_{22} - E_{12}^2 \quad (6.31)$$

$$\Delta = C_1 E_{11} + C_2 E_{12} + C_3 E_{13} \quad (6.32)$$

then

$$\dot{\omega}_1 = (D_1 C_1 + D_2 C_2 + D_3 C_3) / \Delta \quad (6.33)$$

$$\dot{\omega}_2 = (D_1 C_2 + D_2 C_4 + D_3 C_5) / \Delta \quad (6.34)$$

$$\dot{\omega}_3 = (D_1 C_3 + D_2 C_5 + D_3 C_6) / \Delta \quad (6.35)$$

Eqs. (6.33)-(6.35) are readily amenable to numerical (digital computer) integration which yields time histories of  $\omega_1$ ,  $\omega_2$ ,  $\omega_3$  provided that the initial values of  $\omega_1$ ,  $\omega_2$ ,  $\omega_3$  are given, that  $m_A$ ,  $m_B$ , and the  $A_{ij}$  defined by Eq. (6.16) are known, and that time histories of the quantities defined by Eqs. (6.17)-(6.21) are available. When this is the case,  $\dot{\omega}_1$ ,  $\dot{\omega}_2$ ,  $\dot{\omega}_3$  may be computed at each step of the integration by proceeding as follows:

(1) The instantaneous values of  $E_{11}$ ,  $E_{12}$ ,  $E_{13}$ ,  $E_{22}$ ,  $E_{23}$ ,  $E_{33}$  and of the  $D$ 's are calculated using Eqs. (6.23)-(6.25) with appropriate permutations of the indices.

(2) The  $C$ 's and  $\Delta$  are calculated from Eqs. (6.26)-(6.32).

(Note: for these calculations only six of the nine  $E$ 's are required because of their symmetry.)

(3) Finally,  $\dot{\omega}_1$ ,  $\dot{\omega}_2$ ,  $\dot{\omega}_3$  are determined from Eqs. (6.33)-(6.35). Of course, the nature of the  $F_i$ ,  $T_i$ ,  $B_{ij}$  and of the  $r_i$ ,  $\Omega_i$ , and their derivatives, all of which appear in Eqs. (6.23)-(6.25), has not been discussed and, indeed, no more can be said until a particular two-body system and relative motion have been chosen. In the following section, expressions for some of these terms are found for one class of motions of  $B$  relative to  $A$ .

## 6.2 Kinematics of Two Hinged Bodies

In general, a rigid body  $B$  possesses six degrees of freedom relative to a rigid body  $A$ . However, if the two bodies are connected by a

simple hinge,  $B$  possesses only a single degree of freedom relative to  $A$ . The quantities  $B_{ij}$ ,  $r_i$ , and  $\Omega_i$  of Eqs. (6.19)-(6.21) can then be expressed in relatively simple terms which depend only on the location and orientation in each body of the hinge axis and on the generalized coordinate used to describe the attitude of  $B$  relative to  $A$ .

In Fig. 6.2,  $L$  designates the hinge axis,  $C$  is a point on  $L$ , chosen arbitrarily, and the position vectors of  $C$  relative to  $A^*$  and  $B^*$  are denoted by  $\underline{a}$  and  $\underline{b}$ , respectively. Two sets of three mutually perpendicular unit vectors,  $\underline{a}_1, \underline{a}_2, \underline{a}_3$  and  $\underline{b}_1, \underline{b}_2, \underline{b}_3$ , are fixed in  $A$  and  $B$ , respectively; a unit vector  $\underline{h}$  lies parallel to  $L$ ; and unit vectors  $\underline{n}_A$  and  $\underline{n}_B$ , both normal to  $L$ , are fixed in  $A$  and  $B$ , respectively. Finally, the angle  $\alpha$  between  $\underline{n}_A$  and  $\underline{n}_B$  is regarded as increasing when  $\underline{\omega}^{AB}$ , the angular velocity of  $B$  in  $A$ , has the same sense as  $\underline{h}$ .

When  $B$  rotates relative to  $A$  about  $L$ , suitable expressions for  $B_{ij}$ ,  $r_i$ , and  $\Omega_i$  (see Eqs. (6.19)-(6.21)) may not be readily available, but can always be constructed. For instance, one may have been given the moments and products of inertia of  $B$  for  $B^*$ , i.e.,  $I_{ij}^B$  where

$$I_{ij}^B = \underline{b}_i \cdot \underline{I}^B \cdot \underline{b}_j \quad i, j = 1, 2, 3 \quad (6.36)$$

in which case one must determine a direction cosine matrix  $[c]$  such that

$$[\underline{a}_1, \underline{a}_2, \underline{a}_3] = [\underline{b}_1, \underline{b}_2, \underline{b}_3] [c] \quad (6.37)$$

after which one can express  $B_{ij}$  as

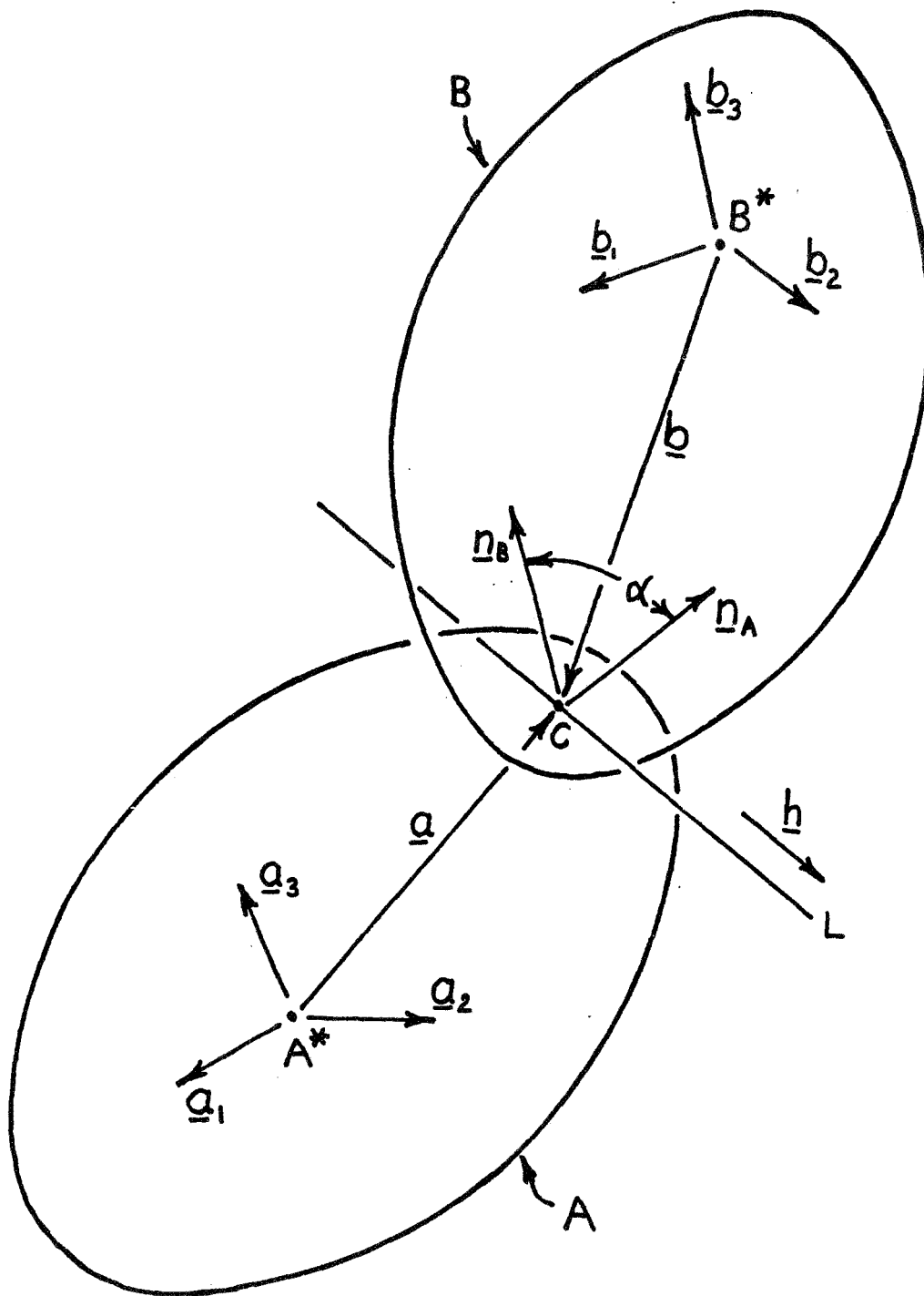


Fig. 6.2

Two hinged bodies



$$B_{ij} = \sum_{m=1}^3 \sum_{n=1}^3 I_{mn}^B c_{mi} c_{nj} \quad i, j = 1, 2, 3 \quad (6.38)$$

where  $c_{mi}$  denotes the element in the  $m^{\text{th}}$  row and  $i^{\text{th}}$  column of  $[c]$ .

To express  $[c]$  in terms of quantities which govern the orientation of  $\underline{h}$  and  $\underline{n}_A$  in  $A$ , and of  $\underline{h}$  and  $\underline{n}_B$  in  $B$ , one may proceed as follows: Express  $\underline{h}$  and  $\underline{n}_A$  in terms of  $\underline{a}_1, \underline{a}_2, \underline{a}_3$  by means of two sets of direction cosines,  $p_{11}, p_{12}, p_{13}$  and  $p_{31}, p_{32}, p_{33}$ , i.e., let

$$\underline{h} = \sum_{i=1}^3 p_{1i} \underline{a}_i \quad (6.39)$$

$$\underline{n}_A = \sum_{i=1}^3 p_{3i} \underline{a}_i \quad (6.40)$$

and, similarly, express  $\underline{h}$  and  $\underline{n}_B$  as

$$\underline{h} = \sum_{i=1}^3 q_{1i} \underline{b}_i \quad (6.41)$$

$$\underline{n}_B = \sum_{i=1}^3 q_{3i} \underline{b}_i \quad (6.42)$$

Next, let  $\underline{m}_A$  and  $\underline{m}_B$  be unit vectors defined as

$$\underline{m}_A = \underline{n}_A \times \underline{h} \quad (6.43)$$

$$\underline{m}_B = \underline{n}_B \times \underline{h} \quad (6.44)$$

and designate by  $[p]$  and  $[q]$  the direction cosine matrices such that

$$[\underline{a}_1, \underline{a}_2, \underline{a}_3] = [\underline{h}, \underline{m}_A, \underline{n}_A] [p] \quad (6.45)$$

and

$$[\underline{b}_1, \underline{b}_2, \underline{b}_3] = [\underline{h}, \underline{m}_B, \underline{n}_B] [q] \quad (6.46)$$

Furthermore, note that

$$[\underline{h}, \underline{m}_B, \underline{n}_B] = [\underline{h}, \underline{m}_A, \underline{n}_A] [r] \quad (6.47)$$

where

$$[r] = \begin{bmatrix} 1 & 0 & 0 \\ 0 & \cos \alpha & -\sin \alpha \\ 0 & \sin \alpha & \cos \alpha \end{bmatrix} \quad (6.48)$$

Then, if a superscript T is used to denote transposition,

$$\begin{aligned} [\underline{a}_1, \underline{a}_2, \underline{a}_3] &= [\underline{h}, \underline{m}_B, \underline{n}_B] [r]^T [p] \\ &\quad (6.45, 6.47) \\ &= [\underline{b}_1, \underline{b}_2, \underline{b}_3] [q]^T [r]^T [p] \\ &\quad (6.46) \end{aligned} \quad (6.49)$$

and comparison with (6.37) shows that  $c_{ij}$  is the element in the  $i^{\text{th}}$  row and  $j^{\text{th}}$  column of  $[q]^T [r]^T [p]$ ; i.e.,

$$c_{ij} = d_{ij} + e_{ij} \sin \alpha + f_{ij} \cos \alpha \quad i, j = 1, 2, 3 \quad (6.50)$$

where

$$d_{ij} = q_{1i} p_{1j} \quad i, j = 1, 2, 3 \quad (6.51)$$

$$e_{ij} = q_{2i} p_{3j} - q_{3i} p_{2j} \quad i, j = 1, 2, 3 \quad (6.52)$$

$$f_{ij} = q_{2i} p_{2j} + q_{3i} p_{3j} \quad i, j = 1, 2, 3 \quad (6.53)$$

and  $p_{ij}$  and  $q_{ij}$  are, of course, the elements in the  $i^{\text{th}}$  row and  $j^{\text{th}}$  column of  $[p]$  and  $[q]$ , respectively. When using these relationships, one should keep in mind that the elements in the first and third rows of the matrices  $[p]$  and  $[q]$  specify the orientation of  $\underline{h}$  and  $\underline{n}_A$  in A, and of  $\underline{h}$  and  $\underline{n}_B$  in B (see Eqs. (6.39)-(6.42)); the elements in the second rows of  $[p]$  and  $[q]$  can be expressed in terms of the elements of the first and third rows of the matrices by reference to Eqs. (6.43) and (6.44). For example,

$$p_{21} = p_{32} p_{13} - p_{33} p_{12} \quad (6.54)$$

and

$$q_{23} = q_{31} q_{12} - q_{32} q_{11} \quad (6.55)$$

The quantity  $r_i$  appearing in Eq. (6.20) may be expressed in a convenient form by noting that the position vector  $\underline{r}$  is given by (see Fig. 6.2)

$$\underline{r} = \underline{a} - \underline{b} \quad (6.56)$$

and that, if  $a_i$  and  $b_i$  are defined as

$$a_i = \underline{a} \cdot \underline{a}_i \quad i = 1, 2, 3 \quad (6.57)$$

and

$$b_i = \underline{b} \cdot \underline{b}_i \quad i = 1, 2, 3 \quad (6.58)$$

then (see (6.56)-(6.58), (6.37), (6.50))

$$r_i = u_i - v_i \sin \alpha - w_i \cos \alpha \quad i = 1, 2, 3 \quad (6.59)$$

where

$$u_i = a_i - \sum_{j=1}^3 b_j d_{ji} \quad i = 1, 2, 3 \quad (6.60)$$

$$v_i = \sum_{j=1}^3 b_j e_{ji} \quad i = 1, 2, 3 \quad (6.61)$$

$$w_i = \sum_{j=1}^3 b_j f_{ji} \quad i = 1, 2, 3 \quad (6.62)$$

The time derivatives of  $r_i$  required for use in Eq. (6.25) can now be found easily:

$$\dot{r}_i = (w_i \sin \alpha - v_i \cos \alpha) \dot{\alpha} \quad i = 1, 2, 3 \quad (6.63)$$

$$\begin{aligned} \ddot{r}_i &= (w_i \sin \alpha - v_i \cos \alpha) \ddot{\alpha} \\ &+ (v_i \sin \alpha + w_i \cos \alpha) \dot{\alpha}^2 \quad i = 1, 2, 3 \end{aligned} \quad (6.64)$$

Finally, for hinged systems, the angular velocity of B in A is given by

$$\underline{\omega}^{A/B} = \dot{\alpha} \underline{h} \quad (6.65)$$

and  $\Omega_i$  of Eq. (6.21) can be expressed as

$$\Omega_i = \dot{\alpha} p_{1i} \quad i = 1, 2, 3 \quad (6.66)$$

(6.65, 6.39)

Furthermore, it then follows that

$$\dot{\Omega}_i = \ddot{\alpha} p_{1i} \quad i = 1, 2, 3 \quad (6.67)$$

(6.66)

Thus, if body B is hinged to body A and if the following information is given:

- (1) the direction cosines  $p_{ij}$  which specify the orientation of  $\underline{h}$  and  $\underline{n}_A$  in A (see Eqs. (6.39) and (6.40)),
- (2) the direction cosines  $q_{ij}$  which specify the orientation of  $\underline{h}$  and  $\underline{n}_B$  in B (see Eqs. (6.41) and (6.42)),
- (3) the time history of  $\alpha$ ,
- (4) the quantities  $I_{ij}^B$  which are centroidal moments and products of B referred to the  $\underline{b}_1, \underline{b}_2, \underline{b}_3$  directions (see Eqs. (6.36)), and
- (5) the quantities  $a_i$  and  $b_i$  which are components of the position vectors  $\underline{a}$  and  $\underline{b}$  referred to directions fixed in A and B, respectively (see Eqs. (6.57) and (6.58)),

then the quantities  $B_{ij}, r_i, \dot{r}_i, \ddot{r}_i, \Omega_i$  and  $\dot{\Omega}_i$ , appearing in Eq. (6.25), can be found as follows:

- (I) The second rows of matrices  $[p]$  and  $[q]$  are found using Eqs. (6.54), (6.55), and cyclic permutations thereof.
- (II) The quantities  $d_{ij}, e_{ij}, f_{ij}$  are formed by reference to Eqs. (6.51)-(6.53).
- (III) The quantities  $u_i, v_i, w_i$  are formed by reference to Eqs. (6.60)-(6.62).
- (IV) The quantities  $c_{ij}$  are determined by using Eqs. (6.50), and then the  $B_{ij}$  are computed from (6.38).
- (V) The quantities  $r_i, \dot{r}_i, \ddot{r}_i$  are formed from Eqs. (6.59),

(6.63), and (6.64), respectively.

(VI) Finally,  $\Omega_i$  and  $\dot{\Omega}_i$  are obtained from Eqs. (6.66) and (6.67).

The formulation in this section proves advantageous when the equations of motion (6.33)-(6.35) are integrated numerically. Then steps I, II, and III can be completed once and for all prior to the integration. Steps IV, V, and VI must be performed at every step of the integration, but are relatively straightforward once  $\alpha$ ,  $\dot{\alpha}$ ,  $\ddot{\alpha}$ ,  $\sin \alpha$ , and  $\cos \alpha$  are known.

### 6.3 Computer Program

Analytical solutions of the equations for the attitude motion of systems comprised of two rigid bodies are difficult to obtain; and these solutions are mainly restricted to systems which perform relatively simple motions or which possess an extremely simple geometry. In the remainder of cases, including those considered in the sequel, only a numerical integration of the equations of motion is possible; and this is not a feasible task without a digital computer.

In this section, four FORTRAN computer subroutines capable of performing the calculations outlined in Secs. 6.1 and 6.2 are described. (A complete listing of these subroutines is contained in Appendix A.2.) Of these four subroutines, two deal exclusively with hinged bodies and perform computations discussed in Sec. 6.2; a third subroutine performs only those operations described in Sec. 6.1 and can be used either with the first two subroutines when hinged systems are being considered or without these first two when more general relative motions are involved.

The fourth subroutine performs numerical integration.

The most important of the subroutines is entitled TWOBOD. This subroutine computes  $E_{ij}$  and  $D_i$  of Eqs. (6.23)-(6.25), and solves Eqs. (6.22) to obtain the instantaneous values of  $\dot{\omega}_1$ ,  $\dot{\omega}_2$ ,  $\dot{\omega}_3$  in accordance with Eqs. (6.33)-(6.35). Thus, TWOBOD deals exclusively with computations in Sec. 6.1 and, hence, with general relative motions of two-body systems. Certain quantities pertaining to the inertia and geometrical properties and to the relative motion of the bodies must be supplied to TWOBOD. Those quantities which remain constant, namely  $A_{ij}$ ,  $\frac{m_A m_B}{M}$ , and  $\frac{m_B}{M}$  are supplied to it by means of a COMMON block named BODBLK. One of the subroutines, BODIES, which deals with hinged bodies and which will be discussed shortly, is equipped to pass these constant quantities to TWOBOD. When subroutine BODIES is not included in the user's program, some other part of that program must contain a COMMON block named BODBLK and must define these constants. Those quantities which are time-varying, namely  $F_i$ ,  $T_i$ ,  $B_{ij}$ , and  $r_i$ ,  $\Omega_i$ , and their derivatives (see Eqs. (6.17)-(6.21)) are supplied by a subroutine named INTRNL which is called by TWOBOD.

The numerical integration itself is performed by subroutine DFEQS1 which must be called by a main program each time that integration over a time interval is desired. Subroutine DFEQS1 was obtained from the subprogram library of the Stanford University Computation Center and employs a Kutta-Merson procedure for numerical integration (e.g., see Fox [44]). Since DFEQS1 calls subroutine TWOBOD at least five times during each step of the integration, an attempt was made to streamline TWOBOD to speed the computations. To this end, most array elements in TWOBOD are

initially redefined as real variables and the expressions for each of the quantities  $E_{ij}$  and  $D_i$  of Eqs. (6.23)-(6.25) are coded explicitly, rather than having the computer manipulate indices.

A subroutine named INTRNL, which supplies TWOBOD with time histories of the quantities  $F_i$ ,  $T_i$ ,  $B_{ij}$ , and of  $r_i$ ,  $\Omega_i$ , and their derivatives (see Eqs. (6.17)-(6.21)), must be supplied regardless of the nature of the motion of B relative to A. However, when A and B are hinged, the results of Sec. 6.2 may be embodied in INTRNL; and exactly such a version of INTRNL is included in Appendix A.2. In this particular version, the quantities  $F_i$  and  $T_i$  are equated to zero since the problems to be considered in the sequel deal only with torque-free motion. This feature can be easily modified, should the user so elect. The sole purpose of this version of INTRNL is to compute the quantities  $B_{ij}$ ,  $r_i$ ,  $\dot{r}_i$ ,  $\ddot{r}_i$ ,  $\Omega_i$ , and  $\ddot{\Omega}_i$  in accordance with Eqs. (6.38), (6.59), (6.63), (6.64), (6.66), and (6.67), respectively. To achieve this end, INTRNL must obtain the instantaneous values of the angle  $\alpha$  and its derivatives,  $\dot{\alpha}$  and  $\ddot{\alpha}$ . These values are supplied by a subroutine ALPHA which is called by INTRNL. In the course of its computations, INTRNL must also determine the quantities  $c_{ij}$  by means of Eq. (6.50).

In the derivation of Sec. 6.2, great care was taken to separate the quantities which depend on the angle  $\alpha$  (i.e., the time-varying terms) from those quantities, such as  $I_{ij}^B$ ,  $d_{ij}$ , and  $u_{ij}$ , which remain constant. This was done so that, in a computer program, this same separation could be effected. It is the task of subroutine BODIES to compute these constant terms once and for all prior to integration and to pass them to subroutine INTRNL via a block of COMMON named INTBLK. Recall



that BODIES also passes constants to subroutine TWOBOD via a COMMON block named BODBLK.

In order to supply subroutine BODIES with the requisite geometrical and inertia properties, it was decided to also assign BODIES the task of reading the data cards on which these properties are provided. Consequently, BODIES first reads four cards which contain the following quantities:

Card 1 -  $A_{11}$  ,  $A_{22}$  ,  $A_{33}$  ,  $A_{12}$  ,  $A_{13}$  ,  $A_{23}$  ,  $m_A$

Card 2 -  $a_1$  ,  $a_2$  ,  $a_3$  ,  $p_{11}$  ,  $p_{12}$  ,  $p_{13}$  ,  $p_{31}$  ,  $p_{32}$  ,  $p_{33}$

Card 3 -  $I_{11}^B$  ,  $I_{22}^B$  ,  $I_{33}^B$  ,  $I_{12}^B$  ,  $I_{13}^B$  ,  $I_{23}^B$  ,  $m_B$

Card 4 -  $b_1$  ,  $b_2$  ,  $b_3$  ,  $q_{11}$  ,  $q_{12}$  ,  $q_{13}$  ,  $q_{31}$  ,  $q_{32}$  ,  $q_{33}$

Next, the quantities  $p_{2i}$  ,  $q_{2i}$  ,  $d_{ij}$  ,  $e_{ij}$  ,  $f_{ij}$  ,  $u_i$  ,  $v_i$  , and  $w_i$  are computed following Eqs. (6.54), (6.55), (6.51)-(6.53) and (6.60)-

(6.62); and the quantities  $\frac{m_A m_B}{M}$  and  $\frac{m_B}{M}$  are also determined.

Finally, the quantities  $A_{ij}$  ,  $\frac{m_A m_B}{M}$  , and  $\frac{m_B}{M}$  are available to TWOBOD,

and  $d_{ij}$  ,  $e_{ij}$  ,  $f_{ij}$  ,  $u_i$  ,  $v_i$  ,  $w_i$  ,  $p_{ij}$  , and  $I_{ij}^B$  are available to

INTRNL since these quantities have been declared in the appropriate

COMMON statements.

Tables 6.1 through 6.5 summarize the features of these four subroutines. Table 6.1 lists the input data read by subroutine BODIES and Table 6.2 itemizes the terms stored in COMMON blocks by BODIES. Tables 6.3, 6.4, and 6.5 describe the quantities in the parameter lists of subroutines INTRNL, TWOBOD, and DFEQS1 and provide other useful information.

Table 6.1

Data Cards read by Subroutine BODIES

Symbol in BODIES	Symbol in analysis	Variable type	Definition
Card No. 1: Format (7F10.3)			
A(1,1) A(2,2) A(3,3) A(1,2) A(1,3) A(2,3)	$A_{11}$ $A_{22}$ $A_{33}$ $A_{12}$ $A_{13}$ $A_{23}$	Real Array	Moments & products of inertia of body A for $A^*$ , referred to $\underline{a}_1, \underline{a}_2, \underline{a}_3$ . See (6.16).
MA	$m_A$	Real	Mass of body A.
Card No. 2: Format (3F10.3, 2X, 6F8.3)			
A1 A2 A3	$a_1$ $a_2$ $a_3$	Real	Components of $\underline{a}$ , the position vector of C relative to $A^*$ , referred to $\underline{a}_1, \underline{a}_2, \underline{a}_3$ . See (6.57).
P11 P12 P13	$p_{11}$ $p_{12}$ $p_{13}$	Real	Components of $\underline{h}$ , the unit vector parallel to the hinge, referred to $\underline{a}_1, \underline{a}_2, \underline{a}_3$ . See (6.39).
P31 P32 P33	$p_{31}$ $p_{32}$ $p_{33}$	Real	Components of $\underline{n}_A$ , a unit vector fixed in A & normal to $\underline{h}$ , referred to $\underline{a}_1, \underline{a}_2, \underline{a}_3$ . See (6.40).
Card No. 3: Format (7F10.3)			
IB11 IB22 IB33 IB12 IB13 IB23	$I_{11}^B$ $I_{22}^B$ $I_{33}^B$ $I_{12}^B$ $I_{13}^B$ $I_{23}^B$	Real	Moments & products of inertia of body B for $B^*$ , referred to $\underline{b}_1, \underline{b}_2, \underline{b}_3$ . See (6.36).
MB	$m_B$	Real	Mass of body B.

Table 6.1 (continued)

Symbol in BODIES	Symbol in analysis	Variable type	Definition
Card No. 4:      Format (3F10.3, 2X, 6F8.3)			
B1 B2 B3	$b_1$ $b_2$ $b_3$	Real	Components of $\underline{b}$ , the position vector of C relative to $B^*$ , referred to $\underline{b}_1$ , $\underline{b}_2$ , $\underline{b}_3$ . See (6.58).
Q11 Q12 Q13	$q_{11}$ $q_{12}$ $q_{13}$	Real	Components of $\underline{h}$ , the unit vector parallel to the hinge, referred to $\underline{b}_1$ , $\underline{b}_2$ , $\underline{b}_3$ . See (6.41).
Q31 Q32 Q33	$q_{31}$ $q_{32}$ $q_{33}$	Real	Components of $\underline{n}_B$ , a unit vector fixed in B and normal to $\underline{h}$ , referred to $\underline{b}_1$ , $\underline{b}_2$ , $\underline{b}_3$ . See (6.42).

Subroutine BODIES has no parameter list .

Subroutines called: None

Named COMMON blocks: /BODBLK/ , /INTBLK/

Subroutine BODIES is called by the Main Program.

Table 6.2

Named COMMON /BODBLK/

Contained in subroutines BODIES and TWOBOD

Symbol in program	Symbol in analysis	Variable type	Definition
A	$\underline{I}^A$	Real Array	The $A_{ij}$ ; the inertia dyadic of body A for $A^*$ . See (6.16).
MM	$\frac{m_A m_B}{M}$	Real	See (6.25).
MBM	$\frac{m_B}{M}$	Real	See (6.25).

Named COMMON /INTBLK/

Contained in subroutines BODIES and INTRNL

Symbol in program	Symbol in analysis	Variable type	Definition
D11	$d_{11}$	Real	See (6.51).
D12	$d_{12}$		
D13	$d_{13}$		
D21	$d_{21}$		
D22	$d_{22}$		
D23	$d_{23}$		
D31	$d_{31}$		
D32	$d_{32}$		
D33	$d_{33}$		
E11	$e_{11}$	Real	See (6.52).
E12	$e_{12}$		
E13	$e_{13}$		
E21	$e_{21}$		
E22	$e_{22}$		
E23	$e_{23}$		
E31	$e_{31}$		
E32	$e_{32}$		
E33	$e_{33}$		

Table 6.2 (continued)

Symbol in program	Symbol in analysis	Variable type	Definition
F11	$f_{11}$	Real	See (6.53).
F12	$f_{12}$		
F13	$f_{13}$		
F21	$f_{21}$		
F22	$f_{22}$		
F23	$f_{23}$		
F31	$f_{31}$		
F32	$f_{32}$		
F33	$f_{33}$		
U1	$u_1$	Real	See (6.60).
U2	$u_2$		
U3	$u_3$		
V1	$v_1$	Real	See (6.61).
V2	$v_2$		
V3	$v_3$		
W1	$w_1$	Real	See (6.62).
W2	$w_2$		
W3	$w_3$		
P11	$p_{11}$	Real	$\underline{h} \cdot \underline{a}_1$
P12	$p_{12}$		$\underline{h} \cdot \underline{a}_2$
P13	$p_{13}$		$\underline{h} \cdot \underline{a}_3$
IB11	$I_{11}^B$	Real	Moments and products of inertia of B for $B^*$ , referred to $\underline{b}_1$ , $\underline{b}_2$ , $\underline{b}_3$ . See (6.36).
IB12	$I_{12}^B$		
IB13	$I_{13}^B$		
IB22	$I_{22}^B$		
IB23	$I_{23}^B$		
IB33	$I_{33}^B$		

Table 6.3

Subroutine INTRNL (T,F,MA,B,WBA,DWBA,R,DR,DDR)

Symbol in parameter list	Symbol in analysis	Variable type	Definition
T	t	Real	Time.
F	$\underline{F}$	Real Array	$(F_1, F_2, F_3)$ ; the resultant of the forces acting on bodies A & B . See (6.17).
MA	$\underline{T}$	Real Array	$(T_1, T_2, T_3)$ ; the moment of the force system about $A^*$ . See (6.18).
B	$\underline{I}^B$	Real Array	Centroidal inertia dyadic of body B , referred to $\underline{a}_1, \underline{a}_2, \underline{a}_3$ ; the $B_{ij}$ . See (6.19) and (6.38).
WBA	$\underline{\omega}^{A/B}$	Real Array	$(\Omega_1, \Omega_2, \Omega_3)$ ; the angular velocity of B in A . See (6.21) and (6.66).
DWBA	$\frac{d}{dt} \underline{\omega}^{A/B}$	Real Array	$(\dot{\Omega}_1, \dot{\Omega}_2, \dot{\Omega}_3)$ ; the time derivative in A of $\underline{\omega}^{A/B}$ . See (6.67).
R	$\underline{r}$	Real Array	$(r_1, r_2, r_3)$ ; the position vector of $B^*$ relative to $A^*$ . See (6.20) and (6.59).
DR	$\frac{d}{dt} \underline{r}$	Real Array	$(\dot{r}_1, \dot{r}_2, \dot{r}_3)$ ; the time derivative in A of $\underline{r}$ . See (6.63).
DDR	$\frac{d^2}{dt^2} \underline{r}$	Real Array	$(\ddot{r}_1, \ddot{r}_2, \ddot{r}_3)$ ; the second time derivative in A of $\underline{r}$ . See (6.64).

Subroutines called: ALPHA (T,ALF,DALF,DDALF)

Named COMMON blocks: /INTBLK/

Subroutine INTRNL is called by subroutine TWOBOD .

Table 6.4

Subroutine TWOBOD (T,WAF,DWAF)

Symbol in parameter list	Symbol in analysis	Variable type	Definition
T	t	Real	Time.
WAF	$\underline{\omega}^A$	Real Array	$(\omega_1, \omega_2, \omega_3)$ ; the inertial angular velocity of body A . See (6.15).
DWAF	$\underline{\dot{\omega}}^A$	Real Array	$(\dot{\omega}_1, \dot{\omega}_2, \dot{\omega}_3)$ ; the inertial angular acceleration of body A . See (6.33)- (6.35).

Subroutines called: INTRNL (T,F,MA,B,WBA,DWBA,R,DR,DDR)

Named COMMON blocks: /BODBLK/

Subroutine TWOBOD is called by subroutine DFEQS1.

Table 6.5

Subroutine DFEQS1 (NEQ,X,STEP,Y,F,EPS,\*)

(Courtesy Stanford Computation Center)

Symbol in parameter list	Symbol in analysis	Variable type	Definition
NEQ	3	Integer	Size of dependent variable array.
X	t	Real	Independent variable (time).
STEP		Real	Length of integration interval.
Y	$\underline{A}$ $\underline{\omega}$	Real Array	Array of dependent variables, e.g., ( $\omega_1$ , $\omega_2$ , $\omega_3$ ).
F		Sub- routine	Subroutine providing the differen- tial equations, e.g., TWOBOD.
EPS		Real	Relative error tolerance per integra- tion step, typically $10^{-5}$ .
*		Return Label	Transfers control to main program if specified accuracy cannot be obtained.

Subroutines called: F (i.e., TWOBOD)

Named COMMON blocks: None

Subroutine DFEQS1 is called by the Main Program.

(The Main Program must contain an EXTERNAL TWOBOD statement.)



Of course, these four subroutines alone do not comprise a complete computer program. Unfortunately, the additional subprograms which are required depend more heavily on the nature of the particular problem being considered and on the input-output format desired by the user. Consequently, it is more difficult to maintain generality while documenting additional subprograms. Nevertheless, to perform the computations outlined in the sequel, a complete program must be written and one will be described here with the understanding that it may not be suitable, or even readily adaptable, for other purposes. In fact, this version of the program cannot even be used to generate data points for some of the illuminating, but non-essential, graphs in the sequel (e.g., Figs. 7.4, 7.6, or the graph of  $\varphi$  in Fig. 8.2). There are three subprograms to be considered, subroutines ALPHA and OUTPUT, and the main program, itself. Complete listings of these subprograms are contained in Appendix A.3.

The medium for prescribing motions of  $B$  relative to  $A$  is a subroutine ALPHA which is called by INTRNL and which must provide the instantaneous values of the angle  $\alpha$  and of its time derivatives,  $\dot{\alpha}$  and  $\ddot{\alpha}$ . Thus far, no functional form for  $\alpha$  has been presented and, indeed, finding appropriate forms is the central topic of Sec. 7.3. However, for illustrative purposes, a subroutine ALPHA which performs computations discussed in Secs. 7.3 and 8.2 is presented in Appendix A.3. The particular function for  $\alpha$  prescribed therein is of the form of Eq. (7.27) which is plotted in Fig. 7.2. This function has the nature of a pulse and is dependent on two parameters, an amplitude and a period, which are supplied to ALPHA by the main program via a COMMON block named ALFBLK. Thus, the main program is somewhat related to the nature of subroutine

ALPHA. It is probable that the user will wish to prescribe a different type of time history for  $\alpha$ , in which case he must write a new subroutine and must, perhaps, rewrite parts of the main program. This new subroutine must also be named ALPHA if it is to be called by the present version of subroutine INTRNL.

We next consider the varied roles of the main program whose first duty is to write a heading for the first page of output. The main program then calls on subroutine BODIES to read in values of inertia properties. Next, the main program reads in the initial conditions for the motion, namely, the initial time, the initial values of  $\omega_1$ ,  $\omega_2$ ,  $\omega_3$ , and an integer  $N$  which indicates the number of pulses of the relative motion to be performed. Then, a succession of  $N$  data cards, each containing a pulse amplitude and period, and an integer indicating the number of print-outs to be made during that pulse, are read by the main program. All that remains is for the main program to call DFEQS1 each time that a step of integration is to be performed. Two time variables are maintained in the main program. One, TIME, starts at an initial value indicated on a data card and increases continually, representing real time; a second variable,  $T$ , is reset to zero at the beginning of every pulse of relative motion. Finally, the one remaining task of the main program is that of periodically calling subroutine OUTPUT which writes out the instantaneous values of TIME,  $\alpha$ ,  $\omega_1$ ,  $\omega_2$ , and  $\omega_3$ . If there are additional items which one wishes to compute and which are functions of the angular rates and of  $\alpha$ ,  $\dot{\alpha}$ , and  $\ddot{\alpha}$  (e.g., the kinetic energy, as seen in Fig. 7.4), these computations can often be incorporated into subroutine OUTPUT.

The program whose parts are listed in Appendices A.2 and A.3 may be employed to verify some of the results presented in the sequel or may be used to perform similar calculations. To accomplish these ends, the program user need only know how to furnish data cards. Table 6.6 presents a list of symbols, definitions, and formats for these data cards. Sample data cards for two examples considered in the sequel (see Figs. 7.3, 7.5, and  $\alpha$  of Fig. 8.2) are given at the end of Appendix A.3; and the corresponding output pages for these examples are presented in Appendix A.4. Any number of examples can be handled, in turn, by the program, provided that a complete set of data cards is submitted for each example. Additional information concerning the main program is contained in Table 6.7; and complete definitions of the items appearing in the parameter lists of subroutines ALPHA and OUTPUT are presented in Tables 6.8 and 6.9, respectively.

Two additional points should be made: Firstly, any compatible system of units can be employed for time, length, and mass; the only restrictions on units employed in the program under consideration are that initial angular rates be specified in radians per time unit (see Data Card No. 5 in Table 6.6) and that the amplitude of  $\alpha$  be given in degrees (see Data Cards Nos. 5+I in Table 6.6). Secondly, it will be convenient in the sequel to non-dimensionalize time in such a way that the system of two bodies, when spinning as a quasi-rigid body about a particular principal axis, performs one revolution per time unit. This can be accomplished by choosing the initial angular velocities (see Data Card No. 5 in Table 6.6) in such a way that the magnitude of the angular velocity of the system, when spinning about this principal axis, becomes  $2\pi$ . This procedure is followed in both examples in Appendix A.4.

Table 6.6

Data Cards:

The first 4 data cards are read in by subroutine BODIES.

See Table 6.1 for details.

The following data cards are read by the Main Program.

Symbol in program	Symbol in analysis	Variable type	Description
Card No. 5: Format (4F10.3,I10)			
TO		Real	Initial time.
W(1) W(2) W(3)		Real Array	Initial values of $\omega_1$ , $\omega_2$ , $\omega_3$ , the components of the angular velocity of A, in radians per time unit.
N		Integer	The number of cards which follow, each containing parameters for one pulse of relative motion.
Cards Nos. 5 + I, I = 1,N Format (2F10.2,I10)			
AMPL(I)	$\Gamma_i$	Element of Real Array	Amplitude of the $i^{\text{th}}$ cycle of relative motion, in degrees. See (7.27) and Fig. 7.2.
PD(I)	$T_i$	Element of Real Array	Period of the $i^{\text{th}}$ cycle of relative motion. See (7.27) and Fig. 7.2.
NPRNT(I)		Element of Integer Array	Number of print-outs to occur during the $i^{\text{th}}$ cycle of relative motion.

Table 6.7

Main Program

Subroutines called: BODIES  
 OUTPUT (TIME,T,WAF)  
 OUT2 (a second entry to OUTPUT)  
 DFEQS1 (NEQ,X,STEP,Y,F,EPS,\*)

Named COMMON blocks: /ALFBLK/

Symbol in /ALFBLK/	Symbol in analysis	Variable type	Definition
PERIOD	T	Real	Duration of pulse of $\alpha$ . See (7.27) and Fig. 7.2.
AMPLTD	$\Gamma$	Real	Amplitude, in radians, of pulse of $\alpha$ . See (7.27) and Fig. 7.2.

Table 6.8

Subroutine ALPHA (T,ALF,DALF,DDALF)

Symbol in parameter list	Symbol in analysis	Variable type	Definition
T	$\xi$	Real	Time from the start of a cycle of relative motion. See (7.27).
ALF	$\alpha$	Real	The angle between $\underline{n}_A$ and $\underline{n}_B$ . See Fig. 6.2.
DALF	$\dot{\alpha}$	Real	Time derivative of $\alpha$ .
DDALF	$\ddot{\alpha}$	Real	Second derivative of $\alpha$ .

Subroutines called: None

Named COMMON blocks: /ALFBLK/

Subroutine ALPHA is called by subroutine INTRNL.

Table 6.9

Subroutine OUTPUT (TIME,T,WAF)

Symbol in parameter list	Symbol in analysis	Variable type	Definition
TIME	t	Real	Time.
T	$\xi$	Real	Time from start of a cycle of relative motion. See (7.27).
WAF	$\underline{\omega}^A$	Real Array	$(\omega_1, \omega_2, \omega_3)$ ; the inertial angular velocity of body A. See (6.15).

Symbol in  
Output

TIME	t	Real	Time.
ALPHA	$\alpha$	Real	Angle between $\underline{n}_A$ and $\underline{n}_B$ . See Fig. 6.2.
W(1) W(2) W(3)	$\omega_1$ $\omega_2$ $\omega_3$	Elements of Real Array	The inertial angular velocity of body A. See (6.15).

Subroutines called: ALPHA(T,ALF,DALF,DDALF)

Named COMMON blocks: None

Subroutine OUTPUT is called by the Main Program.

## 7. Alteration of Attitude Motions of a Tumbling Man

### 7.1 Description

Suppose that a man in free fall is tumbling while holding his limbs in the position of "attention." He may wish to convert this motion, by means of limb maneuvers, into a simple spin in which he again assumes the original quasi-rigid state (i.e., in which he again occupies a position of "attention"). In all probability, he would wish to be spinning about an axis parallel to his roll axis, because this is the axis of maximum centroidal moment of inertia, and the associated rotation thus proceeds with minimum angular speed. For example, if the initial motion was also a simple spin, but about the yaw axis, conversion of the motion to roll would reduce the spin rate by a factor of 13.4.

If we require the man to maneuver by swinging one arm in a torso-fixed plane while keeping all other limbs fixed relative to the torso, then he can be modelled as a system of two hinged rigid bodies; the analyses in Secs. 6.1 and 6.2 are applicable; and the equations of motion (6.33)-(6.35) can be integrated (numerically), once initial values of the components of the inertial angular velocity of the torso have been given, provided that a suitable expression for the function governing the motion of the arm relative to the torso is available. A procedure for obtaining functions which cause a tumbling motion to be converted to simple spin is presented in Sec. 7.3. First, however, an appropriate model of the man is described in Sec. 7.2.

## 7.2 Model

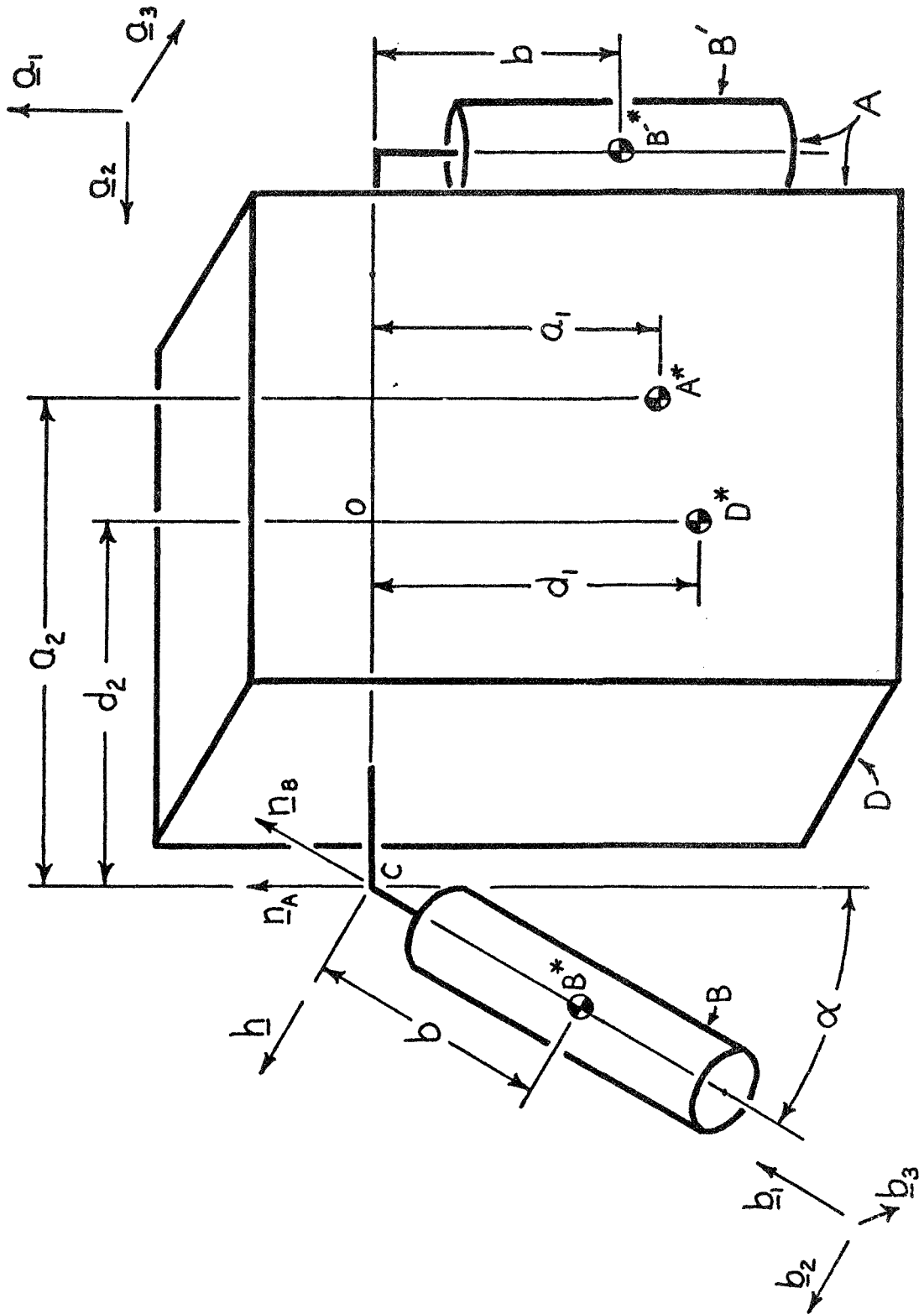
The human is modelled as a system of two rigid bodies, A and B, hinged together about an axis passing through a point C. The main body A is comprised of the torso, head, straightened legs, and, say, the left arm. Body B represents the movable right arm and C represents the shoulder joint.

Body B is assumed to be axially symmetric about a line joining its mass center  $B^*$  to C, the distance from  $B^*$  to C being  $b$ . Arm B has a mass  $m_B$  and moments of inertia  $I_1^B$  about its symmetry axis and  $I_2^B$  about any line passing through  $B^*$  and normal to the symmetry axis. Mutually perpendicular unit vectors,  $\underline{b}_1, \underline{b}_2, \underline{b}_3$ , are fixed in B, with  $\underline{b}_1$  parallel to the symmetry axis and with the direction of  $\underline{b}_3$  chosen arbitrarily (provided, of course, that it is normal to  $\underline{b}_1$ ).

The mass center  $A^*$  of body A is located relative to C by a distance  $a_2$  parallel to the pitch axis and a distance  $a_1$  parallel to the yaw axis (see Fig. 7.1). Letting  $\underline{a}_1, \underline{a}_2, \underline{a}_3$  be mutually perpendicular unit vectors parallel to the yaw, pitch, and roll axes, respectively, then quantities  $A_{ij}$  represent the centroidal moments and products of inertia of A referred to the  $\underline{a}_i$  and  $\underline{a}_j$  directions. Finally, the mass of A is  $m_A$ .

Although body A is rigid, it may be regarded as being composed of two bodies. One, D, represents the torso, head, and legs and the other, B', represents the left arm and is identical to B. Body D has a mass  $m_D$  and centroidal principal moments of inertia  $D_1, D_2, D_3$  about the yaw, pitch, and roll axes, respectively. ( $D_1, D_2, D_3$  correspond to





Model of man moving one arm

Fig. 7.1

$I_3^A$ ,  $I_2^A$ ,  $I_1^A$ , respectively, in the case where the legs are straight in Table 4.1.) The mass center  $D^*$  of  $D$  is located on the yaw axis at a distance  $d_1$  from the midpoint  $O$  of a line of length  $2d_2$  joining the shoulders (see Fig. 7.1).

In terms of the inertia properties of  $D$  and  $B'$ , the mass of  $A$  is given by

$$m_A = m_D + m_B \quad (7.1)$$

the moments and products of inertia of  $A$  for  $A^*$  by

$$A_{11} = D_1 + I_1^B + \frac{m_B m_D}{m_A} d_2^2 \quad (7.2)$$

$$A_{22} = D_2 + I_2^B + \frac{m_B m_D}{m_A} (d_1 - b)^2 \quad (7.3)$$

$$A_{33} = D_3 + I_2^B + \frac{m_B m_D}{m_A} [(d_1 - b)^2 + d_2^2] \quad (7.4)$$

$$A_{12} = A_{21} = \frac{m_B m_D}{m_A} (d_1 - b) d_2 \quad (7.5)$$

$$A_{13} = A_{31} = A_{23} = A_{32} = 0 \quad (7.6)$$

and the distances relating  $A^*$  to  $C$  by

$$a_1 = \frac{m_D d_1 + m_B b}{m_A} \quad (7.7)$$

$$a_2 = \left( \frac{m_D + 2m_B}{m_A} \right) d_2 \quad (7.8)$$

Table 7.1 lists appropriate values of the inertia properties of bodies  $A$  and  $B$  for an average man (see Sec. 1.3) holding his legs straight, with and without five-pound weights in his hands.

Table 7.1

Symbol	With no weights	With 5-lb. weights in each hand	Units
Body A			
$m_A$	4.74	4.89	slugs
$a_1$	1.447	1.465	feet
$a_2$	0.705	0.725	feet
$A_{11}$	0.536	0.594	slug-ft. <sup>2</sup>
$A_{22}$	8.35	8.40	slug-ft. <sup>2</sup>
$A_{33}$	8.67	8.78	slug-ft. <sup>2</sup>
$A_{12} , A_{21}$	0.1054	0.0514	slug-ft. <sup>2</sup>
Body B			
$m_B$	0.289	0.445	slugs
$b$	0.899	1.291	feet
$I_1^B$	0.0030	0.0030	slug-ft. <sup>2</sup>
$I_2^B$	0.1331	0.261	slug-ft. <sup>2</sup>

The inertia properties of bodies A and B have been presented in forms suitable for use with the equations of motion in Secs. 6.1 and 6.2. For instance, the centroidal inertia dyadic of A may be expressed as

$$\underline{I}^A = \sum_{i=1}^3 \sum_{j=1}^3 A_{ij} \underline{a}_i \underline{a}_j \quad (7.9)$$

The inertia dyadic of B for  $B^*$  is given by

$$\underline{I}^B = I_1^B \underline{b}_1 \underline{b}_1 + I_2^B \underline{b}_2 \underline{b}_2 + I_3^B \underline{b}_3 \underline{b}_3 \quad (7.10)$$

and  $\underline{a}$  and  $\underline{b}$ , the position vectors of C relative to  $A^*$  and  $B^*$ , respectively, are given by (see Fig. 7.1)

$$\underline{a} = a_1 \underline{a}_1 + a_2 \underline{a}_2 \quad (7.11)$$

$$\underline{b} = b \underline{b}_1 \quad (7.12)$$

Motion of arm B relative to A may be described in terms of three unit vectors,  $\underline{n}_A$ ,  $\underline{n}_B$ , and  $\underline{h}$  (see Sec. 6.2). Vectors  $\underline{n}_A$  and  $\underline{n}_B$  are parallel to  $\underline{a}_1$  and  $\underline{b}_1$ , respectively, so that the angle  $\alpha$  between them is zero when the arm is held at the side (see Fig. 7.1). The hinge vector  $\underline{h}$  must then be parallel to the yaw plane and defines the normal to the torso-fixed plane in which the symmetry axis of the arm moves. For instance, when  $\underline{h}$  is equal to  $-\underline{a}_3$ , the arm's symmetry axis must remain in the roll plane.

Finally, it will be helpful in the sequel to know some of the inertia properties of the system comprised of A and B in its quasi-rigid state (i.e., when  $\alpha$  is zero). Letting  $I_1$ ,  $I_2$ ,  $I_3$  denote the centroidal principal moments of inertia of the system about axes parallel to the yaw, pitch, and roll axes, respectively, one can express  $I_1$ ,  $I_2$ , and  $I_3$  as

$$I_1 = D_1 + 2I_1^B + 2m_B d_2^2 \quad (7.13)$$

$$I_2 = D_2 + 2I_2^B + \frac{2m_B m_D}{m_D + 2m_B} (b - d_1)^2 \quad (7.14)$$

$$I_3 = D_3 + 2I_2^B + 2m_B \left[ d_2^2 + \frac{m_D}{m_D + 2m_B} (b - d_1)^2 \right] \quad (7.15)$$

Values for  $I_1$ ,  $I_2$ , and  $I_3$  for a man standing at attention with, and without, five-pound weights in his hands are listed in Table 7.2.

Table 7.2

Symbol	With no weights	With 5-lb. weights in each hand	Units
$I_1$	0.674	0.811	slug-ft. <sup>2</sup>
$I_2$	8.57	8.67	slug-ft. <sup>2</sup>
$I_3$	9.02	9.26	slug-ft. <sup>2</sup>

### 7.3 Procedure

A procedure employing the concepts in Sec. 5.1 will now be applied to the following problem: How can one find an analytical expression for  $\alpha$  as a function of time  $t$  such that, if a man is initially spinning about his yaw axis and if he moves his arm relative to his torso in accordance with that function, his motion will be converted into a spin about the roll axis at the instant when his arm returns to his side? Essentially this is a boundary value problem in which  $\alpha$ , its time derivative, and the components  $\omega_1$ ,  $\omega_2$ ,  $\omega_3$  of the inertial angular velocity of the torso of the man are prescribed at an initial and at an, as yet unspecified, final time.

It is helpful to designate by  $\Omega_0$  the magnitude of the initial angular velocity. Then a non-dimensional time  $\tau$  can be defined as

$$\tau = \frac{\Omega_o t}{2\pi} \quad (7.16)$$

and, thus, one non-dimensional time unit is the time required for the man to complete one revolution about the yaw axis in his initial state of motion.

If  $\tau_o$  represents the initial non-dimensional time and  $\tau_n$  (for reasons which will soon become apparent) represents the time at which the arm maneuver terminates, then the boundary conditions on  $\omega_1$ ,  $\omega_2$ ,  $\omega_3$  are given at  $\tau_o$  by

$$\omega_1(\tau_o) = \Omega_o, \quad \omega_2(\tau_o) = \omega_3(\tau_o) = 0 \quad (7.17)$$

and at  $\tau_n$  by

$$\omega_1(\tau_n) = \omega_2(\tau_n) = 0, \quad \omega_3(\tau_n) = \Omega_n \quad (7.18)$$

where, in view of angular momentum considerations,

$$|\Omega_n| = \frac{I_1}{I_3} |\Omega_o| \quad (7.19)$$

and  $I_1$  and  $I_3$  are obtained from Table 7.2. The function  $\alpha(\tau)$  also must satisfy boundary conditions which insure that the man assumes his quasi-rigid state at  $\tau_o$  and  $\tau_n$ ; i.e.,

$$\alpha(\tau_o) = 0, \quad \alpha'(\tau_o) = 0 \quad (7.20)$$

$$\alpha(\tau_n) = 0, \quad \alpha'(\tau_n) = 0 \quad (7.21)$$

where the prime denotes differentiation with respect to  $\tau$ . Physical constraints when the arm is at the side or above the head require, roughly, that

$$0 \leq \alpha(\tau) \leq 180^\circ \quad (7.22)$$

for  $\tau$  in the open interval  $(\tau_o, \tau_n)$ .

We proceed by computing  $K(\tau_o)$ , the kinetic energy at  $\tau_o$ , and  $K(\tau_n)$ , the desired kinetic energy at  $\tau_n$ :

$$K(\tau_o) = \frac{1}{2} I_1 \Omega_o^2 \quad (7.23)$$

(5.4, 7.17)

$$K(\tau_n) = \frac{1}{2} I_1 \left( \frac{I_1}{I_3} \right) \Omega_o^2 \quad (7.24)$$

(5.4, 7.18, 7.19)

Next,  $\alpha(\tau)$  is determined in a piecewise manner. As the first step, a function  $\gamma(\xi; \Gamma, T)$  is chosen which satisfies

$$\gamma(0; \Gamma, T) = 0, \quad \gamma'(0; \Gamma, T) = 0 \quad (7.25)$$

$$\gamma(T; \Gamma, T) = 0, \quad \gamma'(T; \Gamma, T) = 0 \quad (7.26)$$

One choice of such a function is (see Fig. 7.2)

$$\gamma(\xi; \Gamma, T) = \left\{ \begin{array}{ll} \Gamma \left[ 2 \frac{\xi}{T} - \frac{1}{2\pi} \sin 4\pi \frac{\xi}{T} \right] & 0 \leq \xi \leq \frac{T}{2} \\ \Gamma \left[ 2 \left( 1 - \frac{\xi}{T} \right) + \frac{1}{2\pi} \sin 4\pi \frac{\xi}{T} \right] & \frac{T}{2} \leq \xi \leq T \end{array} \right\} \quad (7.27)$$

The parameters  $\Gamma$  and  $T$  control the amplitude and period, respectively, of the pulse shown in Fig. 7.2. These can be chosen arbitrarily, provided

$$0 \leq \Gamma \leq 180^\circ \quad (7.28)$$

in order to satisfy Eq. (7.22). Suppose that values for  $\Gamma$  and  $T$ ,

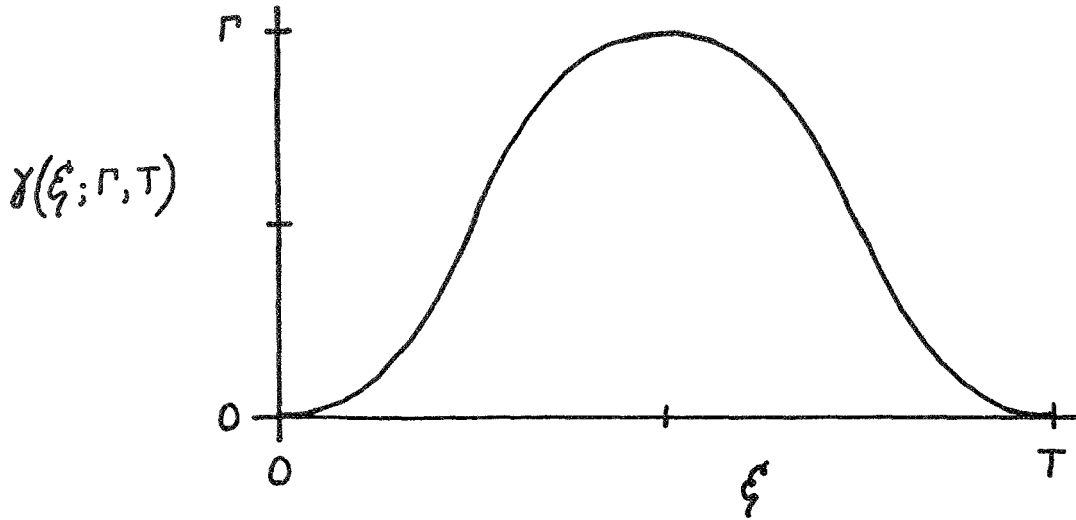


Fig. 7.2

$\gamma(\xi; \Gamma, T)$

designated  $\Gamma_1$  and  $T_1$ , are chosen and the equations of motion (6.33)-(6.35), with  $\alpha(t)$  replaced by  $\gamma(\tau - \tau_0; \Gamma_1, T_1)$  are integrated\* for  $\tau_0 \leq \tau \leq \tau_1$  where

$$\tau_1 = \tau_0 + T_1 \quad (7.29)$$

The kinetic energy at time  $\tau_1$  can be calculated using Eq. (5.4) and compared to  $K(\tau_0)$  and  $K(\tau_n)$  (see (7.23), (7.24)). If the relation

$$\left| K(\tau_1) - K(\tau_n) \right| < \left| K(\tau_0) - K(\tau_n) \right| \quad (7.30)$$

---

\*The computer program, documented in Sec. 6.3, may be employed for this integration by setting  $\omega_1(0) = 2\pi$  to obtain the proper relationship between time and initial angular rates. The components of angular velocity printed out by the computer should then be regarded as  $2\pi \omega_1 / \Omega_0$ ,  $2\pi \omega_2 / \Omega_0$ ,  $2\pi \omega_3 / \Omega_0$  and the time should be regarded as non-dimensional.



is not satisfied, new choices of values for  $\Gamma_1$  and  $T_1$  can be tried until values are found for which (7.30) is satisfied. In most cases, some choice of values for  $\Gamma_1$  and  $T_1$  can be found which lead to satisfaction of (7.30). There are, however, cases in which this is not so, and this possibility will be discussed later.

With Eq. (7.30) satisfied,  $\omega_1(\tau_1)$ ,  $\omega_2(\tau_1)$ ,  $\omega_3(\tau_1)$  become new initial conditions at a new initial time  $\tau_1$ . New choices of  $\Gamma$  and  $T$ , designated  $\Gamma_2$  and  $T_2$ , are made and the equations of motion, now using  $\gamma(\tau - \tau_1; \Gamma_2, T_2)$  in place of  $\alpha(t)$  are integrated for  $\tau_1 \leq \tau \leq \tau_2$  where

$$\tau_2 = \tau_1 + T_2 \quad (7.31)$$

The kinetic energy  $K(\tau_2)$  at time  $\tau_2$  is compared to  $K(\tau_1)$  and  $K(\tau_n)$ . If

$$|K(\tau_2) - K(\tau_n)| < |K(\tau_1) - K(\tau_n)| \quad (7.32)$$

then the values of  $\Gamma_2$  and  $T_2$  are accepted; and if (7.32) does not hold, new values must be selected for  $\Gamma_2$  and  $T_2$ .

This process may be repeated indefinitely and, in this manner, a series of cycles of the form of (7.27) is generated and, at the end of each cycle, the kinetic energy is brought closer to  $K(\tau_n)$ . The process may be terminated after, say, the  $n^{\text{th}}$  cycle when  $\omega_1$ ,  $\omega_2$ ,  $\omega_3$  are as close as desired to their values in (7.18) and  $\tau_n$  is given by

$$\tau_n = \sum_{i=1}^n T_i \quad (7.33)$$

The function  $\alpha(\tau)$ , which is the solution to the problem governed by Eqs. (6.33)-(6.35) and (7.17)-(7.22), is

$$\alpha(\tau) = \left\{ \begin{array}{ll} \gamma(\tau - \tau_0; \Gamma_1, T_1) & \tau_0 \leq \tau \leq \tau_1 \\ \gamma(\tau - \tau_1; \Gamma_2, T_2) & \tau_1 \leq \tau \leq \tau_2 \\ \dots\dots\dots & \\ \gamma(\tau - \tau_{n-1}; \Gamma_n, T_n) & \tau_{n-1} \leq \tau \leq \tau_n \end{array} \right\} \quad (7.34)$$

The solution can be specified by providing a functional form such as (7.27) and by tabulating the duration  $T_i$  and amplitude  $\Gamma_i$  of each of the  $n$  cycles.

This method of solution is also suitable for problems in which the initial motion is one of tumbling rather than spin. In fact, in the procedure just discussed, the motion of the man in his quasi-rigid state prior to every cycle of arm motion, except the first, is one of tumbling. If the desired final motion is other than a simple spin about the axes corresponding to  $I_1$  and  $I_3$ , however, this procedure fails since an infinite number of combinations of  $\omega_1, \omega_2, \omega_3$  are compatible with a given angular momentum and kinetic energy other than  $K_1$  and  $K_3$  as defined in Eqs. (5.9) and (5.10).

Finally, we consider the possibility that no choice of values for  $\Gamma$  and  $T$  will lead to an improvement in the value of the kinetic energy. Such a situation will always occur when the initial motion of two hinged bodies is one of simple spin and the relative motion of the bodies is such that the orientation in the main body of the principal axis which

is originally aligned with the angular velocity vector remains unchanged. In this case, a new form of relative motion must be chosen. (One such example appears in Sec. 7.4.)

It is more probable, however, that the range of values of  $\Gamma$  and  $T$  under consideration is limited for physical or computational reasons (e.g., see (7.28)). In this case, it may occur that no values of  $\Gamma$  and  $T$  within the permissible range lead to improvements in the value of the kinetic energy. One way to overcome this difficulty is to change the functional form of  $\gamma$ . Often, however, it is simpler to set  $\Gamma$  equal to zero for a short time and thus to allow the system to tumble in its quasi-rigid state. While this leads to no change in kinetic energy, it may yield more favorable initial conditions from which a change in energy is possible in the next cycle with a choice of  $\Gamma$  and  $T$  from the range of permissible values.

#### 7.4 Results

The procedure described in the previous section allows considerable leeway in the manner in which values of  $\Gamma$  and  $T$  are chosen. Let us employ a specific algorithm to make these choices and consider the problem posed in Sec. 7.3, assuming, in addition, that the man is holding a five-pound weight in each hand and that  $\underline{h}$  is equal to  $-\underline{a}_3$ . Taking  $\tau_0$  equal to zero (e.g., in (7.17), (7.20), and (7.23)) and deciding arbitrarily to set  $\Gamma_1$  equal to 135 degrees, we can select various values for  $T$  between, say, zero and eleven time units and can integrate the equations of motion for  $0 \leq \tau \leq T$ . The value of  $T$  (to within  $\pm .2$  time units) which causes  $K(T)$  to be a minimum will be designated  $T_1$ .

Thus  $T_1$  is found to be 2.8 time units. This process may be repeated, and  $T_2$ ,  $T_3$ , and  $T_4$  are found to be 2.8, 7.0, and 10.2 time units, respectively. The function  $\alpha(\tau)$  representing these four cycles is plotted in Fig. 7.3 and is presented in tabular form in Table 7.3.

Table 7.3

Cycle	1	2	3	4
$\Gamma_i$	135°	135°	135°	135°
$T_i$	2.8	2.8	7.0	10.2
$\tau_i$	2.8	5.6	12.6	22.8

At the conclusion of the fourth cycle of arm maneuver (i.e., when  $\tau = \tau_4 = 22.8$ ), the kinetic energy  $K$  is sufficiently close to  $K(\tau_n)$  (see (7.24)), the minimum attainable value, and so  $n$  is taken to be 4. In Fig. 7.4,  $K$  is plotted as a function of  $\tau$  and it can be seen that  $K$  decreases from  $K_1$ , the maximum possible value (compatible with the initial motion) which the man can attain in his quasi-rigid state, to  $K_3$ , the minimum possible value. Notice that sometimes (e.g., when  $\tau = 9.0$  or  $\tau = 18.0$ ) the value of  $K$  becomes less than  $K_3$ . This should not be construed as contradicting statement (1) of Sec. 5.1 since the remarks regarding the boundedness of  $K$  apply only when the system is in its quasi-rigid state, a situation which occurs only when  $\tau$  is less than or equal to  $\tau_0$ , equal to  $\tau_1$ ,  $\tau_2$ , or  $\tau_3$ , and equal to or greater than  $\tau_4$ .

Fig. 7.3  $\alpha$  as a function of  $\tau$  (see Table 7.3)

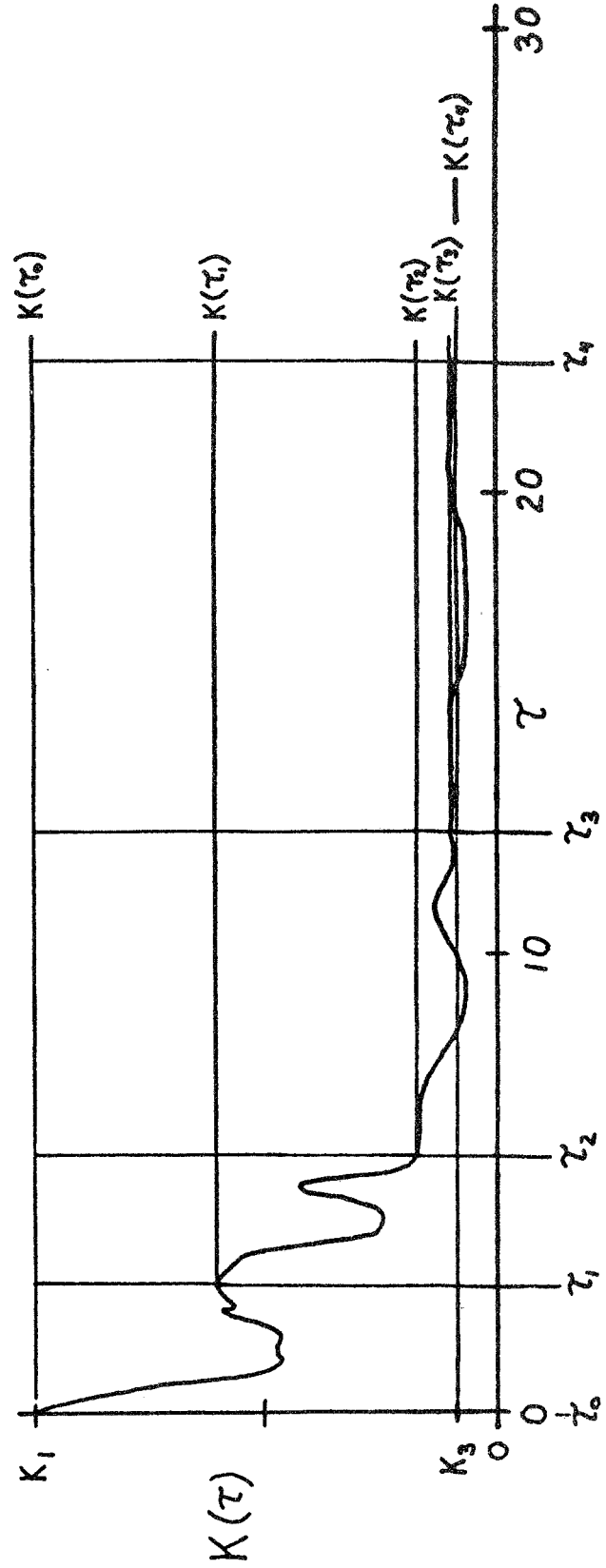
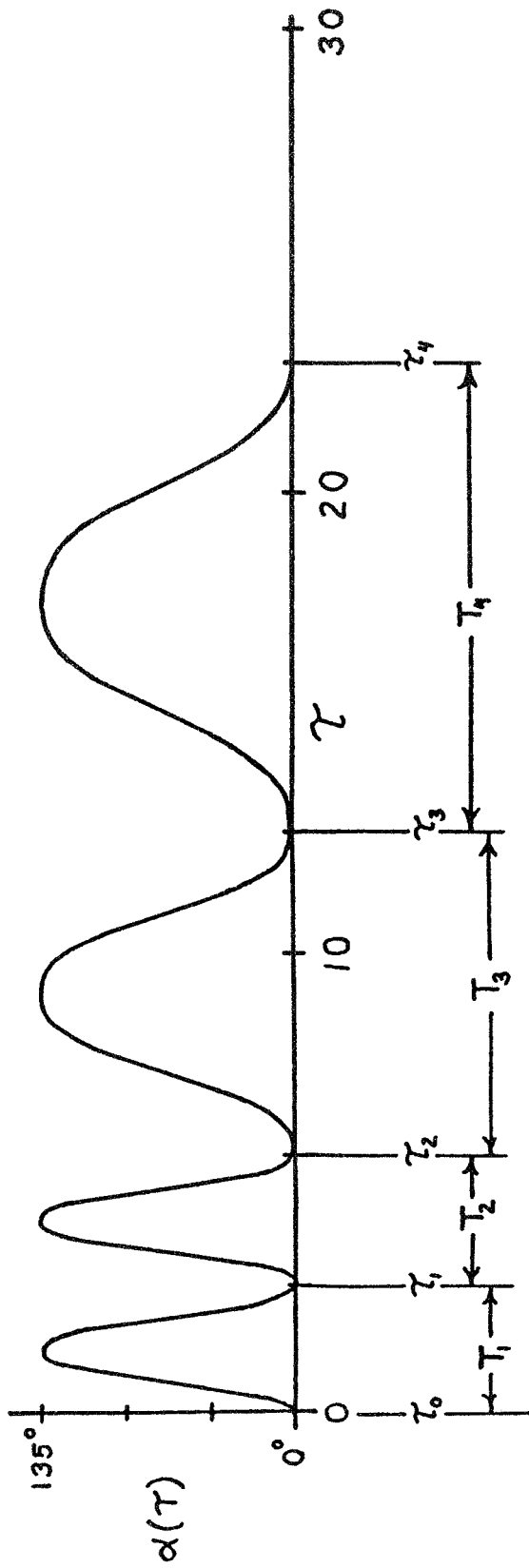


Fig. 7.4 Kinetic energy as a function of  $\tau$

The plot of  $\alpha$  as a function of  $\tau$  in Fig. 7.3 provides a fairly graphic description of the motion of the arm relative to the torso. Attempts to describe the motion of the torso in inertial space, however, are rendered difficult by the complexity of the motion. For instance, the components of the angular velocity of the torso, referred to  $\underline{a}_1$ ,  $\underline{a}_2$ ,  $\underline{a}_3$  (see Fig. 7.1), can be plotted as functions of time. Such a graph is presented in Fig. 7.5; and a first glance reveals the highly oscillatory nature of  $\omega_1$ ,  $\omega_2$ ,  $\omega_3$ . It is possible to verify that the boundary conditions (i.e., Eqs. (7.17)-(7.19)) for  $\omega_1$ ,  $\omega_2$ ,  $\omega_3$  are indeed satisfied; when  $\tau$  is equal to  $\tau_0$ ,  $\omega_1$  is the only non-zero component of angular velocity and, when  $\tau$  equals  $\tau_n$ ,  $\omega_3$  is non-zero and  $\omega_1$  and  $\omega_2$  are sufficiently close to zero.

Perhaps a more helpful way of illustrating attitude motion is to consider attitude variables rather than angular rates. For instance,  $\theta_r$ , the angle between the roll axis of the man and the direction of the (inertially fixed) angular momentum vector  $\underline{H}$ , is plotted as a function of  $\tau$  in Fig. 7.6. Initially  $\theta_r$  is 90 degrees since, at the start of the maneuver, the yaw axis must be aligned with  $\underline{H}$ . Ultimately,  $\theta_r$  becomes 180 degrees, indicating that the roll axis is aligned with  $\underline{H}$ , but that  $\underline{a}_3$ , the forward-pointing torso-fixed unit vector, has a sense opposite to  $\underline{H}$ . Thus, if the angular momentum vector is regarded as pointing "upward," then the initial motion is one of leftward yaw with the man in an "upright" position and the final motion is leftward roll in a "face down" position.

Solutions for  $\alpha(\tau)$ , generated using the procedures of Sec. 7.3, are by no means unique, and equally acceptable solutions may be obtained

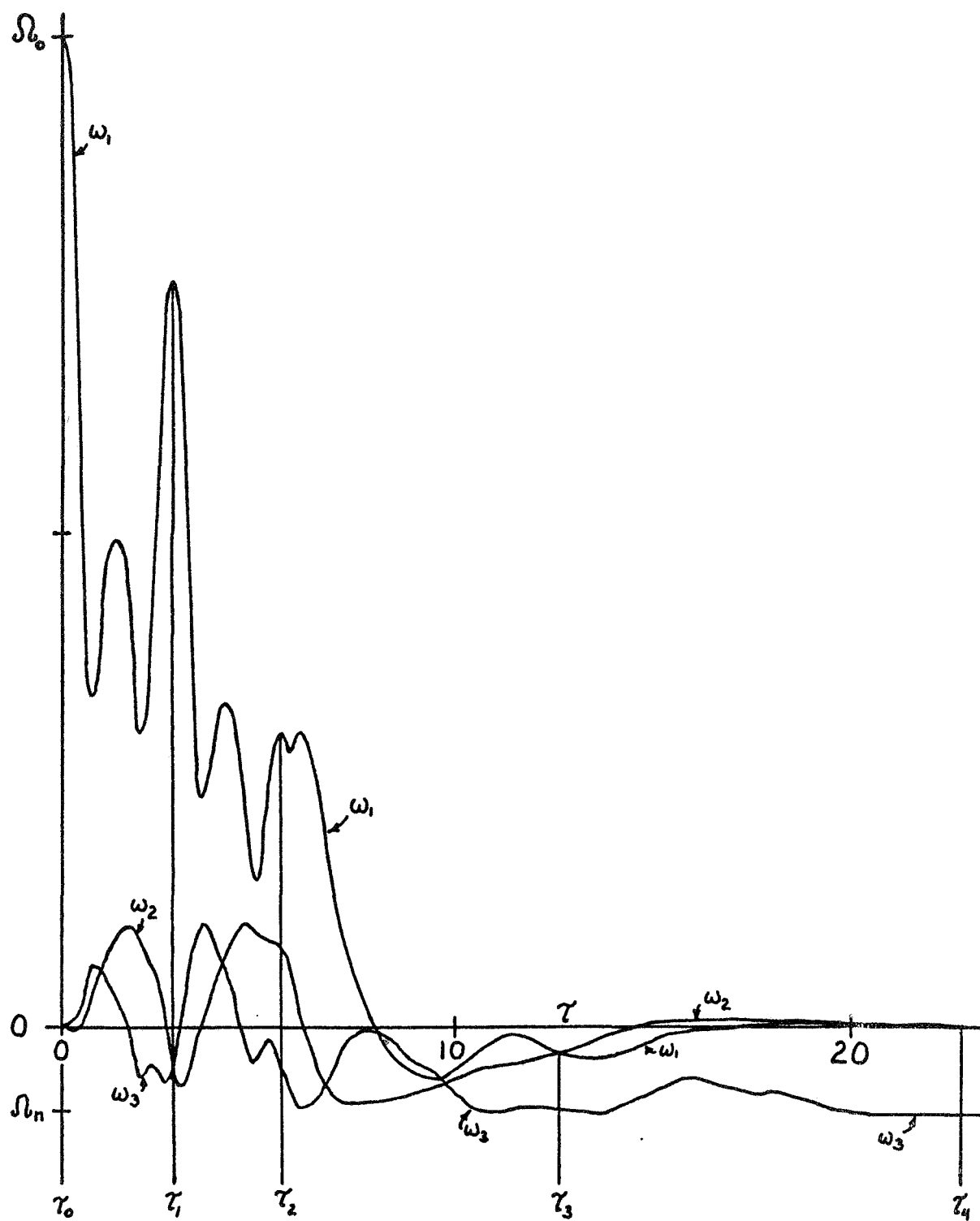
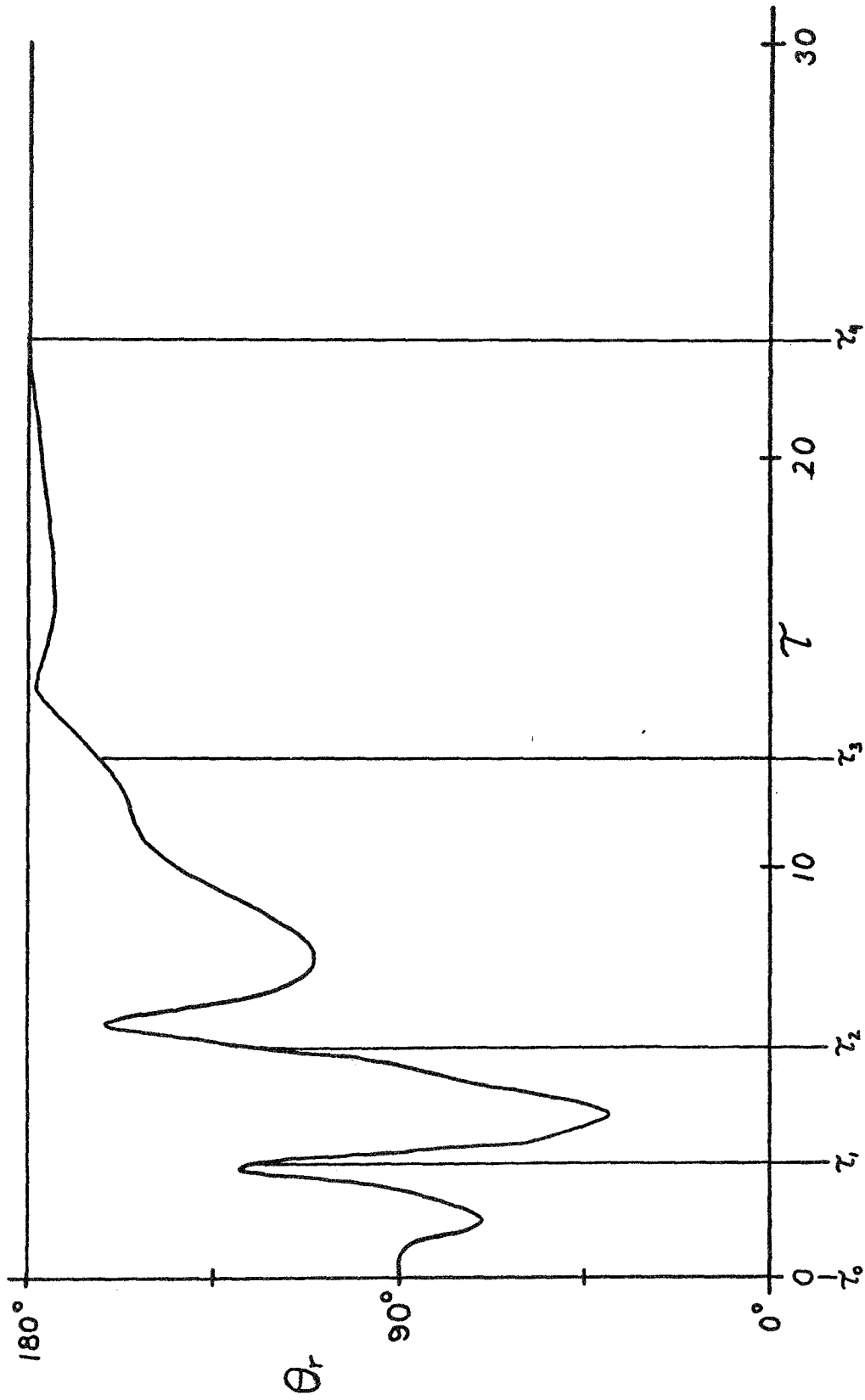


Fig. 7.5 Angular velocity components as functions of  $\tau$



$\theta_r$  as a function of  $\tau$

Fig. 7.6



by modifying the algorithms governing the choice of the  $\Gamma_i$  and  $T_i$ . For example, an alternative function  $\alpha(\tau)$  which produces the same change in attitude motion is plotted in Fig. 7.7 and presented in tabular form in Table 7.4. This function was generated as follows:

Table 7.4

Cycle	1	2	3	4	5	6	7	8
$\Gamma_i$	90°	90°	90°	135°	135°	0°	100°	100°
$T_i$	4.0	5.0	1.8	7.8	1.0	2.0	10.6	4.0
$\tau_i$	4.0	9.0	10.8	18.6	19.6	21.6	32.2	36.2

For the first three cycles, the amplitude was arbitrarily set equal to 90 degrees and the periods between zero and six time units which led to the lowest values of  $K$  were determined. After the third cycle, no value for  $T_4$  between zero and six, with  $\Gamma_4$  equal to 90 degrees, would lead to a reduction in  $K$ . The amplitude was then arbitrarily set at 135 degrees, periods between zero and eleven time units were considered, and two more cycles were thus obtained. At time  $\tau_5$ , no choice of  $T_6$  between zero and eleven, with  $\Gamma_6$  equal to 135 degrees, would lead to a further reduction of  $K$ . The system was then allowed to tumble in its quasi-rigid state for two time units (i.e.,  $\Gamma_6 = 0$ ,  $T_6 = 2.0$ ). Then the amplitude was arbitrarily set to 100 degrees and periods between zero and eleven time units were again considered, thus leading to the last two cycles. At time  $\tau_8$ , the kinetic energy was sufficiently close

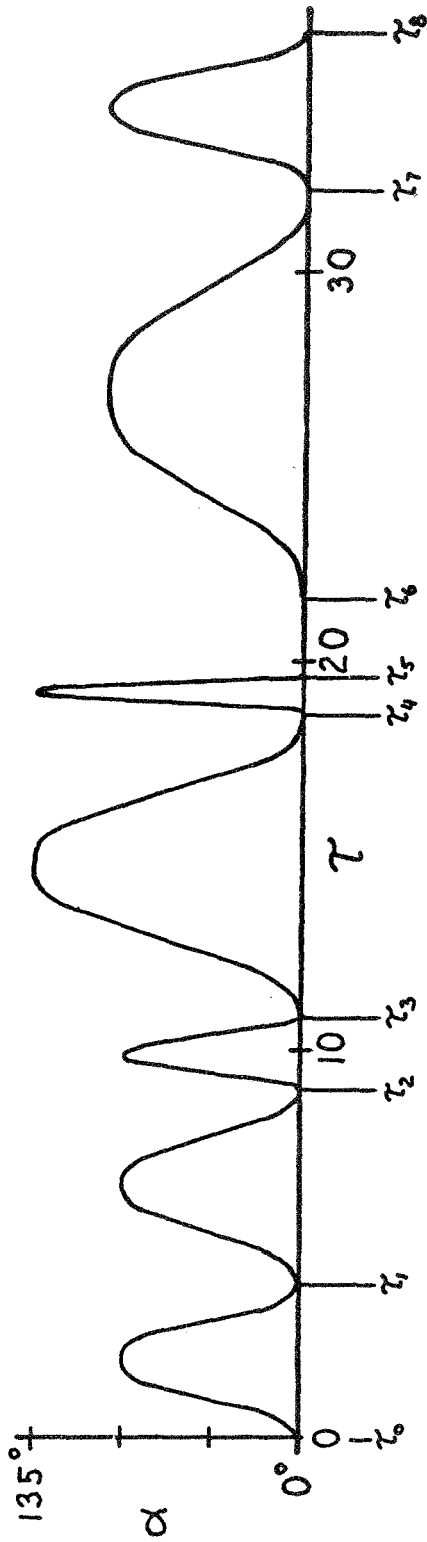


Fig. 7.7 Alternative solution for  $\alpha$  as a function of  $\tau$  (see Table 7.4)

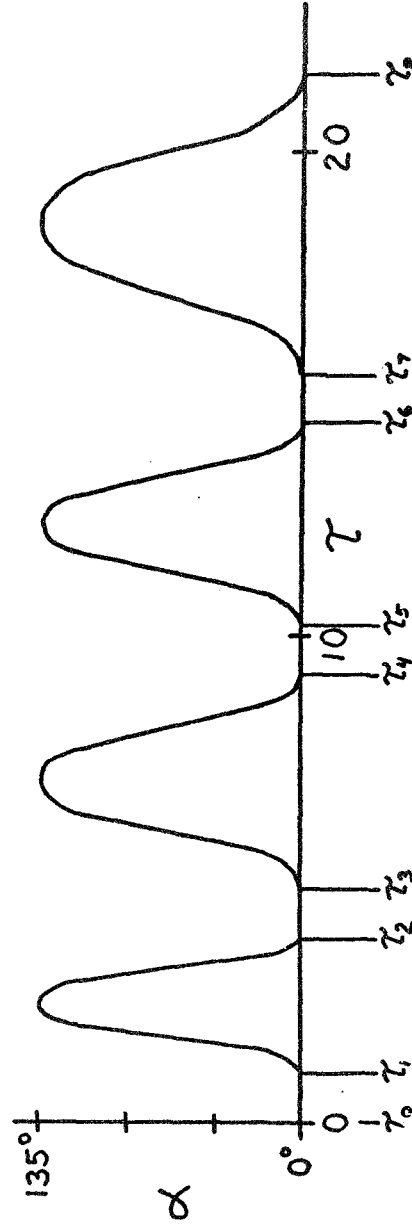


Fig. 7.8 Alternative solution for  $\alpha$  as a function of  $\tau$  with unit lapses between cycles (see Table 7.5)

to its lowest bound. This solution best illustrates the techniques discussed in the last paragraph of Sec. 7.3.

Another interesting solution for  $\alpha(\tau)$  is graphed in Fig. 7.8 and tabulated in Table 7.5. This solution was obtained employing the same procedure used in the solution presented in Table 7.3; that is, the amplitude of the arm motion was arbitrarily set at 135 degrees and periods between zero and eleven time units were examined to find the ones that led to the lowest values for  $K$ . However, prior to each cycle of arm motion, the man was required to tumble in a position of "attention" for one time unit. Originally, these one unit time lapses were intended to simulate "thinking time," that is, time during which the man observed his motion and decided what to do next. However, these time lapses seem to lead to more favorable conditions from which to start the next cycle in that the resulting arm maneuver can be performed in less time and employs shorter periods for the cycles than does the solution in Table 7.3.

Table 7.5

Cycle	1	2	3	4	5	6	7	8
$\Gamma_i$	0	135°	0	135°	0	135°	0	135°
$T_i$	1.0	2.8	1.0	4.4	1.0	4.2	1.0	6.2
$\tau_i$	1.0	3.8	4.8	9.2	10.2	14.4	15.4	21.6

When the same task, that of converting yaw motion to roll motion, is attempted without the use of the five-pound weights, one finds that more cycles of arm motion are usually required. For example, Table 7.6 presents

an eight-cycle solution obtained using techniques similar to those employed in generating Table 7.3. Typically, use of the weights roughly halves the time required to obtain the desired change in attitude motion.

Table 7.6

Cycle	1	2	3	4	5	6	7	8
$\Gamma_i$	135°	135°	135°	135°	135°	135°	135°	135°
$T_i$	2.0	1.6	2.2	2.8	5.4	11.8	6.0	11.2
$\tau_i$	2.0	3.6	5.8	8.6	14.0	25.8	31.8	43.0

It is of interest to know how sensitive these solutions are to errors in performance; that is, if a man makes a small error in performing a cycle of the arm motion, will the resulting attitude motions differ greatly from the desired final state of motion? A single example will suffice to indicate that there is a high degree of sensitivity to error. When the arm motion characterized by Table 7.3 is performed with a one percent error in amplitude, i.e., if  $\Gamma_1$ ,  $\Gamma_2$ ,  $\Gamma_3$ , and  $\Gamma_4$  are taken to be 136.35 degrees rather than 135 degrees, then  $\theta_r$  can be plotted as a function of  $\tau$  and compared to Fig. 7.6. Such a plot is presented in Fig. 7.9 and, at a glance, one can see the marked differences in attitude motion. Although the behavior of  $\theta_r$  in Fig. 7.9 conforms closely to  $\theta_r$  of Fig. 7.6 during the first two cycles of arm maneuver, the error gradually grows until, at time  $\tau_4$ ,  $\theta_r$  is 95.4 degrees rather than 180 degrees. If the man resumes rigid body motion at time  $\tau_4$ , he will tumble rather than simply spin, and  $\theta_r$  will oscillate as depicted in Fig. 7.9 for times greater than  $\tau_4$ .

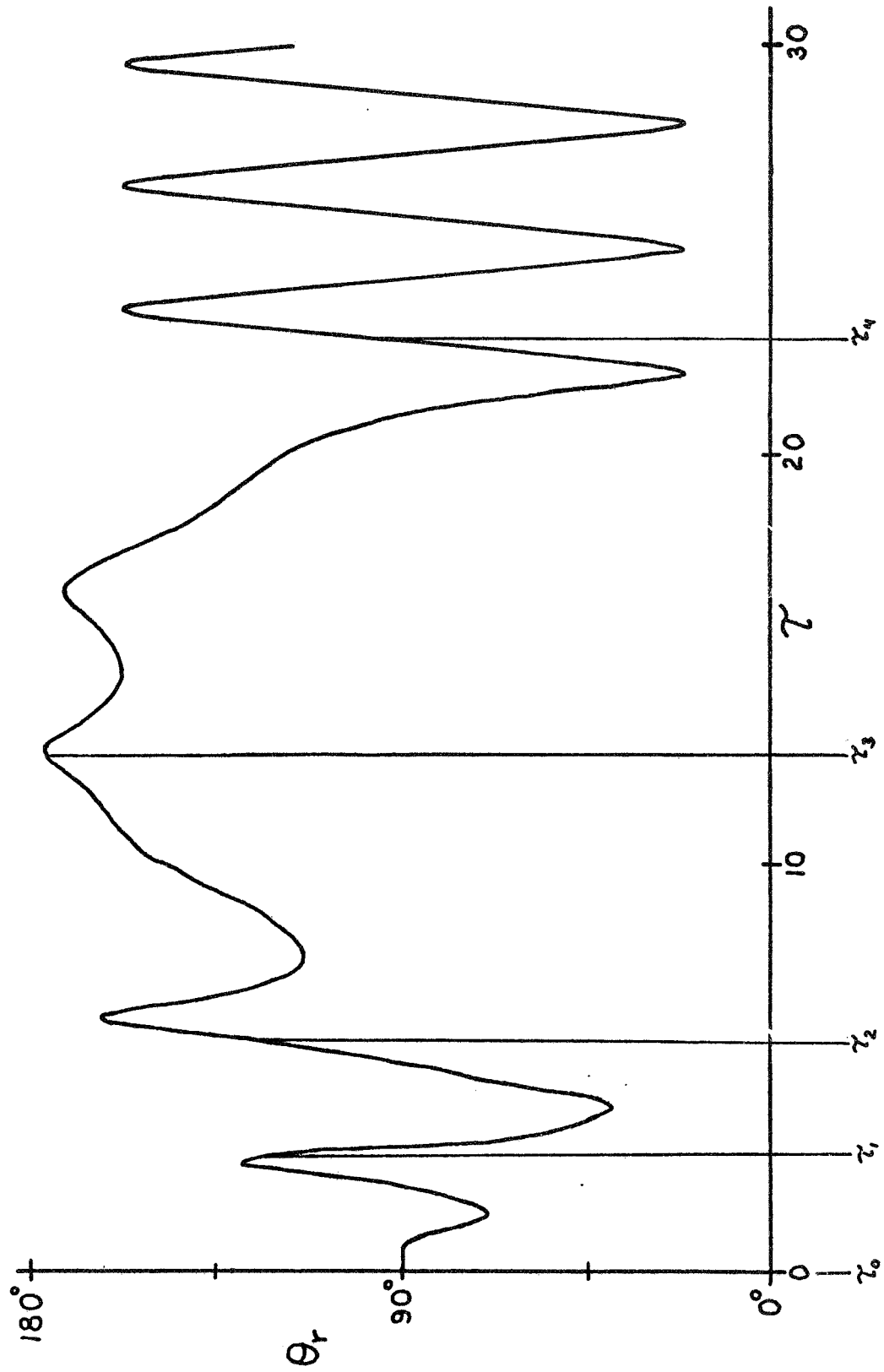


Fig. 7.9  $\theta_r$  as a function of  $\tau$  with a 1% error in  $\Gamma$

Thus far, the problem under consideration has been that of converting yaw to roll or, equivalently, that of lowering the kinetic energy  $K$  from  $K_1$  to  $K_3$ . There is, however, no obstacle to consideration of the converse problem, that of raising kinetic energy and converting roll to yaw. A sample solution is illustrated in Fig. 7.10 where  $\alpha$  and  $K$  are plotted as functions of  $\tau$ . Note that initially  $K$  equals  $K_3$  and, at time  $\tau_4$ ,  $K$  equals  $K_1$ . The most interesting feature of this problem is that it illustrates a point made in the latter part of Sec. 7.3. In the present case, the hinge axis unit vector  $\underline{h}$  (see Fig. 7.1) is taken equal to  $\underline{a}_2$  so that the arm moves in a plane passing through the shoulder and parallel to the pitch plane. If  $\underline{h}$  were equal to  $-\underline{a}_3$ , as in the preceding examples, the initial rolling motion could not be altered because the motions of the arm would not affect the orientation of the principal axis of the system which is initially aligned with the angular velocity vector.

In conclusion, although a method for determining how to use limb motions to alter the attitude motion of a human has been devised, one must deduce from the preceding examples that, from a practical point of view, the feasibility of this method, and the possibility of using limb motions at all, appears dubious for the following reasons:

- (1) The arm motions must be performed with a high degree of accuracy.
- (2) The man's initial angular rates must be determined with great accuracy.
- (3) The times required to obtain the desired alterations in attitude motion are relatively long, even when weights are used.

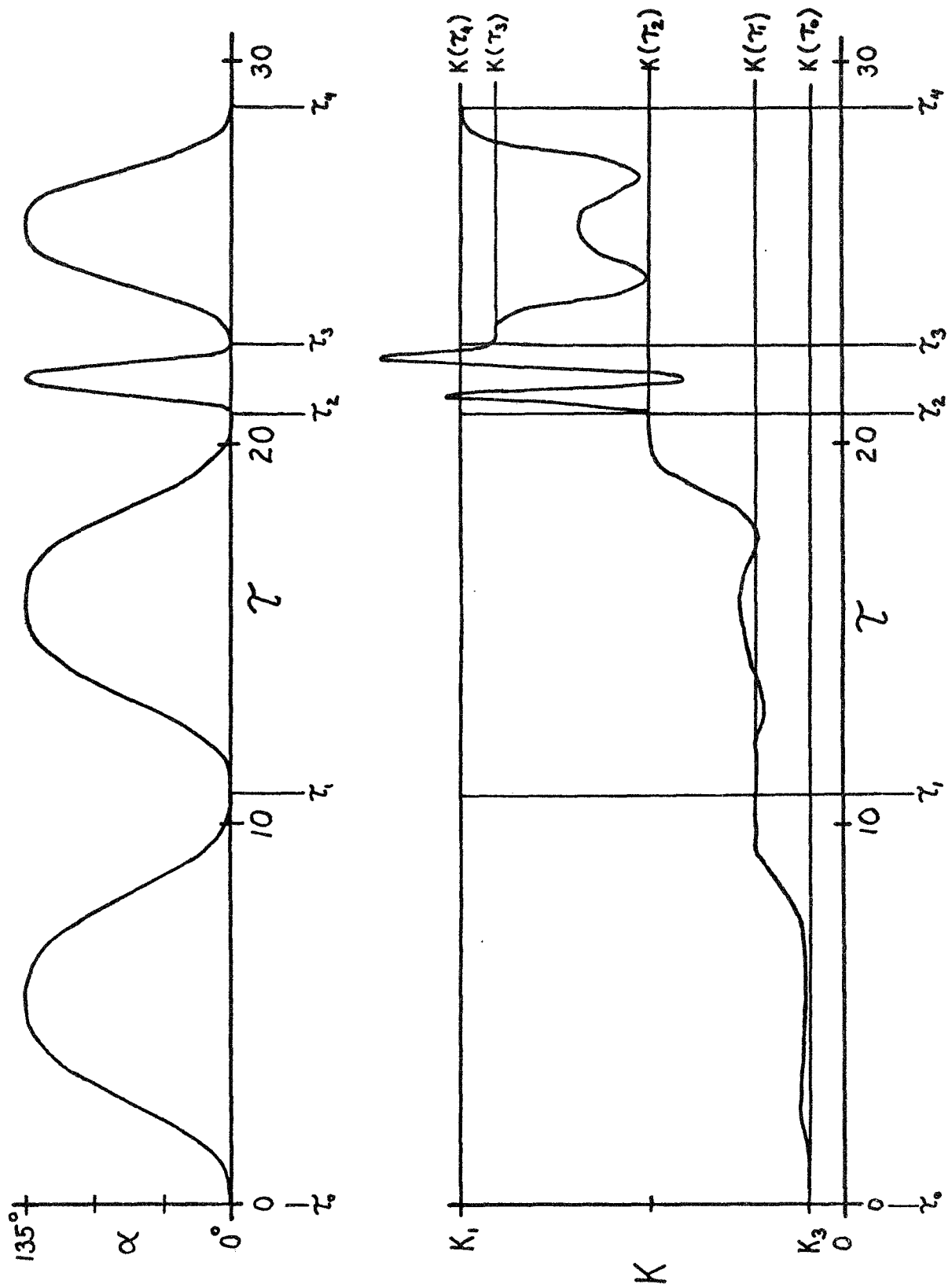


Fig. 7.10  $\alpha$  and kinetic energy as functions of  $\tau$  when converting roll to yaw ( $\bar{h} = \bar{a}_2$ )

- (4) Extensive numerical computations are involved.
- (5) The maneuvers can not be learned prior to the time when they are needed because each set of initial conditions requires a different maneuver.

It may occur to the reader that some maneuver, other than swinging one arm, may lead to more acceptable solutions. In fact, the leg was considered as an alternative, but it is less effective than the arm because physical constraints limit the angles through which it can be moved. Other maneuvers, possibly involving the use of several limbs simultaneously or bending at the waist, have not been considered for two reasons. Firstly, the introduction of more degrees of freedom both complicates the equations of motion and enlarges the parameter space explored in the trial-and-error procedure of Sec. 7.3; and secondly, a more complex maneuver would be difficult to perform accurately.



## 8. Symmetric Two-Body Satellite

### 8.1 Description

While it does not appear to be feasible for a man to control his rotational motion by means of limb maneuvers, the underlying principles can be successfully applied to control the attitude motions of multi-body artificial satellites. In particular, when a satellite possesses an axis of symmetry in its quasi-rigid state, the remarks in Sec. 5.2, concerning the relationship of the state of motion to the angle  $\varphi$  between the symmetry axis and the direction of the angular momentum vector, are applicable. For example, in some space missions it is required only that the satellite spin about its symmetry axis, regardless of the orientation of that axis in space. The primary control problem is then one of "capture," that is, one of converting the initial motion (i.e.,  $\varphi \neq 0$ ) into a simple spinning motion in which the symmetry axis and the angular momentum vector are aligned (i.e.,  $\varphi = 0$ ). The present attitude control scheme is well suited for such missions.

As an example, we consider a system comprised of a solid, uniform, right-circular cylinder A to which is attached a pendulum B consisting of a rigid "massless" rod at whose tip is placed a particle P (see Fig. 8.1) of mass  $m$ . The pendulum has a length  $L$  and is hinged to the center of one face of A about a diametral line D. Cylinder A has a radius  $L$ , a height  $L$ , and a mass  $10m$ . It is assumed that B can be driven relative to A in a prescribed manner; that is, the angle  $\alpha$  between B and the symmetry axis S of A can be prescribed as a

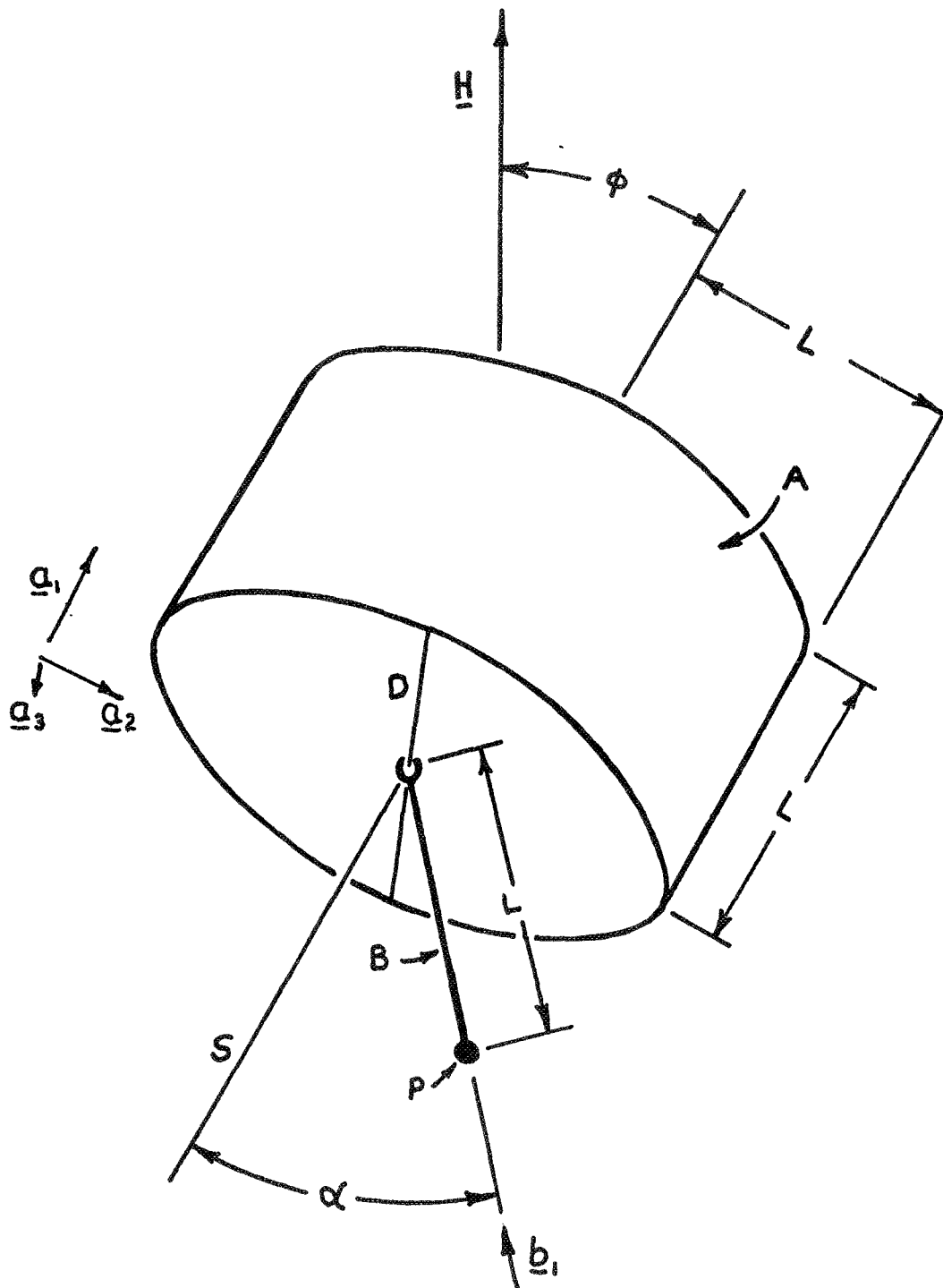


Fig. 8.1

Symmetric two-body satellite

function of time;  $\alpha$  is zero when the system moves in its quasi-rigid state. The angle  $\varphi$  between  $S$  and the (inertially fixed) angular momentum vector  $\underline{H}$  is also shown in Fig. 8.1.

For this system, the control problem is to find how to vary  $\alpha$  as a function of time, and ultimately restore its value to zero, in such a manner that an attitude motion in which  $\varphi$  is initially non-zero is converted to a motion in which  $\varphi$  becomes zero (or 180 degrees) at the instant that the value of  $\alpha$  returns to zero. Some appropriate time histories for  $\alpha$  are presented in Sec. 8.3; but, first, some analytical aspects of the problem are considered.

## 8.2 Analytical Aspects

Appropriate equations of motion for this system have been derived in Secs. 6.1 and 6.2 and can be used once elements of  $\underline{I}^A$  and  $\underline{I}^B$  and components of  $\underline{a}$  and  $\underline{b}$ , as defined by Eqs. (6.16), (6.36), (6.57), and (6.58), have been obtained. ( $\underline{I}^A$  and  $\underline{I}^B$  are the centroidal inertia dyadics of  $A$  and  $B$ ; and  $\underline{a}$  and  $\underline{b}$  are the position vectors from the mass centers of  $A$  and  $B$ , respectively, to the hinge point.) Letting  $\underline{a}_1, \underline{a}_2, \underline{a}_3$  be mutually perpendicular unit vectors fixed in  $A$ , with  $\underline{a}_1$  parallel to  $S$  and  $\underline{a}_3$  parallel to  $D$ , and letting  $\underline{b}_1$  and  $\underline{b}_3$  be perpendicular unit vectors fixed in pendulum  $B$  with  $\underline{b}_1$  parallel to the rod (see Fig. 8.1), one can express  $\underline{I}^A, \underline{I}^B, \underline{a}$ , and  $\underline{b}$  as

$$\underline{I}^A = 5 \text{ mL}^2 \underline{a}_1 \underline{a}_1 + \frac{10}{3} \text{ mL}^2 \underline{a}_2 \underline{a}_2 + \frac{10}{3} \text{ mL}^2 \underline{a}_3 \underline{a}_3 \quad (8.1)$$

$$\underline{I}^B = 0 \quad (8.2)$$

$$\underline{a} = -\frac{L}{2} \underline{a}_1, \quad \underline{b} = L \underline{b}_1 \quad (8.3)$$

Moreover, the unit vectors  $\underline{h}$  and  $\underline{n}_A$  fixed in A, and  $\underline{h}$  and  $\underline{n}_B$  fixed in B, which reflect the orientation of the hinge and define the angle through which B rotates relative to A (see Sec. 6.2), can be chosen as

$$\underline{h} = -\underline{a}_3 = -\underline{b}_3 \quad (8.4)$$

$$\underline{n}_A = \underline{a}_1, \quad \underline{n}_B = \underline{b}_1 \quad (8.5)$$

It will be helpful in the sequel to know the moments of inertia of the entire system in its quasi-rigid state. Applying the parallel axis theorem for moments of inertia,  $I_1, I_2, I_3$ , the centroidal principal moments of inertia for the  $\underline{a}_1, \underline{a}_2, \underline{a}_3$  directions, respectively, are found to be

$$I_1 = 5 mL^2 \quad (8.6)$$

$$I_2 = I_3 = 5.379 mL^2 \quad (8.7)$$

Note that, in this particular example, the moment of inertia of the quasi-rigid system about S is the system's minimum centroidal moment of inertia, whereas the moment of inertia of the cylinder A about S is the cylinder's maximum. Furthermore, conversion of some initial motion of the system to a spinning motion about S corresponds to raising the system's kinetic energy to its upper bound.

It is convenient to non-dimensionalize time in the following manner: First, the magnitude of the angular momentum can be determined from

$\omega_1, \omega_2, \omega_3$ , the components of the angular velocity of A referred to the  $\underline{a}_1, \underline{a}_2, \underline{a}_3$  directions, at any instant when the system is in its quasi-rigid state, i.e.,

$$|\underline{H}| = \sqrt{I_1^2 \omega_1^2 + I_3^2 (\omega_2^2 + \omega_3^2)} \quad (8.8)$$

(5.3, 8.7)

Next, the magnitude  $\Omega$  of the angular velocity which the system would possess if it were simply spinning about its symmetry axis is given by

$$\Omega = \frac{|\underline{H}|}{I_1} \quad (8.9)$$

and, finally, a non-dimensional time variable  $\tau$  is defined as

$$\tau = \frac{\Omega t}{2\pi} \quad (8.10)$$

so that the system will perform one revolution per time unit when spinning about its axis of symmetry. Moreover, as  $I_2$  equals  $I_3$  (see Eq. (8.7)),  $\varphi$  is given by

$$\varphi = \arccos \frac{\omega_1}{\Omega} \quad 0 \leq \varphi \leq \pi \quad (8.11)$$

(5.14, 8.8, 8.9)

We now wish to determine a function  $\alpha(\tau; \varphi_0)$  which will lead to capture of the satellite when the initial motion is one in which  $\varphi$  has the value  $\varphi_0$ . Since  $\varphi$  remains constant as long as the rigid body motion of the satellite persists, one can wait to begin the motion of B relative to A until some easily recognized, convenient starting condition is reached. More specifically, regardless of the value of  $\varphi_0$  (other than 0, 90, or 180 degrees), the hinge axis D passes periodically through the plane determined by S and  $\underline{H}$  (see Fig. 8.1), at which

instants  $\omega_2$  equals zero. Moreover,  $\omega_1$ , the angular velocity component parallel to the symmetry axis, must remain constant while, at the instants when  $\omega_2$  is zero,  $\omega_3$  is alternately greater than or less than zero. Consequently, a convenient starting time for the relative motion can be taken to be the instant when  $\omega_2$  is zero and when  $\omega_3$  is, say, greater than zero.

Finally, a trial-and-error procedure analogous to that described in Sec. 7.3 is used to obtain functions for  $\alpha$  which convert the initial motion to a simple spin. In this procedure, changes in  $\varphi$ , rather than in kinetic energy, can be used as criteria for selecting the parameters  $\Gamma$  and  $T$  which denote the amplitude and period, respectively, of the function  $\gamma(\xi; \Gamma, T)$  (see Eq. (7.27)) which is chosen to represent one cycle in the time history of  $\alpha(\tau; \varphi_0)$ . For this particular system, we require  $\alpha$ , and hence  $\Gamma$ , to be bounded between -90 and 90 degrees so that the pendulum will not pass through the face of the cylinder. It also proves advantageous to employ algorithms for the choice of  $\Gamma$  and  $T$  which differ from those described in Sec. 7.4 by allowing more latitude in finding the most advantageous values of  $\Gamma$  and  $T$  for each cycle.

### 8.3 Results

We now turn to consideration of time histories of  $\alpha$  which are appropriate for use with given initial conditions. Fig. 8.2 contains graphs of  $\alpha$  and  $\varphi$  as functions of  $\tau$  for the case where  $\tau_0$  is zero,  $\varphi_0$  is 60 degrees,  $\omega_2(\tau_0)$  is zero,  $\omega_1(\tau_0)$  and  $\omega_3(\tau_0)$  are positive, and  $\varphi_f$ , the final value of  $\varphi$ , is zero. A most welcome

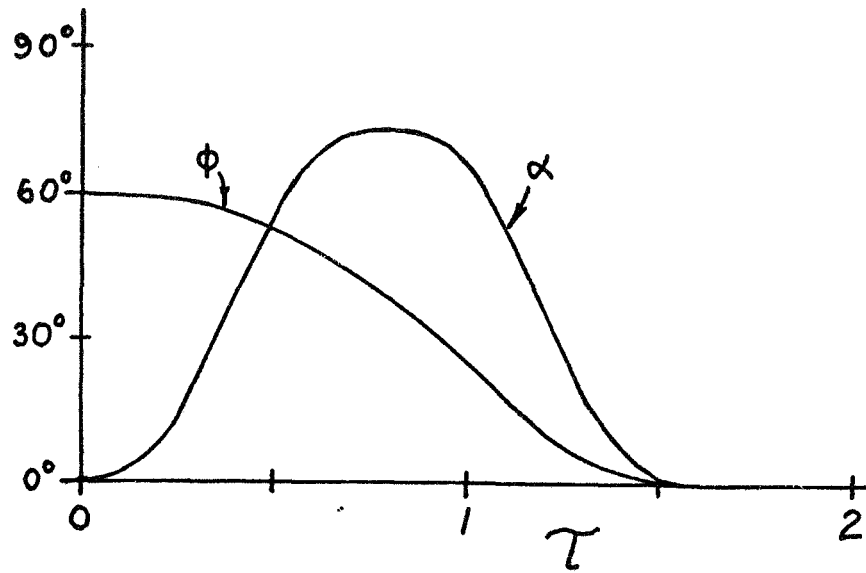


Fig. 8.2 Reduction of  $\varphi$  from  $60^\circ$  to  $0^\circ$

result is immediately observed, namely, that only one cycle of control motion is required, and that cycle has a period  $T$  of only 1.6 time units. Furthermore,  $\varphi$  changes from  $\varphi_0$  to  $\varphi_f$  in a monotonic fashion. In these two respects, the graphs in Fig. 8.2 are typical of time histories of  $\alpha$  and  $\varphi$  for values of  $\varphi_0$  between 0 and 90 degrees when the choice of initial conditions is made in the above manner and  $\alpha$  is of the form of  $\gamma(\xi; \Gamma, T)$  in Eq. (7.27).

Values for the amplitude  $\Gamma$  and period  $T$  for several selected values of  $\varphi_0$  between 0 and 180 degrees are presented in Table 8.1 for two possible initial conditions, i.e.,  $\omega_3(\tau_0)$  less than zero and greater than zero. Note that the sign of  $\Gamma$  varies with the choice of initial condition, but  $T$  is unaffected. Moreover, a time history of  $\alpha$  appropriate for an angle  $\varphi_0$  is also appropriate for the supplement of  $\varphi_0$ . Table 8.1 also lists the resulting value of  $\varphi_f$ , that value being zero when  $\varphi_0$  is less than 90 degrees and being 180 degrees when  $\varphi_0$  is greater than 90 degrees.

Table 8.1

$\varphi_0$	$\frac{\omega_1(\tau_0)}{\Omega}$	$\Gamma$		T	$\varphi_f$
		$\omega_3(\tau_0) > 0$	$\omega_3(\tau_0) < 0$		
5°	0.996	19°	-19°	0.36	0°
10°	0.985	55°	-55°	0.26	0°
20°	0.940	80°	-80°	0.40	0°
30°	0.866	84°	-84°	0.60	0°
45°	0.707	79°	-79°	1.00	0°
60°	0.500	73°	-73°	1.60	0°
75°	0.259	67°	-67°	2.62	0°
85°	0.087	70°	-70°	3.88	0°
95°	-0.087	70°	-70°	3.88	180°
105°	-0.259	67°	-67°	2.62	180°
120°	-0.500	73°	-73°	1.60	180°
135°	-0.707	79°	-79°	1.00	180°
150°	-0.866	84°	-84°	0.60	180°
160°	-0.940	80°	-80°	0.40	180°
170°	-0.985	55°	-55°	0.26	180°
175°	-0.996	19°	-19°	0.36	180°

The case when  $\varphi_0$  equals 90 degrees requires special consideration. In this event,  $\omega_1$  is zero and  $\omega_2$  and  $\omega_3$  remain constant as long as the system is rigid. Unfortunately, the initial condition employed thus far, i.e.,  $\omega_2(\tau_0)$  equal to zero, may not occur and, if it does, then any motion of the pendulum relative to the cylinder about D fails to



misalign the principal axis which is initially parallel to the angular velocity vector of the system and, thus, no change in the state of motion can be obtained. Now, when  $\varphi_0$  is 90 degrees and  $\omega_2(\tau_0)$  is non-zero, a different function for  $\alpha$  must be obtained for each combination of values of  $\omega_2(\tau_0)$  and  $\omega_3(\tau_0)$ . As an illustrative example, Fig. 8.3 contains appropriate time histories of  $\alpha$  and  $\varphi$  for the case when  $\varphi_0$  is 90 degrees,  $\omega_3(\tau_0)$  is initially zero, and  $\omega_2(\tau_0)$  is positive.

Two additional points regarding the nature of this system should be made. First, any function  $\gamma(\xi; \Gamma, T)$  which satisfies Eqs. (7.25) and (7.26) may be used in the trial-and-error procedure by which appropriate values of  $\Gamma$  and  $T$  are determined. For instance, taking  $\gamma$  to be

$$\gamma = \Gamma \sin^3 \pi \frac{\xi}{T} \quad (8.12)$$

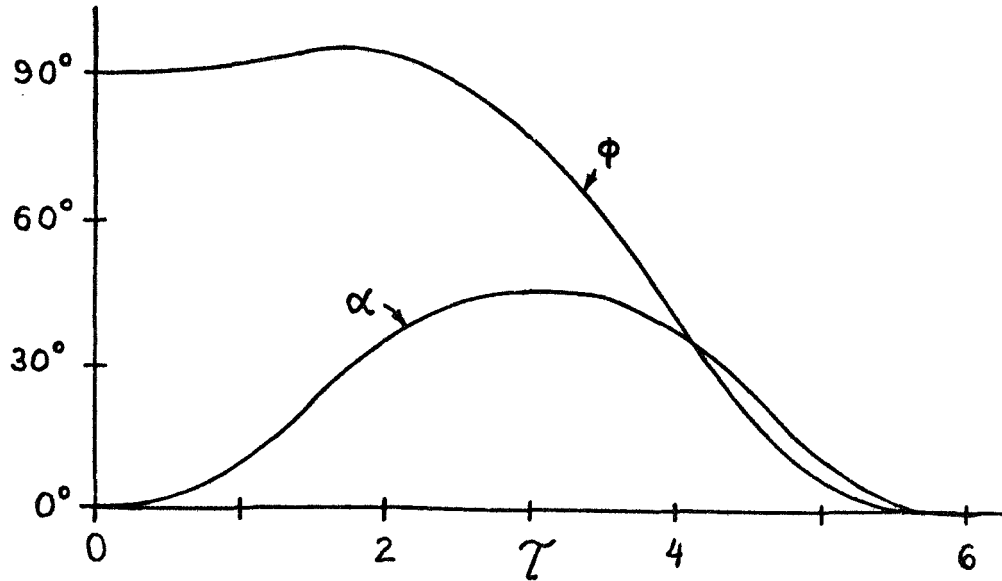


Fig. 8.3

Reduction of  $\varphi$  from 90° to 0°

and seeking values of  $\Gamma$  and  $T$  to reduce  $\varphi$  from 60 degrees to zero, when initially  $\omega_2(\tau_0)$  is zero and  $\omega_3(\tau_0)$  is positive, we obtain the time histories for  $\alpha$  and  $\varphi$  shown in Fig. 8.4. Comparing these time histories to those in Fig. 8.2 which were obtained using the function  $\gamma$  of Eq. (7.27), we see that small changes in the form of  $\gamma$  can lead to significant changes in values for  $\Gamma$  and  $T$ . Here  $\Gamma$  and  $T$  are 80 degrees and 1.73 time units, respectively, whereas in Fig. 8.2,  $\Gamma$  is 73 degrees and  $T$  is 1.60 time units. The fact that  $\gamma$  does not have to be of a specific form may be expected to prove helpful in the design of hardware. The second point to be made is that any value of  $\varphi_f$ , in addition to 0 and 180 degrees, can be obtained. For instance, Fig. 8.5 contains time histories of  $\alpha$  and  $\varphi$  during which  $\varphi$  is reduced from 60 to 30 degrees. In this case, the form of  $\gamma$  is given by Eq. (8.12) where  $\Gamma$  is 38.1 degrees and  $T$  is 2 time units.

#### 8.4 Feasibility

Turning from specific examples to questions of practical feasibility, we note, first, that it is possible to surmount the drawbacks mentioned in Sec. 7.4 which precluded the possibility of having a man control his attitude motions by means of limb motions. For instance, from Table 8.1 it is evident that the times required for the control motions may be reasonably short and that, for appropriate choices of inertia properties and initial conditions, only one cycle of control motion needs to be performed. The angular rates of the satellite,  $\omega_1$ ,  $\omega_2$ ,  $\omega_3$ , which are required as inputs to the control system, may be obtained with reasonable accuracy from an inertial navigation system consisting of a

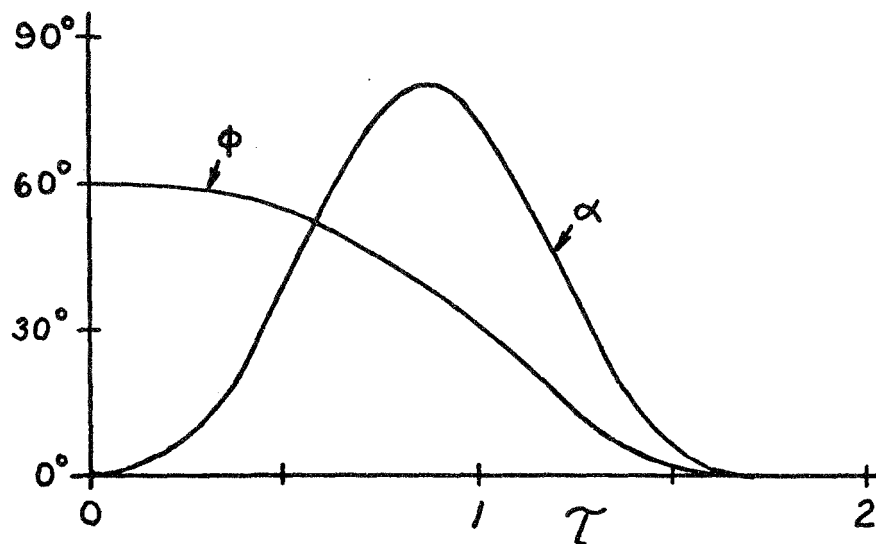


Fig. 8.4 Reduction of  $\varphi$  from  $60^\circ$  to  $0^\circ$  when  $\alpha = \Gamma \sin^3 \pi \frac{\tau}{T}$

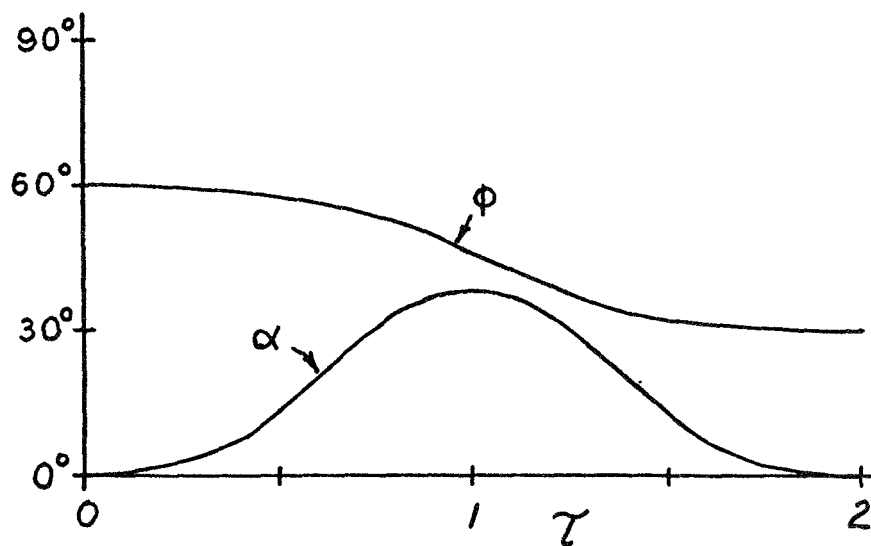


Fig. 8.5 Reduction of  $\varphi$  from  $60^\circ$  to  $30^\circ$

stable platform which is gimballed to the satellite body. Such navigation systems are currently available (e.g., see [45]). Furthermore, motion of the pendulum can be guaranteed to conform to the function  $\gamma$  by choosing for the form of  $\gamma$  an expression which reflects the capabilities of the actual hardware being employed.

It may appear that the present attitude control scheme requires extensive on-board computational facilities. This is not necessarily true. For example, in the case of a symmetric vehicle for which the desired value of  $\varphi_f$  is known, a catalog of functions  $\alpha(\tau; \varphi_0)$  suitable for use with particular values of  $\varphi_0$  can be compiled once and for all prior to launch. For example, the entries in Table 8.1 might appear in the catalog for a satellite which is ultimately to spin with  $\varphi_f$  equal to either 0 or 180 degrees. When the vehicle is in orbit,  $\Omega$  need be determined only once from Eqs. (8.8) and (8.9); and  $\varphi_0$  can then be calculated from Eq. (8.11); both of these computations require only simple algebraic operations involving the moments of inertia (e.g., see Eqs. (8.6) and (8.7)) and the instantaneous values of  $\omega_1$ ,  $\omega_2$ ,  $\omega_3$ ; and the required time history for  $\alpha$  may be selected from the catalog without further computation. Should unavoidable non-rigidity of the system lead to later deviations of the motion from one of simple spin, it is only necessary to recompute  $\varphi_0$  (or perhaps only  $\frac{\omega_1}{\Omega}$ ) and again determine the appropriate control motion from the catalog. Another possibility is that the assumption of free fall will be invalid in that unforeseen external torques might act on the system, altering both the magnitude and direction of  $\underline{H}$ . Should these torques act only occasionally, or should they be sufficiently small, the system could recompute  $\Omega$  and  $\varphi_0$  and correct its motion repeatedly.

An additional desirable feature of this attitude control scheme, applicable to general as well as symmetric satellites, is that energy requirements may be kept quite low. Letting  $K(\tau_o)$  and  $K(\tau_n)$  denote the kinetic energy of the system in the initial and final states of motion, respectively, then the total energy required is  $K(\tau_n) - K(\tau_o)$ , a quantity which depends on (1) the design of the satellite, (2) its initial motion, and (3) the desired final attitude motion. Recalling that  $I_1$  and  $I_3$  represent the minimum and maximum centroidal principal moments of inertia of the quasi-rigid system, respectively, and that  $\underline{a}_1$  and  $\underline{a}_3$  are parallel to the corresponding principal directions, suppose that the desired final attitude motion is to be simple spin about the  $\underline{a}_1$  direction. Then  $\Delta E$ , the upper bound on the energy required to convert any initial motion to simple spin, is given by

$$\Delta E = \frac{H^2}{2} \left( \frac{1}{I_1} - \frac{1}{I_3} \right) \quad (8.13)$$

(i.e., by  $K_1 - K_3$  where  $K_1$  and  $K_3$  are given by Eqs. (5.9) and (5.10)). This energy cost is associated with initial spin about the  $\underline{a}_3$  direction. If the satellite is inserted into orbit with the same angular momentum and with any other attitude motion, then the cost is reduced. Clearly, energy costs can also be reduced by releasing the satellite with as little angular motion as possible, thereby keeping  $H^2$  small. Finally, by designing the satellite so that  $I_1$  and  $I_3$  are nearly equal (i.e., if the inertia ellipsoid of the quasi-rigid satellite is nearly spherical) the energy costs may be kept low.

On the other hand, it is more probable that the desired final motion will be spin about the  $\underline{a}_3$  direction. Then (electrical) energy may be

generated rather than expended. This generated energy cannot exceed  $\Delta E$  of Eq. (8.13), and the remarks concerning initial motion and design apply in reverse. For instance, designing the satellite to obtain a large difference between  $I_1$  and  $I_3$  will increase the energy acquired when the control system alters the attitude motion to spin about the  $\underline{a}_3$  direction.

In conclusion, it may be of interest to compare the attitude control scheme under consideration to other available systems. The most versatile active control systems employ gas jets and are thus capable of altering the magnitude and direction of angular momentum to achieve a desired orientation as well as a desired attitude motion. These gas jet systems are essential for missions with precise attitude requirements, but must carry a fuel supply and therefore have a limited life. They generally also require some onboard computing capability.

A second class of active control systems employ control moment gyroscopes or reaction wheels. Without the use of gas jets, these systems cannot alter their angular momentum vector and therefore are suitable for the same missions as is the present active attitude control system. Although gyroscopes and reaction wheels are subject to saturation, nevertheless these systems are widely used, often in conjunction with a gas jet system, because their feedback control feature provides prompt elimination of nutation. These systems also require some computational facilities and a power supply for the motors which drive the rotating parts.

Finally, there are passive dissipative control systems. Some of these employ pendulous dampers and therefore seem to resemble the present active control system. However, these two attitude control schemes differ

from each other in four major respects. Firstly, a passive damper cannot be used to produce spin about the axis of minimum moment of inertia, whereas this is readily possible with the active method as shown in Figs. 8.2 and 8.3. Secondly, a passive damper does not possess the capability of obtaining non-zero values of  $\phi_f$ , but active control can lead to such a result as illustrated in Fig. 8.5. Thirdly, the time required to obtain the desired objective can be expected to be substantially greater for the passive device than for the active one. This becomes clear in view of the fact that Table 8.1 contains entries which lead to elimination of nutation in times less than the time consumed by only four rotations of the system about its axis of symmetry. And fourthly, in a dissipative device, kinetic energy is converted to heat, whereas, in the active system, it may be possible to convert the kinetic energy to more readily usable electrical energy.

## 9. Conclusion

### 9.1 Changes in Orientation

Although detailed conclusions have been drawn in each of the preceding chapters, it may be helpful to summarize them briefly.

A number of investigators have studied limb maneuvers which lead to changes in the orientation of the torso of a man who is initially without rotational motion. However, some of these investigators proposed maneuvers without attempting to gauge their effectiveness, others developed complex equations of motion, but drew no conclusions, and still others analyzed maneuvers which are physically impossible. A few practically feasible maneuvers have been analyzed correctly, but enough gaps have remained so that it has been impossible to thoroughly instruct an astronaut in self-rotation techniques.

Numerical results from the present analyses show that significant pitch, yaw, and roll reorientations can be achieved by employing the maneuvers under consideration. By using his arms, the average man can obtain about 30 degrees of either pitch or yaw, and about 20 degrees of roll, per cycle of such a maneuver. The use of hand-held weights significantly enhances the effectiveness of the pitch and roll maneuvers, but adds little to the effectiveness of the yaw maneuver. However, the legs are highly effective in yaw, producing rotations of about 70 degrees per cycle. Finally, the asymmetries involved in moving the arms to the starting positions, the precision required in locating the cone axes correctly, and the interference between the knees and the arms when the



legs are tucked all tend to make the roll maneuver less desirable than the other two. It is suggested, therefore, that an astronaut perform a yaw-pitch-yaw sequence when he wishes to acquire a general reorientation.

## 9.2 Changes in Attitude Motion

The possibility of altering attitude motions by means of prescribed cyclical relative motions of the parts of a system has been recognized for a long time. What remained to be done, was the determination of suitable relative motions.

From a dynamical point of view, the problem of converting a general attitude motion of a quasi-rigid body to a simple spin corresponds to bringing the kinetic energy associated with the rotational motion of the quasi-rigid system to either its upper or lower bound. An algorithm which employs a trial-and-error technique can be used to analytically determine relative motions which bring a system "sufficiently close" to the desired final state of motion. The computations involved in this process, even for a system of only two bodies with one degree of freedom of relative motion, are lengthy and complex, and invariably require high-speed computational facilities.

In the case of a man swinging one arm, time and accuracy requirements, in addition to computational difficulties, suggest that he cannot easily learn to control his rotational motion while still returning to a position of "attention." Nevertheless, such control is possible in principle, and it may be advantageous for satellite attitude control systems to exploit these same principles. When a satellite has a favorable symmetry and is equipped with accurate rate sensors, reliable

servo-mechanisms, and minimal computational facilities, it can, indeed, control its attitude motion by driving one of its appendages and ultimately returning that appendage to its initial relative position. For certain space missions, particularly those with minimal pointing requirements and long lifetimes, the proposed control system may become practically useful.

A. Appendix

A.1 Tables of Inertia Properties

Table A.1

Inertia Properties for a Nine-Segment Model of the USAF 5th Percentile Man  
(Refer to Fig. 1.1 and Table 1.1.)

Segment	$m_i$	$I_x^i$	$I_y^i$	$I_z^i$	$L_i$	$d_i$
$B_1$	2.30	1.231	1.157	0.1733	1.539	0.578
$B_2, B_2'$	0.1194	0.01169	0.01169	0.00114	0.914	0.368
$B_3, B_3'$	0.1058	0.01347	0.01347	0.00072	0.992	0.550
$B_4, B_4'$	0.419	0.0564	0.0564	0.01055	1.333	0.637
$B_5, B_5'$	0.261	0.0517	0.0550	0.00570	1.271	0.681

$$s_1 = 0.595$$

$$s_2 = 0.244$$

$$\text{Total mass} = 4.11$$

(All lengths in feet, masses in slugs, and moments of inertia in slug-feet<sup>2</sup>.)

Table A.2

Inertia Properties for a Nine-Segment Model of the USAF 25<sup>th</sup> Percentile Man

(Refer to Fig. 1.1 and Table 1.1.)

Segment	$m_i$	$I_x^i$	$I_y^i$	$I_z^i$	$L_i$	$d_i$
$B_1$	2.57	1.505	1.418	0.217	1.510	0.606
$B_2, B_2'$	0.1409	0.01472	0.01472	0.00155	0.935	0.368
$B_3, B_3'$	0.1196	0.01638	0.01638	0.00090	1.032	0.564
$B_4, B_4'$	0.469	0.0651	0.0651	0.01358	1.467	0.755
$B_5, B_5'$	0.297	0.0639	0.0677	0.00691	1.333	0.709

$$s_1 = 0.636$$

$$s_2 = 0.248$$

$$\text{Total mass} = 4.62$$

(All lengths in feet, masses in slugs, and moments of inertia in slug-feet<sup>2</sup>.)

Table A.3

Inertia Properties for a Nine-Segment Model of the USAF 75<sup>th</sup> Percentile Man  
(Refer to Fig. 1.1 and Table 1.1.)

Segment	$m_i$	$I_x^i$	$I_y^i$	$I_z^i$	$L_i$	$d_i$
$B_1$	3.02	1.990	1.880	0.306	1.550	0.641
$B_2, B_2'$	0.1782	0.0207	0.0207	0.00239	0.975	0.372
$B_3, B_3'$	0.1433	0.0217	0.0217	0.00124	1.091	0.586
$B_4, B_4'$	0.555	0.0802	0.0802	0.01962	1.550	0.823
$B_5, B_5'$	0.358	0.0872	0.0921	0.00927	1.429	0.747

$$s_1 = 0.696$$

$$s_2 = 0.258$$

$$\text{Total mass} = 5.48$$

(All lengths in feet, masses in slugs, and moments of inertia in slug-feet<sup>2</sup>.)

Table A.4

Inertia Properties for a Nine-Segment Model of the USAF 95<sup>th</sup> Percentile Man

(Refer to Fig. 1.1 and Table 1.1.)

Segment	$m_i$	$I_x^i$	$I_y^i$	$I_z^i$	$L_i$	$d_i$
$B_1$	3.40	2.43	2.30	0.394	1.576	0.655
$B_2, B_2'$	0.211	0.0267	0.0267	0.00327	1.009	0.373
$B_3, B_3'$	0.1639	0.0265	0.0265	0.00157	1.131	0.601
$B_4, B_4'$	0.630	0.0952	0.0952	0.0253	1.617	0.871
$B_5, B_5'$	0.411	0.1092	0.1151	0.01147	1.500	0.778

$$s_1 = 0.749$$

$$s_2 = 0.264$$

$$\text{Total mass} = 6.24$$

(All lengths in feet, masses in slugs, and moments of inertia in slug-feet<sup>2</sup>.)

Table A.5

Inertia Properties for a Five-Segment Model of the USAF 5th Percentile Man  
(Refer to Fig. 1.2 and Table 1.3.)

Segment	$m_i$	$I_x^i$	$I_y^i$	$I_z^i$	$L_i$	$d_i$
$B_1$	2.30	1.231	1.157	0.1733	1.539	0.578
$B_2, B_2'$	0.225	0.0925	0.0925	0.00186	1.906	0.883
$B_3, B_3'$	0.680	0.413	0.416	0.01625	2.60	1.166

$$s_1 = 0.595$$

$$s_2 = 0.244$$

$$\text{Total mass} = 4.11$$

Table A.6

Inertia Properties for a Five-Segment Model of the USAF 25th Percentile Man  
(Refer to Fig. 1.2 and Table 1.3.)

Segment	$m_i$	$I_x^i$	$I_y^i$	$I_z^i$	$L_i$	$d_i$
$B_1$	2.57	1.505	1.418	0.217	1.510	0.606
$B_2, B_2'$	0.260	0.1138	0.1138	0.00245	1.967	0.887
$B_3, B_3'$	0.766	0.496	0.500	0.0205	2.80	1.305

$$s_1 = 0.636$$

$$s_2 = 0.248$$

$$\text{Total mass} = 4.62$$

(All lengths in feet, masses in slugs, and moments of inertia in slug-feet<sup>2</sup>.)

Table A.7

Inertia Properties for a Five-Segment Model of the USAF 75<sup>th</sup> Percentile Man  
(Refer to Fig. 1.2 and Table 1.3.)

Segment	$m_i$	$I_x^i$	$I_y^i$	$I_z^i$	$L_i$	$d_i$
$B_1$	3.02	1.990	1.880	0.306	1.550	0.641
$B_2, B_2'$	0.321	0.1546	0.1546	0.00364	2.07	0.902
$B_3, B_3'$	0.913	0.641	0.645	0.0289	2.98	1.401

$$s_1 = 0.696 \quad s_2 = 0.258$$

Total mass = 5.48

Table A.8

Inertia Properties for a Five-Segment Model of the USAF 95<sup>th</sup> Percentile Man  
(Refer to Fig. 1.2 and Table 1.3.)

Segment	$m_i$	$I_x^i$	$I_y^i$	$I_z^i$	$L_i$	$d_i$
$B_1$	3.40	2.43	2.30	0.394	1.576	0.655
$B_2, B_2'$	0.375	0.1942	0.1942	0.00484	2.14	0.914
$B_3, B_3'$	1.041	0.783	0.788	0.0368	3.12	1.473

$$s_1 = 0.749 \quad s_2 = 0.264$$

Total mass = 6.24

(All lengths in feet, masses in slugs, and moments of inertia in slug-feet<sup>2</sup>.)



## A.2 Subroutines BODIES, INTRNL, TWOBOD, and DFEQS1

### SUBROUTINE BODIES

```

C
C THIS SUBROUTINE READS IN THE INERTIA PROPERTIES AND DETERMINES
C THE VALUES STORED IN NAMED COMMON /BODBLK/ AND /INTBLK/
C
REAL IB11,IB12,IB13,IB22,IB23,IB33,A(3,3),MA,MB,MM,MBM
C
COMMON BLOCKS
COMMON /BODBLK/ A,MM,MBM
COMMON /INTBLK/ D11,D12,D13,D21,D22,D23,D31,D32,D33,
1 E11,E12,E13,E21,E22,E23,E31,E32,E33,
2 F11,F12,F13,F21,F22,F23,F31,F32,F33,
3 U1,U2,U3, V1,V2,V3, W1,W2,W3, P11,P12,P13,
4 IB11,IB12,IB13,IB22,IB23,IB33
C
C INERTIA PROPERTIES ARE READ IN ON FOUR CARDS AS FOLLOWS:
C CARD (1): FORMAT (7F10.3):
C A(1,1), A(2,2), A(3,3), A(1,2), A(1,3), A(2,3), MA
C A IS INERTIA DYADIC OF BODY A FOR A*
C MA IS MASS OF BODY A
C CARD (2): FORMAT (3F10.3, 2X, 6F8.3):
C A1, A2, A3, P11, P12, P13, P31, P32, P33
C (A1,A2,A3) IS POSITION VECTOR OF HINGE C RELATIVE TO A*
C (P11,P12,P13) IS UNIT VECTOR HA PARALLEL TO THE HINGE
C (P31,P32,P33) IS UNIT VECTOR NA NORMAL TO THE HINGE
C CARD (3): FORMAT (7F10.3):
C IB11, IB22, IB33, IB12, IB13, IB23, MB
C IB IS INERTIA DYADIC OF B FOR B*
C MB IS MASS OF BODY B
C CARD (4): FORMAT (3F10.3, 2X, 6F8.3):
C B1, B2, B3, Q11, Q12, Q13, Q31, Q32, Q33
C (B1,B2,B3) IS POSITION VECTOR OF HINGE C RELATIVE TO B*
C (Q11,Q12,Q13) IS UNIT VECTOR HB PARALLEL TO THE HINGE
C (Q31,Q32,Q33) IS UNIT VECTOR NB NORMAL TO THE HINGE
C
READ (5,110,END=200,ERR=200) A(1,1), A(2,2), A(3,3), A(1,2),
1 A(1,3), A(2,3), MA
READ (5,120,END=200,ERR=200) A1,A2,A3, P11,P12,P13, P31,P32,P33
READ (5,110,END=200,ERR=200) IB11,IB22,IB33,IB12,IB13,IB23, MB
READ (5,120,END=200,ERR=200) B1,B2,B3, Q11,Q12,Q13, Q31,Q32,Q33
C
C FORMATS
110 FORMAT (7F10.3)
120 FORMAT (3F10.3, 2X, 6F8.3)
C

```

```

C      WRITE INPUT
      WRITE (6,150) (A(1,1), I=1,3), MA, A(1,2),A(2,2),A(2,3), A(1,3),
1      A(2,3),A(3,3), A1,P11,P31, A2,P12,P32, A3,P13,P33,
2      IB11,IB12,IB13, MB, IB12,IB22,IB23, IB13,IB23,IB33,
3      B1,Q11,Q31, B2,Q12,Q32, B3,Q13,Q33
150  FORMAT ('0'/'0INPUT INERTIA PROPERTIES: '/
1      '0',4X,'INERTIA DYADIC OF A FOR A*', A(1,J)',7X,
2      'MASS MA'/' ',4(1PE15.6)/' ',3E15.6/' ',3E15.6/
3      '0',4X,'VECTORS: '/' ',4X,'A',18X,'HA',13X,'NA'/' ',E15.6,
4      2(0PF15.6)/' ',1PE15.6,2(0PF15.6)/' ',1PE15.6,2(0PF15.6)/
5      '0',4X,'INERTIA DYADIC OF B FOR B*', IB(1,J)',6X,
6      'MASS MB'/' ',4(1PE15.6)/' ',3E15.6/' ',3E15.6/
7      '0',4X,'VECTORS: '/' ',4X,'B',18X,'HB',13X,'NB'/' ',E15.6,
8      2(0PF15.6)/' ',1PE15.6,2(0PF15.6)/' ',1PE15.6,2(0PF15.6))

C
C      DEFINE THE TERMS IN NAMED COMMON /BODBLK/
      MBM = MB/(MA + MB)
      MM = MA*MBM

C
C      DEFINE HELPFUL CONSTANTS (EQ. (6.54))
      P21 = P32*P13 - P33*P12
      P22 = P33*P11 - P31*P13
      P23 = P31*P12 - P32*P11

C
C      SEE EQ. (6.55).
      Q21 = Q32*Q13 - Q33*Q12
      Q22 = Q33*Q11 - Q31*Q13
      Q23 = Q31*Q12 - Q32*Q11

C
C      DEFINE TERMS IN NAMED COMMON /INTBLK/
      SEE EQ. (6.51).
      D11 = Q11*P11
      D12 = Q11*P12
      D13 = Q11*P13
      D21 = Q12*P11
      D22 = Q12*P12
      D23 = Q12*P13
      D31 = Q13*P11
      D32 = Q13*P12
      D33 = Q13*P13

C
C      SEE EQ. (6.52).
      E11 = Q21*P31 - Q31*P21
      E12 = Q21*P32 - Q31*P22
      E13 = Q21*P33 - Q31*P23
      E21 = Q22*P31 - Q32*P21
      E22 = Q22*P32 - Q32*P22
      E23 = Q22*P33 - Q32*P23
      E31 = Q23*P31 - Q33*P21
      E32 = Q23*P32 - Q33*P22
      E33 = Q23*P33 - Q33*P23

```

```
C
C   SEE EQ. (6.53).
F11 = Q21*P21 + Q31*P31
F12 = Q21*P22 + Q31*P32
F13 = Q21*P23 + Q31*P33
F21 = Q22*P21 + Q32*P31
F22 = Q22*P22 + Q32*P32
F23 = Q22*P23 + Q32*P33
F31 = Q23*P21 + Q33*P31
F32 = Q23*P22 + Q33*P32
F33 = Q23*P23 + Q33*P33

C
C   SEE EQ. (6.60).
U1 = A1 - B1*D11 - B2*D21 - B3*D31
U2 = A2 - B1*D12 - B2*D22 - B3*D32
U3 = A3 - B1*D13 - B2*D23 - B3*D33

C
C   SEE EQ. (6.61).
V1 = B1*E11 + B2*E21 + B3*E31
V2 = B1*E12 + B2*E22 + B3*E32
V3 = B1*E13 + B2*E23 + B3*E33

C
C   SEE EQ. (6.62).
W1 = B1*F11 + B2*F21 + B3*F31
W2 = B1*F12 + B2*F22 + B3*F32
W3 = B1*F13 + B2*F23 + B3*F33
RETURN

C
C   END OF DATA
200 WRITE (6,250)
250 FORMAT ('0','0END OF DATA OR ERROR IN DATA HAS BEEN ENCOUNTERED '
1      'IN SUBROUTINE BODIES'/'1')
STOP

C
C   END OF SUBROUTINE BODIES
END
```

SUBROUTINE INTRNL (T,F,MA,B,WBA,DWBA,R,DR,DDR)

THIS SUBROUTINE SUPPLIES PROPERTIES OF THE MOTION WHICH ARE  
DEPENDENT ON THE ANGLE ALF WHEN THE TWO HINGED BODIES PERFORM  
RELATIVE MOTION.

REAL T, F(3), MA(3), B(3,3), WBA(3), DWBA(3), R(3), DR(3), DDR(3),  
1 IB11,IB12,IB13,IB22,IB23,IB33

CONSTANTS IN NAMED COMMON /INTBLK/ ARE DEFINED IN SUBR BODIES.

COMMON /INTBLK/ D11,D12,D13,D21,D22,D23,D31,D32,D33,  
1 E11,E12,E13,E21,E22,E23,E31,E32,E33,  
2 F11,F12,F13,F21,F22,F23,F31,F32,F33,  
3 U1,U2,U3, V1,V2,V3, W1,W2,W3, P11,P12,P13,  
4 IB11,IB12,IB13,IB22,IB23,IB33

OBTAIN INTERNAL VARIABLE & ITS DERIVATIVES  
CALL ALPHA (T,ALF,DALF,DDALF)

SAL = SIN(ALF)  
CAL = COS(ALF)  
DALF2 = DALF\*DALF

DETERMINE EXTERNAL FORCE AND MOMENT  
NOTE: IN THIS CASE, THERE IS NO EXTERNAL FORCE SYSTEM.  
THE FOLLOWING DO-LOOP CAN BE REPLACED WITH NON-ZERO FORCES  
IF DESIRED.

DO 10 I=1,3  
F(I) = 0.0  
10 MA(I) = 0.0

ESTABLISH COSINE MATRIX BETWEEN A AND B. SEE EQ. (6.50).

C11 = D11 + E11\*SAL + F11\*CAL  
C12 = D12 + E12\*SAL + F12\*CAL  
C13 = D13 + E13\*SAL + F13\*CAL  
C21 = D21 + E21\*SAL + F21\*CAL  
C22 = D22 + E22\*SAL + F22\*CAL  
C23 = D23 + E23\*SAL + F23\*CAL  
C31 = D31 + E31\*SAL + F31\*CAL  
C32 = D32 + E32\*SAL + F32\*CAL  
C33 = D33 + E33\*SAL + F33\*CAL

COMPUTE INERTIA DYADIC OF B. SEE EQS. (6.38).

B(1,1) = IB11\*C11\*C11 + IB22\*C21\*C21 + IB33\*C31\*C31  
1 + 2.0\*( IB12\*C11\*C21 + IB13\*C11\*C31 + IB23\*C21\*C31 )  
B(2,2) = IB11\*C12\*C12 + IB22\*C22\*C22 + IB33\*C32\*C32  
1 + 2.0\*( IB12\*C12\*C22 + IB13\*C12\*C32 + IB23\*C22\*C32 )  
B(3,3) = IB11\*C13\*C13 + IB22\*C23\*C23 + IB33\*C33\*C33  
1 + 2.0\*( IB12\*C13\*C23 + IB13\*C13\*C33 + IB23\*C23\*C33 )  
B(1,2) = IB11\*C11\*C12 + IB22\*C21\*C22 + IB33\*C31\*C32 + IB12\*(C11\*C22 +  
1 C12\*C21) + IB13\*(C11\*C32 + C31\*C12) + IB23\*(C21\*C32 + C22\*C31)  
B(1,3) = IB11\*C11\*C13 + IB22\*C21\*C23 + IB33\*C31\*C33 + IB12\*(C11\*C23 +  
1 C13\*C21) + IB13\*(C11\*C33 + C13\*C31) + IB23\*(C21\*C33 + C31\*C23)

```

      B(2,3) = IB11*C12*C13 + IB22*C22*C23 + IB33*C32*C33 + IB12*(C12*C23+
1      C13*C22) + IB13*(C12*C33+C13*C32) + IB23*(C22*C33+C32*C23)
C
C      COMPUTE ANGULAR VELOCITY OF B IN A.  SEE EQ. (6.66).
      WBA(1) = P11*DALF
      WBA(2) = P12*DALF
      WBA(3) = P13*DALF
C
C      SEE EQ. (6.67).
      DWBA(1) = P11*DDALF
      DWBA(2) = P12*DDALF
      DWBA(3) = P13*DDALF
C
C      DEFINE TERMS
      SUMA1 = V1*SAL + W1*CAL
      SUMA2 = V2*SAL + W2*CAL
      SUMA3 = V3*SAL + W3*CAL
C
      SUMB1 = W1*SAL - V1*CAL
      SUMB2 = W2*SAL - V2*CAL
      SUMB3 = W3*SAL - V3*CAL
C
C      COMPUTE POSITION OF B* WITH RESPECT TO A*.  SEE EQ. (6.59).
      R(1) = U1 - SUMA1
      R(2) = U2 - SUMA2
      R(3) = U3 - SUMA3
C
C      SEE EQ. (6.63).
      DR(1) = SUMB1*DALF
      DR(2) = SUMB2*DALF
      DR(3) = SUMB3*DALF
C
C      SEE EQ. (6.64).
      DDR(1) = SUMB1*DDALF + SUMA1*DALF2
      DDR(2) = SUMB2*DDALF + SUMA2*DALF2
      DDR(3) = SUMB3*DDALF + SUMA3*DALF2
      RETURN
C
C      END OF SUBROUTINE INTRNL
      END
```

SUBROUTINE TWOBOD (T, WAF, DWAF)

THIS SUBROUTINE COMPUTES TIME-DERIVATIVES OF THE ANGULAR VELOCITY COMPONENTS OF THE MAIN BODY A (ALONG UNIT VECTORS FIXED IN A)

INTERNAL VARIABLES AND APPLIED FORCE SYSTEM IS SUPPLIED BY SUBROUTINE INTRNL.

ARGUMENTS OF SUBROUTINE TWOBOD:

T - TIME  
WAF - ANGULAR VELOCITY OF BODY A IN INERTIAL FRAME, F  
DWAF - ANGULAR ACCELERATION OF BODY A IN F

THE FOLLOWING VECTORS AND DYADIC ARE SUPPLIED BY SUBR. INTRNL:

F - RESULTANT OF ALL FORCES ACTING ON BODIES A & B  
MA - MOMENT OF FORCE SYSTEM ABOUT A\*  
B - INERTIA DYADIC OF BODY B FOR B\* (SEE NOTE BELOW)  
WBA - ANGULAR VELOCITY OF BODY B IN BODY A  
DWBA - ANGULAR ACCELERATION OF BODY B IN BODY A  
R - POSITION VECTOR OF B\* WITH RESPECT TO A\*  
DR - VELOCITY OF B\* IN BODY A  
DDR - ACCELERATION OF B\* IN BODY A

THE FOLLOWING ARE SUPPLIED THRU NAMED COMMON /BODBLK/:

A - INERTIA DYADIC OF BODY A FOR A\*  
MM -  $MA \cdot MB / (MA + MB)$  WHERE MA & MB ARE MASSES OF BODIES A & B  
MBM -  $MB / (MA + MB)$

NOTE: ALL VECTORS AND DYADICS MUST BE RESOLVED ALONG A SET OF MUTUALLY PERPENDICULAR UNIT VECTORS FIXED IN BODY A.

DECLARATIONS

REAL T, WAF(3), DWAF(3), A(3,3), MM, MBM,  
1 F(3), MA(3), B(3,3), WBA(3), DWBA(3), R(3), DR(3), DDR(3)  
COMMON /BODBLK/ A, MM, MBM

OBTAIN INFORMATION ON RELATIVE MOTION

CALL INTRNL (T, F, MA, B, WBA, DWBA, R, DR, DDR)

CONVERT ARRAYS TO CONSTANTS AND DEFINE TERMS.

(MOST ARRAYS ARE CONVERTED TO CONSTANTS TO SPEED COMPUTATIONS.)

B11 = B(1,1)  
B12 = B(1,2)  
B13 = B(1,3)  
B22 = B(2,2)  
B23 = B(2,3)  
B33 = B(3,3)

R1 = R(1)  
R2 = R(2)  
R3 = R(3)

```

AB11 = A(1,1) + B11
AB12 = A(1,2) + B12
AB13 = A(1,3) + B13
AB22 = A(2,2) + B22
AB23 = A(2,3) + B23
AB33 = A(3,3) + B33
C
C FORM EQS. (6.23)
E11 = AB11 + MM*( R2*R2 + R3*R3)
E22 = AB22 + MM*( R1*R1 + R3*R3)
E33 = AB33 + MM*( R1*R1 + R2*R2)
C
C FORM EQS. (6.24)
E12 = AB12 - MM*R1*R2
E13 = AB13 - MM*R1*R3
E23 = AB23 - MM*R2*R3
C
C DEFINE TERMS (EQS. (6.26)-(6.31))
C1 = E22*E33 - E23*E23
C2 = E13*E23 - E12*E33
C3 = E12*E23 - E22*E13
C4 = E11*E33 - E13*E13
C5 = E13*E12 - E11*E23
C6 = E11*E22 - E12*E12
C
C FIND DETERMINANT OF THE E'S. SEE EQ. (6.32)
DET = E11*C1 + E12*C2 + E13*C3
C
C IF (ABS(DET) .GT. 1.0E-25) GO TO 50
WRITE (6,110) DET, T
110 1 FORMAT ('DETERMINANT IN SUBROUTINE TWOBOD =', 1PE15.6,
1 ' AT T =', E15.6, '. EXECUTION TERMINATED')
STOP
C
C CONVERT ARRAYS TO CONSTANTS AND DEFINE TERMS
50 W1 = WAF(1)
W2 = WAF(2)
W3 = WAF(3)
C
F1 = F(1)
F2 = F(2)
F3 = F(3)
C
WB1 = WBA(1)
WB2 = WBA(2)
WB3 = WBA(3)
C
DR1 = DR(1)
DR2 = DR(2)
DR3 = DR(3)
C

```

DDR1 = DDR(1)  
DDR2 = DDR(2)  
DDR3 = DDR(3)

ABW1 = AB11\*W1 + AB12\*W2 + AB13\*W3  
ABW2 = AB12\*W1 + AB22\*W2 + AB23\*W3  
ABW3 = AB13\*W1 + AB23\*W2 + AB33\*W3

DWB1 = DWBA(1) + W2\*WB3 - W3\*WB2  
DWB2 = DWBA(2) + W3\*WB1 - W1\*WB3  
DWB3 = DWBA(3) + W1\*WB2 - W2\*WB1

BW1 = B11\*W1 + B12\*W2 + B13\*W3  
BW2 = B12\*W1 + B22\*W2 + B23\*W3  
BW3 = B13\*W1 + B23\*W2 + B33\*W3

BWB1 = B11\*WB1 + B12\*WB2 + B13\*WB3  
BWB2 = B12\*WB1 + B22\*WB2 + B23\*WB3  
BWB3 = B13\*WB1 + B23\*WB2 + B33\*WB3

WBF1 = W1 + WB1  
WBF2 = W2 + WB2  
WBF3 = W3 + WB3

WXDR1 = W2\*DR3 - W3\*DR2  
WXDR2 = W3\*DR1 - W1\*DR3  
WXDR3 = W1\*DR2 - W2\*DR1

WR = W1\*R1 + W2\*R2 + W3\*R3

FORM RIGHT-HAND-SIDE OF ATTITUDE EQUATION. SEE EQ. (6.25).

D1 = MA(1) + ABW2\*W3 - ABW3\*W2 - B11\*DWB1 - B12\*DWB2 - B13\*DWB3  
1 + BW2\*WB3 - BW3\*WB2 + BWB2\*WBF3 - BWB3\*WBF2 - MBM\*(R2\*F3  
2 - R3\*F2) - MM\*(R2\*DDR3 - R3\*DDR2 + 2.0\*(R2\*WXDR3 - R3\*WXDR2)  
3 + WR\*(R2\*W3 - R3\*W2))

D2 = MA(2) + ABW3\*W1 - ABW1\*W3 - B12\*DWB1 - B22\*DWB2 - B23\*DWB3  
1 + BW3\*WB1 - BW1\*WB3 + BWB3\*WBF1 - BWB1\*WBF3 - MBM\*(R3\*F1  
2 - R1\*F3) - MM\*(R3\*DDR1 - R1\*DDR3 + 2.0\*(R3\*WXDR1 - R1\*WXDR3)  
3 + WR\*(R3\*W1 - R1\*W3))

D3 = MA(3) + ABW1\*W2 - ABW2\*W1 - B13\*DWB1 - B23\*DWB2 - B33\*DWB3  
1 + BW1\*WB2 - BW2\*WB1 + BWB1\*WBF2 - BWB2\*WBF1 - MBM\*(R1\*F2  
2 - R2\*F1) - MM\*(R1\*DDR2 - R2\*DDR1 + 2.0\*(R1\*WXDR2 - R2\*WXDR1)  
3 + WR\*(R1\*W2 - R2\*W1))

COMPUTE ANGULAR ACCELERATION OF BODY A IN F BY CRAMER'S RULE  
SEE EQS. (6.33)-(6.35).

DWAF(1) = (D1\*C1 + D2\*C2 + D3\*C3)/DET  
DWAF(2) = (D1\*C2 + D2\*C4 + D3\*C5)/DET  
DWAF(3) = (D1\*C3 + D2\*C5 + D3\*C6)/DET  
RETURN

END OF SUBROUTINE TWOBOD  
END



SUBROUTINE DFEQS1(NEQ, X, STEP, Y, F, EPS, \*)

SINGLE STEP DIFFERENTIAL EQUATION SOLVER.

INTEGER NEQ

REAL X, STEP, Y(NEQ), F, EPS

EXTERNAL F

KUTTA MERSON INTEGRATES A SYSTEM OF 'NEQ' FIRST ORDER ORDINARY DIFFERENTIAL EQUATIONS .. YPRIME = F(T,Y), FROM X TO X+STEP, WITH ERROR CONTROL, IF REQUESTED BY 'EPS'. WHEN T = T+H, RETURN 1 TAKEN.

SEE.. L. FOX, 'NUMERICAL SOLUTION OF ORDINARY AND PARTIAL DIFFERENTIAL EQUATIONS', 1962, P.24.

CALLING SEQUENCE...

DFEQS1 (NEQ,X,STEP,Y,FUNCT,EPS,&1)

PARAMETERS...

NEQ	FULL WORD INTEGER	THE NUMBER OF FIRST ORDER EQUATIONS IN THE SYSTEM (NEQ.LE.30)
X	REAL VARIABLE SHORT PRECISION	THE INITIAL VALUE OF THE INDEPENDENT VARIABLE, WHICH IS SET TO X + STEP ON RETURN
STEP	REAL VARIABLE SHORT PRECISION	THE LENGTH OF THE INTERVAL THROUGH WHICH THE EQUATIONS ARE TO BE SOLVED (MAY BE POSITIVE OR NEGATIVE)
Y	REAL ARRAY SHORT PRECISION	THE INITIAL VALUES OF THE DEPENDENT VARIABLES Y(1),..., Y(NEQ) AT X. THE ARRAY IS SET TO THE VALUES AT X + STEP BY THE SUBROUTINE.
FUNCT	SUBROUTINE NAME	THE NAME OF A USER SUPPLIED SUBROUTINE SUBPROGRAM WITH PARAMETERS (X,Y,DY), WHICH WHEN GIVEN THE INDEPENDENT VARIABLE X, THE DEPENDENT VARIABLES Y(1),...,Y(NEQ) PLACES THE FIRST DERIVATIVE AT X IN THE ARRAY DY(1),..., DY(NEQ).
EPS	REAL VARIABLE SHORT PRECISION	THE STEP INTERVAL OF THE SUBROUTINE IS ADJUSTED SO THAT THE MAXIMUM OF THE ESTIMATED RELATIVE ERROR IS LESS THAN EPS. IF EPS=0, THE INTERVAL REMAINS UNCHANGED AND EQUAL TO STEP.

```

C
C      &1      STATEMENT LABEL      ERROR RETURN 1
C
C      LIBRARY PROGRAM NUMBER  C015
C      JOHN H. WELSCH (SLAC)
C      MARCH 8,1967
C
      REAL HC/0./
      REAL      FINAL, H2, H3, H6, H8, ERR, TEST, T, H, EPSL,
1      Y1(30), Y2(30), F0(30), F1(30), F2(30)
      INTEGER I
      LOGICAL DBL
C *** CHECK FOR INITIAL ENTRY AND ADJUST HC, IF NECESSARY.
      IF(NEQ.NE.0) GO TO 10
      HC = STEP
      RETURN
10      IF(STEP.EQ.0) RETURN
      IF(HC.EQ.0) HC = STEP
C *** SET LOCAL VARIABLES.
      FINAL = X+STEP
      H = STEP
      EPSL = EPS
C *** CHANGE DIRECTION, IF REQUIRED.
      IF(EPS.EQ.0 .OR. ABS(H) .LE. ABS(HC)) GO TO 15
      IF(H*HC.LE.0) HC = -HC
      H = HC
15      T = X+H
      X = FINAL
      H2 = H/2.
      H3 = H/3.
      H6 = H/6.
      H8 = H/8.
C *** MAIN KUTTA-MERSON STEP
20      IF(H.GT.0 .AND. T.GT.FINAL .OR. H.LT.0.AND.T.LT.FINAL) GOTO 40
21      CALL F(T-H, Y, F0)
      DO 22 I = 1,NEQ
22          Y1(I) = F0(I)*H3+Y(I)
      CALL F(T-2.*H3, Y1, F1)
      DO 23 I = 1,NEQ
23          Y1(I) = (F0(I)+F1(I))*H6+Y(I)
      CALL F(T-2.*H3, Y1, F1)
      DO 24 I = 1,NEQ
24          Y1(I) = (F1(I)*3.+F0(I))*H8+Y(I)
      CALL F(T-H2, Y1, F2)
      DO 25 I = 1,NEQ
25          Y1(I) = (F2(I)*4.-F1(I)*3.+F0(I))*H2 +Y(I)
      CALL F(T, Y1, F1)
      DO 26 I = 1,NEQ
26          Y2(I) = (F2(I)*4.+F1(I)+F0(I))*H6 +Y(I)
C *** DOES THE STEP SIZE H NEED TO BE CHANGED.
      IF(EPSL.EQ.0) GO TO 38
      DBL = .TRUE.

```

```

DO 35 I = 1,NEQ
    ERR = ABS(Y1(I)-Y2(I))*0.2
    TEST = ABS(Y1(I))*EPSL
    IF(ERR.LE.TEST) GO TO 34
C *** HALVE THE STEP SIZE.
    H = H2
    T = T-H2
    IF(T+H.NE.T) GO TO 33
    X = T
    RETURN 1
C *** STEP SIZE TOO SMALL RELATIVE TO T, TAKE RETURN 1.
33    H2 = H/2.
    H3 = H/3.
    H6 = H/6.
    H8 = H/8.
    GO TO 21
34    IF(64.0*ERR.GT.TEST) DBL = .FALSE.
35    CONTINUE
C *** DOUBLE THE STEP SIZE, MAYBE.
    IF(.NOT.DBL) GO TO 38
    H2 = H
    H = 2.*H
    H3 = H/3.
    H6 = H/6.
    H8 = H/8.
38    DO 39 I = 1,NEQ
39    Y(I) = Y2(I)
    T = T+H
    GO TO 20
40    IF(EPSL.EQ.0) RETURN
C *** NOW BE SURE TO HAVE T = FINAL.
    HC = H
    H = FINAL-(T-H)
    IF(ABS(H).LE.ABS(FINAL)*9.536744E-07) RETURN
    T = FINAL
    EPSL = 0
    H2 = H/2.
    H3 = H/3.
    H6 = H/6.
    H8 = H/8.
    GO TO 20
C *** LAST CARD OF SUBROUTINE DFEQ1
END

```

A.3 Main Program and Subroutines ALPHA and OUTPUT

C TWO HINGED BODIES PERFORMING RELATIVE MOTIONS  
C  
C BEGIN MAIN PROGRAM  
C  
C PROGRAM PERFORMS CALCULATIONS OUTLINED IN SECS. 6.1 AND 6.2  
C  
C THIS PROGRAM COMPUTES THE ANGULAR VELOCITY OF BODY A WHEN BODY  
C B , ATTACHED TO A BY A HINGE, IS MOVED RELATIVE TO A.  
C  
C THE MOTION OF B IN A IS DESCRIBED BY 1 ANGLE, ALF,  
C WHICH IS PRESCRIBED IN SUBROUTINE ALPHA.  
C  
C THIS PARTICULAR MAIN PROGRAM IS DESIGNED TO BE USED WITH TIME  
C HISTORIES OF ALF WHICH ARE DESCRIBABLE IN TERMS OF 2 PARAMETERS,  
C AN AMPLITUDE & A PERIOD (E.G., SEE FIG. 7.2), AND IT SHOULD BE  
C MODIFIED, ALONG WITH SUBROUTINE ALPHA, WHEN OTHER FORMS OF  
C RELATIVE MOTION ARE DESIRED.  
C  
C SUBROUTINES REQUIRED:  
C BODIES READS IN AND WRITES OUT INERTIA PROPERTIES AND  
C PERFORMS THE COMPUTATIONS IN EQS. (6.51)-(6.55),  
C (6.60)-(6.62)  
C INTRNL PERFORMS THE COMPUTATIONS OF EQS. (6.50), (6.38),  
C (6.59), (6.63), (6.64), (6.66), (6.67)  
C ALPHA PRESCRIBES A TIME HISTORY OF THE ANGLE ALF AND ITS  
C DERIVATIVES. THIS PARTICULAR FUNCTIONAL FORM IS GIVEN  
C IN EQ. (7.27)  
C TWOBOD PERFORMS COMPUTATIONS IN EQS. (6.23)-(6.35)  
C OUTPUT LABELS COLUMNS AND WRITES OUTPUT  
C DFEQS1 PERFORMS NUMERICAL INTEGRATION VIA THE KUTTA-MERSON  
C METHOD  
C  
C NAMED COMMON INTERCONNECTIONS:  
C /BODBLK/ SUBROUTINE BODIES & SUBROUTINE TWOBOD  
C /INTBLK/ SUBROUTINE BODIES & SUBROUTINE INTRNL  
C /ALFBLK/ MAIN PROGRAM & SUBROUTINE ALPHA  
C  
C INPUT TO THE PROGRAM INCLUDES THE INERTIA PROPERTIES OF A & B ,  
C THE AMPLITUDE AND PERIOD OF EACH OSCILLATION OF B RELATIVE TO A ,  
C AND INITIAL CONDITIONS.  
C  
C INPUT DATA IS READ IN 3 STEPS:  
C STEP 1:  
C FOUR CARDS CONTAINING INERTIA & GEOMETRICAL PROPERTIES ARE READ  
C BY SUBROUTINE BODIES. (SEE BODIES FOR DETAILS.)

```

C      STEP 2:
C      THE MAIN PROGRAM READS ONE CARD WHICH HAS FORMAT (4F10.3,I10)
C      AND WHICH CONTAINS THE FOLLOWING ITEMS DEALING WITH INITIAL
C      CONDITIONS:
C      TO          (REAL)      STARTING TIME
C      W(I)  I=1,3  (REAL AR)  INITIAL ANGULAR RATES
C      N          (INTEGER) THE NUMBER OF CYCLES OF RELATIVE MOTION TO
C                        BE PERFORMED. MUST BE LESS THAN 101.
C
C      STEP 3:
C      THE MAIN PROGRAM READS N CARDS WHICH HAVE FORMAT (2F10.2,I10)
C      AND WHICH CONTAIN THE FOLLOWING ITEMS DESCRIBING THE RELATIVE
C      MOTION:
C      AMPL(I)      (REAL AR) OSCILLATION AMPLITUDE IN DEGREES
C      PD(I)        (REAL AR) OSCILLATION PERIOD
C      NPRNT(I)     (INT. AR) NUMBER OF PRINT-OUTS PER CYCLE
C
C      OUTPUT INCLUDES THE TIME AND ANGULAR VELOCITY COMPONENTS AND IS
C      SUPPLIED BY SUBROUTINE OUTPUT
C
C      VARIABLE DECLARATIONS
C      REAL PD(100), AMPL(100), W(3), RAD/1.745329E-02/
C      INTEGER I, J, NPT, N, NPRNT(100)
C      COMMON /ALFBLK/ PERIOD, AMPLTD
C      EXTERNAL TWOBOD
C
C      WRITE HEADING
C      250 WRITE (6,50)
C      50 FORMAT (1H1, 'TWO HINGED BODIES PERFORMING PRESCRIBED ',
C      1          'RELATIVE MOTIONS' /'0', 'FORWARD INTEGRATION OF ',
C      2          'EQUATIONS (6.33)-(6.35)' ///'0',
C      3          'A INDICATES MAIN BODY B INDICATES SECOND BODY')
C
C      READ IN INERTIA PROPERTIES IN SUBROUTINE BODIES
C      CALL BODIES
C
C      READ IN INITIAL CONDITIONS
C      READ (5,110,ERR=220,END=220) TO, (W(I), I=1,3), N
C      110 FORMAT (4F10.3,I10)
C
C      WRITE OUT INITIAL CONDITIONS
C      WRITE (6,120) TO, (W(I), I=1,3), N
C      120 FORMAT ('0'/'0'INITIAL CONDITIONS: '/
C      1          ' ',5X,'INITIAL TIME =',F8.3/ ' ',5X,'ANGULAR RATES'/
C      2          ' ',5X,'W(1) =', F8.4, ' W(2) =', F8.4, ' W(3) =',
C      3          F8.4 /'0',5X,'NUMBER OF CYCLES =',I4/
C      4          '0',5X,'CYCLE AMPLITUDE PERIOD PRINTS/PERIOD')
C      IF (N .EQ. 0) GO TO 250
C

```

```
C      READ IN, AND WRITE OUT, PARAMETERS FOR RELATIVE MOTION
      DO 480 I=1,N
        READ (5,410,ERR=310,END=310) AMPL(I), PD(I), NPRNT(I)
410    FORMAT (2F10.2,I10)
480    WRITE (6,481) I, AMPL(I), PD(I), NPRNT(I)
481    FORMAT (' ',I8,F13.2,F10.2,I10)
      GO TO 320
310 N = I-1

C
C      INITIALIZE THE INDEPENDENT VARIABLE AND THE INTERNAL INTEGRATION
C      STEP SIZE
320 TIME = TO
      CALL DFEQS1 (0,T,0.5, W,TWOBOD,1.0E-5,&150)

C
C      LABEL OUTPUT COLUMNS USING SECOND ENTRY TO SUBROUTINE OUTPUT
      CALL OUT2

C
C      WRITE OUT INITIAL CONDITIONS
      PERIOD = 1.0
      AMPLTD = 0.0
      CALL OUTPUT (TIME, 0.0, W)

C
C      BEGIN INTEGRATION
      DO 450 I=1,N
        T = 0.0
        AMPLTD = AMPL(I)*RAD
        PERIOD = PD(I)
        NPT = NPRNT(I)
        DT = PERIOD/FLOAT(NPT)

C
        DO 430 J=1,NPT
          CALL DFEQS1 (3,T,DT, W,TWOBOD,1.0E-4,&150)
          TIME = TIME + DT
430    CALL OUTPUT (TIME, T, W)
450    WRITE (6,440)
440    FORMAT (' ')

C
C      END OF INTEGRATION
      GO TO 250

C
C      IF INTEGRATION FAILS
150 T = T/PERIOD
      WRITE (6,210) T
210 FORMAT (' INTEGRATION TERMINATED AT T/PD =',F8.5)
      GO TO 250

C
C      IF DATA CARDS ARE MISSING
220 WRITE (6,290)
290 FORMAT ('0'/ '0DATA MISSING FOR MAIN PROGRAM READ STATEMENTS'/'1')
      RETURN

C
C      END OF MAIN PROGRAM
      END
```

```

C      SUBROUTINE ALPHA (T, ALF, DALF, DDALF)
C
C      THIS SUBROUTINE SUPPLIES THE ANGLE, ALF, DESCRIBING THE ORIENTA-
C      TION OF BODY B IN BODY A. THE PARTICULAR FUNCTIONAL FORM
C      FOR THE TIME HISTORY OF ALF IS GIVEN BY EQ. (7.27). TIME DERIV-
C      ITIVES OF ALF ARE ALSO GIVEN.
C
C      REAL PI2/6.283185/, T, ALF, DALF, DDALF
C      COMMON /ALFBLK/PERIOD,AMPLTD
C
C      COMPUTE HELPFUL CONSTANTS
C      PD2 = PERIOD/2.0
C      AMPPD = AMPLTD/PD2
C      AMPPD2 = PI2*AMPPD/PD2
C
C      DEFINE INDEPENDENT VARIABLE FOR ONE CYCLE OF LIMB MOTION
C      NOTE: IT IS REQUIRED THAT (0.0 .LE. T .LE. PERIOD)
C      TAU = T*PI2/PD2
C      SINT = SIN(TAU)
C
C      START COMPUTATIONS OF ALF AND ITS DERIVATIVES
C      IF (TAU .GT. PI2) GO TO 10
C
C      IF IN THE FIRST HALF OF A CYCLE
C      EQ. (7.27)
C      ALF = AMPLTD*(TAU - SINT)/PI2
C
C      DALF = AMPPD*(1.0 - COS(TAU))
C      DDALF = AMPPD2*SINT
C      RETURN
C
C      IF IN THE SECOND HALF OF A CYCLE
C      EQ. (7.27)
C      10 ALF = AMPLTD*(2.0 - (TAU - SINT)/PI2)
C
C      DALF = -AMPPD*(1.0 - COS(TAU))
C      DDALF = -AMPPD2*SINT
C      RETURN
C
C      END OF SUBROUTINE ALPHA
C      END
```

```

SUBROUTINE OUTPUT (TIME, T, WAF)
C
C THIS SUBROUTINE WRITES THE OUTPUT. THIS SUBROUTINE CAN BE
C ENLARGED TO COMPUTE OTHER QUANTITIES SUCH AS KINETIC ENERGIES.
C
REAL T, TIME, WAF(3), ALF
C
C OBTAIN VALUE OF ALPHA AND CONVERT TO DEGREES
CALL ALPHA (T, ALF, DALF, DDALF)
ALF = ALF/1.745329E-02
C
C WRITE OUTPUT
WRITE (6,120) TIME, ALF, (WAF(I), I=1,3)
120 FORMAT (' ',5F10.2)
RETURN
C
ENTRY OUT2
C
C LABEL OUTPUT COLUMNS
WRITE (6,60)
60 FORMAT ('1      TIME      ALPHA      W(1)      W(2)      W(3)')
RETURN
C
C END OF SUBROUTINE OUTPUT
END

```

Data Cards:

(See Sec. 7.4)

0.5944	8.402	8.777	0.05135	0.0	0.0	4.894	
1.4652	0.7248	0.0	0.0	0.0	-1.0	1.0	0.0
0.00296	0.2607	0.2607	0.0	0.0	0.0	0.4446	
1.2914	0.0	0.0	0.0	0.0	-1.0	1.0	0.0
0.0	6.2832	0.0	0.0	4			
135.0	2.8	7					
135.0	2.8	7					
135.0	7.0	14					
135.0	10.2	17					

(See Sec. 8.3)

5.0	3.333	3.333	0.0	0.0	0.0	10.0	
-0.5	0.0	0.0	0.0	0.0	-1.0	1.0	0.0
0.0	0.0	0.0	0.0	0.0	0.0	1.0	
1.0	0.0	0.0	0.0	0.0	-1.0	1.0	0.0
0.0	3.1416	0.0	5.0582	1			
73.0	1.6	16					



A.4 Computer Output

TWO HINGED BODIES PERFORMING PRESCRIBED RELATIVE MOTIONS  
FORWARD INTEGRATION OF EQUATIONS (6.33)-(6.35)

A INDICATES MAIN BODY      B INDICATES SECOND BODY

INPUT INERTIA PROPERTIES:

INERTIA DYADIC OF A FOR A*, A(I,J)			MASS MA
5.944000E-01	5.135000E-02	0.000000E-01	4.894000E 00
5.135000E-02	8.402000E 00	0.000000E-01	
0.000000E-01	0.000000E-01	8.777000E 00	

VECTORS:

A	HA	NA
1.465200E 00	0.000000	1.000000
7.248000E-01	0.000000	0.000000
0.000000E-01	-1.000000	0.000000

INERTIA DYADIC OF B FOR B*, IB(I,J)			MASS MB
2.960000E-03	0.000000E-01	0.000000E-01	4.446000E-01
0.000000E-01	2.607000E-01	0.000000E-01	
0.000000E-01	0.000000E-01	2.607000E-01	

VECTORS:

B	HB	NB
1.291400E 00	0.000000	1.000000
0.000000E-01	0.000000	0.000000
0.000000E-01	-1.000000	0.000000

INITIAL CONDITIONS:

INITIAL TIME = 0.000

ANGULAR RATES

W(1) = 6.2832      W(2) = 0.0000      W(3) = 0.0000

NUMBER OF CYCLES = 4

CYCLE	AMPLITUDE	PERIOD	PRINTS/PERIOD
1	135.00	2.80	7
2	135.00	2.80	7
3	135.00	7.00	14
4	135.00	10.20	17

TIME	ALPHA	W(1)	W(2)	W(3)
0.00	0.00	6.28	0.00	0.00
0.40	17.62	4.52	-0.01	0.07
0.80	86.47	2.11	0.20	0.38
1.20	132.51	3.00	0.45	0.21
1.60	132.51	2.96	0.62	0.04
2.00	86.47	1.87	0.54	-0.32
2.40	17.62	3.41	0.32	-0.26
2.80	0.00	4.73	-0.21	-0.31
3.20	17.62	3.38	-0.34	0.26
3.60	86.47	1.45	0.02	0.65
4.00	132.51	1.99	0.35	0.41
4.40	132.51	1.93	0.58	0.16
4.80	86.47	1.05	0.61	-0.23
5.20	17.62	1.34	0.56	-0.09
5.60	0.00	1.85	0.45	-0.32
6.10	2.49	1.81	0.04	-0.52
6.60	17.62	1.32	-0.34	-0.38
7.10	48.53	0.62	-0.48	-0.15
7.60	86.47	0.17	-0.49	-0.02
8.10	117.38	-0.09	-0.47	-0.05
8.60	132.51	-0.24	-0.45	-0.16
9.10	135.00	-0.31	-0.42	-0.25
9.60	132.51	-0.33	-0.37	-0.34
10.10	117.38	-0.27	-0.32	-0.46
10.60	86.47	-0.15	-0.28	-0.53
11.10	48.53	-0.07	-0.26	-0.53
11.60	17.62	-0.07	-0.24	-0.51
12.10	2.49	-0.13	-0.22	-0.52
12.60	0.00	-0.17	-0.18	-0.52
13.20	1.41	-0.20	-0.12	-0.54
13.80	10.37	-0.19	-0.05	-0.53
14.40	30.50	-0.14	-0.00	-0.48
15.00	59.58	-0.08	0.03	-0.40
15.60	90.72	-0.05	0.04	-0.34
16.20	115.96	-0.03	0.05	-0.34
16.80	130.41	-0.01	0.05	-0.37
17.40	134.82	0.00	0.05	-0.40
18.00	134.82	0.01	0.05	-0.41
18.60	130.41	0.02	0.04	-0.45
19.20	115.96	0.02	0.04	-0.50
19.80	90.72	0.01	0.03	-0.54
20.40	59.58	0.00	0.03	-0.55
21.00	30.50	-0.00	0.03	-0.55
21.60	10.37	0.00	0.03	-0.55
22.20	1.41	0.01	0.03	-0.55
22.80	0.00	0.02	0.02	-0.55

TWO HINGED BODIES PERFORMING PRESCRIBED RELATIVE MOTIONS  
FORWARD INTEGRATION OF EQUATIONS (6.33)-(6.35)

A INDICATES MAIN BODY            B INDICATES SECOND BODY

INPUT INERTIA PROPERTIES:

INERTIA DYADIC OF A FOR A* , A(I,J)			MASS MA
5.000000E 00	0.000000E-01	0.000000E-01	1.000000E 01
0.000000E-01	3.333000E 00	0.000000E-01	
0.000000E-01	0.000000E-01	3.333000E 00	

VECTORS:		
A	HA	NA
-5.000000E-01	0.000000	1.000000
0.000000E-01	0.000000	0.000000
0.000000E-01	-1.000000	0.000000

INERTIA DYADIC OF B FOR B* , IB(I,J)			MASS MB
0.000000E-01	0.000000E-01	0.000000E-01	1.000000E 00
0.000000E-01	0.000000E-01	0.000000E-01	
0.000000E-01	0.000000E-01	0.000000E-01	

VECTORS:		
B	HB	NB
1.000000E 00	0.000000	1.000000
0.000000E-01	0.000000	0.000000
0.000000E-01	-1.000000	0.000000

INITIAL CONDITIONS:

INITIAL TIME = 0.000  
ANGULAR RATES  
W(1) = 3.1416            W(2) = 0.0000            W(3) = 5.0582

NUMBER OF CYCLES = 1

CYCLE	AMPLITUDE	PERIOD	PRINTS/PERIOD
1	73.00	1.60	16

TIME	ALPHA	W(1)	W(2)	W(3)
0.00	0.00	3.14	0.00	5.06
0.10	0.91	3.14	0.09	5.17
0.20	6.63	3.16	0.04	5.45
0.30	19.16	3.22	-0.20	5.72
0.40	36.50	3.34	-0.62	5.82
0.50	53.84	3.52	-1.15	5.65
0.60	66.37	3.78	-1.70	5.21
0.70	72.09	4.12	-2.21	4.56
0.80	73.00	4.52	-2.62	3.86
0.90	72.09	4.91	-2.95	3.00
1.00	66.37	5.31	-3.03	1.86
1.10	53.84	5.72	-2.68	0.69
1.20	36.50	6.05	-1.91	-0.15
1.30	19.16	6.22	-1.03	-0.48
1.40	6.63	6.28	-0.36	-0.38
1.50	0.91	6.28	-0.05	-0.15
1.60	0.00	6.28	-0.00	-0.03

## References

1. Smith, P.G., The Reorientation of the Human Body in Free Fall, Tech. Report No. 171, Div. of Engineering Mechanics, Stanford Univ., May 1967 (also Ph.D. thesis).
2. Kulwicki, P.V., Schlei, E.J., and Vergamini, P.L., "Weightless Man: Self-Rotation Techniques," Aerospace Medical Research Lab., AMRL-TDR-62-129, Wright-Patterson A.F.B., Oct. 1962.
3. Stepantsov, V., Yereimin, A., and Alekperov, S., "Maneuvering in Free Space," NASA TT-F-9883, Washington, D.C., Jan. 1966.
4. Kane, T.R., and Scher, M.P., "A Dynamical Explanation of the Falling Cat Phenomenon," International J. of Solids and Structures, to appear in 1969.
5. Whitsett, C.E., "Some Dynamic Response Characteristics of Weightless Man," Aerospace Medical Research Lab., AMRL-TDR-63-18, Wright-Patterson A.F.B., April 1963.
6. Hanavan, E.P., "A Mathematical Model of the Human Body," Aerospace Medical Research Lab., AMRL-TR-64-102, Wright-Patterson A.F.B., Oct. 1964.
7. Hanavan, E.P., "A Personalized Mathematical Model of the Human Body," Paper No. 65-498, AIAA Second Annual Meeting, July 1965.
8. McCrank, J.M., and Seger, D.R., Torque Free Rotational Dynamics of a Variable-Configuration Body (Application to Weightless Man), M.S. thesis GAW/Mech 64-19, Air Force Institute of Technology, Wright-Patterson A.F.B., May 1964.
9. Tewell, J.R., and Johnson, C.H., "EVA/IVA Simulation Dynamics," Report R-67-8, Martin Marietta Corp., Denver, Feb. 1967.
10. Smith, P.G., and Kane, T.R., "On the Dynamics of the Human Body in Free Fall," J. of Applied Mechanics, Vol. 35, No. 1, Mar. 1968, pp. 167-168.
11. Riddle, B.C., and Kane, T.R., "Reorientation of the Human Body by Means of Arm Motions," Tech. Report No. 182, Dept. of Applied Mechanics, Stanford Univ., Feb. 1968.
12. Passerello, C., On the Ability of a Man to Reorientate Himself in Space, M.S. thesis, College of Engr., Univ. of Cincinnati, 1968.
13. Kane, T.R., and Scher, M.P., "Human Self-Rotation by Means of Limb Movements," J. of Biomechanics, to appear in 1969.

14. Poli, C.R., "A Study of the Effect of Man's Motion on the Attitude and Orbital Motion of a Satellite," Systems Engineering Group, SEG-TR-65-41, Wright-Patterson A.F.B., Dec. 1965.
15. Tieber, J.A., and Lindemuth, R.W., "An Analysis of the Inertial Properties and Performance of the Astronaut Maneuvering System," Aerospace Medical Research Lab., AMRL-TR-65-216, Wright-Patterson A.F.B., Dec. 1965.
16. Kurzhals, P.R., and Reynolds, R.B., "Development of an Analytical Model of Man and the Effects of His Motion on Orbital Spacecraft," Langley Research Center, LWP No. 442, NASA, 1967.
17. Thomson, W.T., Introduction to Space Dynamics, John Wiley & Sons, Inc., N.Y., 1961, pp. 212-216.
18. Fouché, E., and Fouché, M., "Sur le déplacement de l'axe de rotation d'un corps solide dont une partie est rendue momentanément mobile par rapport au reste de la masse," Comptes Rendus de l'Académie des Sciences, Vol. 123, Paris, July-Dec. 1896, pp. 93-96.
19. Fang, B.T., "Kinetic Energy and Angular Momentum about the Variable Center of Mass of a Satellite," AIAA Journal, Vol. 3, No. 8, Aug. 1965, pp. 1540-1542.
20. Kane, T.R., and Scher, M.P., "A Method of Active Attitude Control Based on Energy Considerations," J. of Spacecraft and Rockets, to appear in 1969.
21. Letvin-Sedoy, M.Z., "Control of Angular Motion of a Body by Means of Rotors," AIAA Journal, Vol. 1, No. 1, Jan. 1963, pp. 275-277.
22. Kane, T.R., and Sobala, D., "A New Method for Attitude Stabilization," AIAA Journal, Vol. 1, No. 6, June 1963, pp. 1365-1367.
23. Gutman, A.S., "Active Damping Concept for Gravity Gradient Satellite Attitude Control," J. of Spacecraft and Rockets, Vol. 4, No. 7, July 1967, pp. 953-955.
24. Gatlin, J.A., Buckingham, A.G., and Pleasants, W.H., "Satellite Attitude Control Using a Torqued, 2-Axis-Gimballed Boom as the Actuator," Paper 68-857, AIAA Guidance, Control, and Flt. Dynamics Conf., Pasadena, Aug. 1968.
25. Lelikov, I., and Miller, D., "Preliminary Analysis of a Reaction-Boom Attitude Control System," Report No. GCS/2379/6212, Lockheed Missiles & Space Co., Sunnyvale, Calif., 1969.
26. Likins, P.W., "Effects of Energy Dissipation on the Free Body Motions of Spacecraft," Tech. Report No. 32-860, Jet Propulsion Lab., Pasadena, July 1966.

27. Alper, J.R., "Analysis of Pendulum Damper for Satellite Wobble Damping," Report No. EM-13-23, TRW Space Technology Labs., Redondo Beach, Calif., July 1963.
28. Haseltine, W.R., "Passive Damping of Wobbling Satellites: General Stability Theory and Example," J. of Aerospace Sciences, Vol. 29, No. 5, May 1962, pp. 543-550.
29. Hrushow, W.K., "Euler's Rotational Equations for Bodies with the Inertia Tensor Varying due to Mass Redistribution and Mass Loss," AIAA Journal, Vol. 7, No. 2, Feb. 1969, pp. 337-339.
30. Chobotov, V., "General Equations of Motion for a Gravitationally Oriented Multiple-Part Satellite," Report No. TDR-269 (4540-70)-8, Aerospace Corp., El Segundo, Calif., Sept. 1964.
31. Grubin, C., "Dynamics of a Vehicle Containing Moving Parts," J. of Applied Mechanics, Vol. 29, No. 3, Sept. 1962, pp. 486-488.
32. Hooker, W.W., and Margulies, G., "The Dynamical Attitude Equations for an n-Body Satellite," J. of Astronautical Sciences, Vol. XII, No. 4, Winter 1965, pp. 123-128.
33. Fletcher, H.J., Rongved, L., and Yu, E.Y., "Dynamics Analysis of a Two-Body Gravitationally Oriented Satellite," Bell System Technical Journal, Vol. XLII, No. 5, Sept. 1963, pp. 2239-2266.
34. Braune, W., and Fischer, O., "Über den Schwerpunkt des menschlichen Körpers mit Rücksicht auf die Ausrüstung des deutschen Infanteristen," Abh. d. math.-phys. Cl. d. k. Sächs. Gesellsch. d. Wissen., Vol. 26, Leipzig, 1889, pp. 561-672.
35. Fischer, O., Theoretische Grundlagen für eine Mechanik der Lebenden Körper mit Speziellen Anwendungen auf den Menschen, sowie auf einige Bewegungs-vorgänge an Maschinen, B.G. Teubner, Leipzig, 1906.
36. Dempster, W.J., "Space Requirements of the Seated Operator," Wright Air Development Center, WADC-TR-55-159, Wright-Patterson A.F.B., July 1955.
37. Weinbach, A.P., "Contour maps, center of gravity, moment of inertia, and surface area of the human body," Human Biology, Vol. 10(3), 1938, pp. 356-371.
38. Drillis, R., and Contini, R., "Body Segment Parameters," Sch. of Engr. & Science, Tech. Rept. No. 1166.03, New York University, Sept. 1966.
39. Santschi, W.R., DuBois, J., and Omoto, C., "Moments of Inertia and Centers of Gravity of the Living Human Body," Aerospace Medical Research Laboratories, AMRL-TDR-63-36, Wright-Patterson A.F.B., May 1963.

40. Hertzberg, H.T.E., Daniels, G.S., and Churchill, E., "Anthropometry of Flying Personnel - 1950," Wright Air Development Center, WADC-TR-52-321, Wright-Patterson A.F.B., March 1950.
41. Barter, J. T., "Estimation of the Mass of Body Segments," Wright Air Development Center, WADC-TR-57-260, Wright-Patterson A.F.B., April 1957.
42. Woolley, C.T., "Segment Masses, Centers of Gravity, and Local Moments of Inertia for an Analytical Model of Man," Langley Research Center, LWP-228, NASA, 1966.
43. Arnold, R.N., and Maunder, L., Gyrodynamics and Its Engineering Applications, Academic Press, London, 1961, p. 105.
44. Fox, L., Numerical Solution of Ordinary and Partial Differential Equations, Pergamon Press, 1962, pp. 24-25.
45. Slater, J.M., "Daylight Star Tracking," Report P4-909/32, Autonetics Div., North American Aviation, Inc., 1965.